QATAR UNIVERSITY

COLLEGE OF ENGINEERING

DEVELOPMENT AND EVALUATION OF A WIRELESS ACTIVE NOISE CONTROL SYSTEM IN AN ENCLOSED ENVIRONMENT

BY

AMIR HAFEZ

A Thesis Submitted to

the College of Engineering

in Partial Fulfillment of the Requirements for the Degree of

Master of Science in Mechanical Engineering

January 2023

COMMITTEE PAGE

The members of the Committee approve the Thesis of
Amir Hafez defended on the 16th of November, 2022.

Dr. Mohammad R.Paurobally
Thesis/Dissertation Supervisor

Dr. Jamil Renno
Committee Member

Dr. Nader Meskin
Committee Member

Dr. John-John Cabibihan
Committee Member

Approved:

Khalid Kamal Naji, Dean, College of Engineering

ABSTRACT

HAFEZ, AMIR, M., Masters : January : [2023:],

Masters of Science in Mechanical Engineering

Title: Development and Evaluation of a Wireless Active Noise Control system in an Enclosed Environment

Supervisor of Thesis: Dr. Mohammad, R, Paurobally.

Active noise control (ANC) is a method used to reduce acoustical vibrations mainly within the low-frequency range. This thesis aims to implement a wireless active noise control system in an enclosed environment, evaluate relevant system performance characteristics and compare it with a wired version of an active noise control system. In doing so, a method to build the wireless ANC system is outlined. The ANC system used the Filtered X-Least Mean Square algorithm (FxLMS) as a standard method to control the noise. In addition, online system identification is implemented to track any changes in the secondary path while a user is moving around. A single-frequency tonal noise source, secondary loudspeakers, and microphones are used for testing and evaluation of the complete wireless system.

It is found that the wireless system works well when validation of a single-channel system is carried out in an air handling duct test rig. Similar noise reduction levels were obtained for the wireless systems when a user wears an in-ear error microphone; it is found that the system performs well for stationary cases. When the user walks at an average pace, the system can diverge if offline system identification is used. However, if online system identification is used, the system performs well.

DEDICATION

To my beloved mother, who has encouraged me and supported me in my own work…

ACKNOWLEDGMENTS

I would like to express my deepest gratitude to my family and my supervisor Dr. Mohammad Paurobally who has guided and supported me in my research work. Afterall, his continuous support and persistent help made me achieve my goal.

Dr. Roshun has always been cooperative, even at busy times, and I am grateful for his honest support throughout my thesis work.

TABLE OF CONTENTS

LIST OF TABLES

LIST OF FIGURES

Chapter 1: Introduction

1.1 Background

Active noise control (ANC) was first introduced by Paul Lueg in 1930. The idea relies on generating a secondary noise signal with equal amplitude and opposite phase (signals with 180-degree phase shift) relative to the primary disturbance source. This causes destructive interference with the disturbance source resulting in silence [1]. In 1950, active noise control received attention from Harry Olson, who carried out experiments with developed feedback control systems. His research was based on attenuating noise at localized positions inside enclosed spaces like interiors of automobiles and aircraft cabins [2].

Today, with the increased global population, and the rise of urban and industrial activities, noise pollution is becoming more apparent than it used to be in the past. Individuals get exposed to noise throughout the day, whether at work, in public areas, or at home. However, when an individual gets exposed to noise, the noise consists of different frequency bands. The main interest in using ANC lies in reducing the Low-frequency Noise (LFN) of the transmitted noise, which is difficult to control using traditional passive control techniques due to the noise characteristics transmitted through walls or structures. Hence ANC is often applied as the most effective LFN control technique.

Commonly, urban districts of any developing country have active work sites where noise is generated by heavy mechanical vehicles (e.g., lorries or heavy-duty trucks). The LFN can be from road traffic, railways and other stationary mechanical systems

such as air-conditioning systems [3]. It can also be present in residential areas nearby airports due to aircraft-inducing noises on the runways causing mechanical and acoustic vibrations [4]. Moreover, residential areas near industrial zones can also be exposed to LFN. With the continuous growth of industrial and urban activities and the numerous increase in transportation, noise is an evident problem for most urban districts. The application of ANC to LFN in practice has thus become more practical and of interest over the last three decades.

1.2 Techniques and Methods of Noise Reduction

Active Noise Control (ANC) and Passive Noise Control (PNC) are two standard methods to reduce acoustical disturbance, as shown in **Fig.** 1.1.

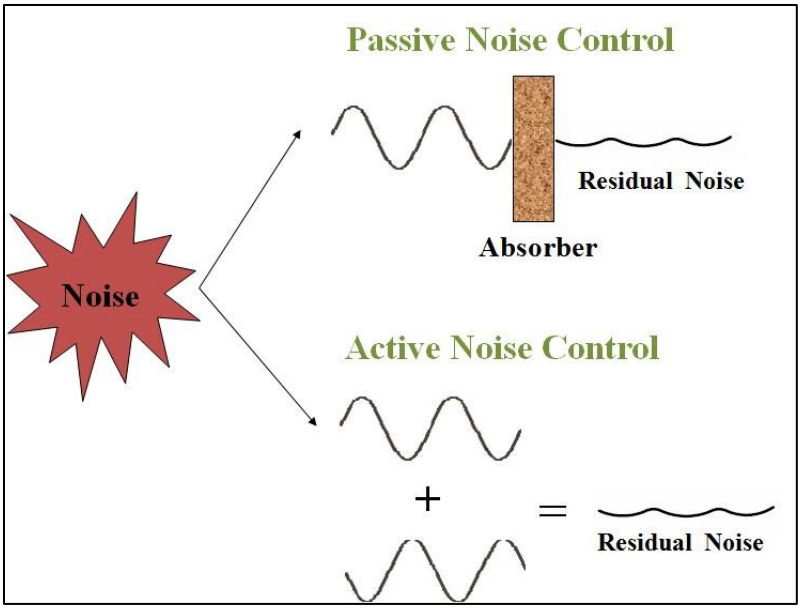

Fig. 1.1. Basic principles of passive noise control and active noise control [5].

1.2.1 Passive Noise Control (PNC)

A common technique to reduce acoustical disturbance is the passive noise reduction method. It is a way to attenuate the noise by using acoustical isolating materials [6]. Unlike ANC systems, passive noise control systems do not need a power source, as they are mainly porous materials with acoustical absorption properties. These materials are typically effective for mid-to-high frequency noise reduction applications. Passive noise control techniques are widely used since individuals experience noises in that range. PNC can absorb medium to high frequencies because of the short wavelength that can be absorbed or reflected by the material. Otherwise, longer wavelengths (at low frequencies) can propagate through them, making it difficult to reduce the noise [7]. The acoustical properties of a mechanical sound absorber can be determined by the type of material, the geometry, and its thickness. Examples of noise-isolating materials are memory foam earpads embedded within headsets, poro-acoustic panels/tiles, plywood applied in construction applications, or exhaust mufflers, considered modern PNC applications. However, PNC is considered inadequate for LFN reduction [8, 9] and can be space-consuming for attenuating LFN by requiring a large thickness of the noise-isolating material. Low-frequency noise is typically considered between 20Hz to 500Hz, which is categorized as a structurally propagative range that can be transmitted through structures [10]. For example, a 27x57 square inch acoustic foam panel with 4 inches thickness can have more than 90% absorption at 500 Hz but a maximum absorption of 30% for 125 Hz of acoustic noise. In general, PNC systems are ineffective for low-frequency applications [11]. They are also ineffective for impulsive noise, which contains mainly low-frequency energy. An example of impulsive noise is a jackhammer for roadworks [12]. For such cases, ANC can help to counteract the LFN better than the passive control method.

1.2.2 Active Noise Control

The other method for reducing noise is active noise control (ANC). In ANC systems, the ‘primary path’ or ‘primary noise’ is the target noise to be reduced or controlled. The ‘secondary loudspeaker’ is driven by the ‘secondary path or control’ signal that aims to reduce the primary noise by using the destructive interference principle [13-15]. In addition to its level of flexibility and improvement in digital systems, ANC has become easily adaptable and a well-researched topic over the past 30 years. Many applications of ANC have been developed, including headphones for noise reduction [16, 17], noise-control systems for industrial machines [18, 19] and noise cancellation for automobiles [20-24]. Unlike the passive noise control strategy, ANC works better in low frequencies [25]. Most real-world scenarios involve exposure to low-frequency noises, such as noise that can reach individuals from vehicle engines, tire contact noise, wind noise [23] and air-conditioning [24, 26].

When constructing an ANC system, the loudspeaker driven by the ANC system produces inverted sound waves opposing the disturbing noises, which attenuates them. Control is effective in the low-frequency range due to the lower complexity of sound waves with long wavelengths and, therefore, better spatial reproducibility of these. The main advantage of using the ANC systems is the use of electrical components such as sensors and actuators to generate anti-noise sound. Using ANC with multiple sensors and actuators is a big step forward in setting up a practical and effective ANC System. This type of setup is referred to as a multi-channel ANC system and is helpful in attenuating sounds in three-dimensional space [27]. However, the wires can occupy

space when constructing a multi-channel ANC with more channels. For that reason, implementing a wireless ANC system is considered attractive in terms of space consumption, less weight (such as in aircraft), and lower cost. In addition, maintenance issues can also be considered attractive in wireless systems eliminating the need to deal with the extensive amount of wiring.

Active Noise Control (ANC) is, therefore, an effective and common way to control low-frequency noise (LFN) [28]. It has been applied successfully, for example, in active headrests for cars and aeroplanes, in yacht cabins, and in bedrooms that are located in noisy environments. In addition, there have been many developments in the aviation industry associated with ANC technology. For example, companies such as Bombardier, King Air and Wolfe Aviation [29] design and offer active noise and vibration control systems specifically designed for aircraft.

1.3 Health risks associated with long-term exposure to loud noises and LFN

Noise can have both auditory and non-auditory prolonged impacts on health. Hearing loss is considered one of the common effects caused by loud noise exposure on a long-term basis [30]. It can cause damage to auditory sensor cells in the ear [31], significantly reducing the quality of life [32]. Noise was ranked as the second environmental threat to human health after air pollution, according to The World Health Organization (WHO) [33]. It can lead to the disruption of brain activity [34]. Children exposed to noise may have lower test scores, memory loss over a long-term period, and lower reading comprehension test scores [35]. If an individual gets exposed to LFN for an extended period, the person may experience unpleasant effects from the extended exposure time. The effects can include disturbed sleep, headache, stress, annoyance, and fatigue [36]. Such annoyance levels can cause sleep disturbance, tired-ness, and possible long-term vibroacoustic diseases (e.g., tinnitus) [37]. In addition, it has been reported that it can lead to atrial fibrillation, which is a heart condition that causes irregular and often abnormally fast heart rate, which can induce blood clots, strokes, and put them at risk for cardiovascular problems such as high blood pressure and high cholesterol[38].

1.4 Aims and Objectives of the research thesis

The overarching aim of the research is to enhance the abilities of ANC systems in an enclosed space using wireless transmission instead of wired transmission. In doing so, it is hoped that it will make the system more mobile, less space consuming and easier to implement on a large scale in future applications.

The main objectives are:

1. To develop a wireless ANC system with specific characteristics, such as electroacoustic delays from the DSP and transceivers.
2. Perform validation experiments of the wireless system to measure system performance by measuring steady-state residual noise in a simple acoustic duct and compare it with the wired version using a single-channel system (one reference, one error, one control).
3. Implement a wireless in-ear microphone system to be used as a mobile error microphone for ANC at the ear.
4. Extend the single-channel error microphone to a dual-error channel microphone system with a single-control loudspeaker for both ears.
5. Test the single and dual-error channel system under stationary and mobile conditions.
6. Draw relevant conclusions from the experimental results, including the wireless ANC system's local and global noise control capabilities.

1.5 Scope of Thesis

The scope of this thesis is mainly concerned with achieving a wireless active noise control system that operates within the low-frequency range with a minimized 'residual noise'. This is achieved by developing a wireless in-ear microphone to be used as the error microphone. A basic study of spatially global and local noise control capabilities is also included. Global noise control applications include ANC in automobiles and aircraft [22, 23, 39-41]. In such cases, the development of a large quiet zone to cover an entire space is desired.

On the other hand, local control aims to achieve control around the error microphone. Only irrespective of increase elsewhere. This can allow multiple users to move around freely within a room using a multi-channel wireless ANC System, as depicted in the example shown in **Fig.** 1.2.

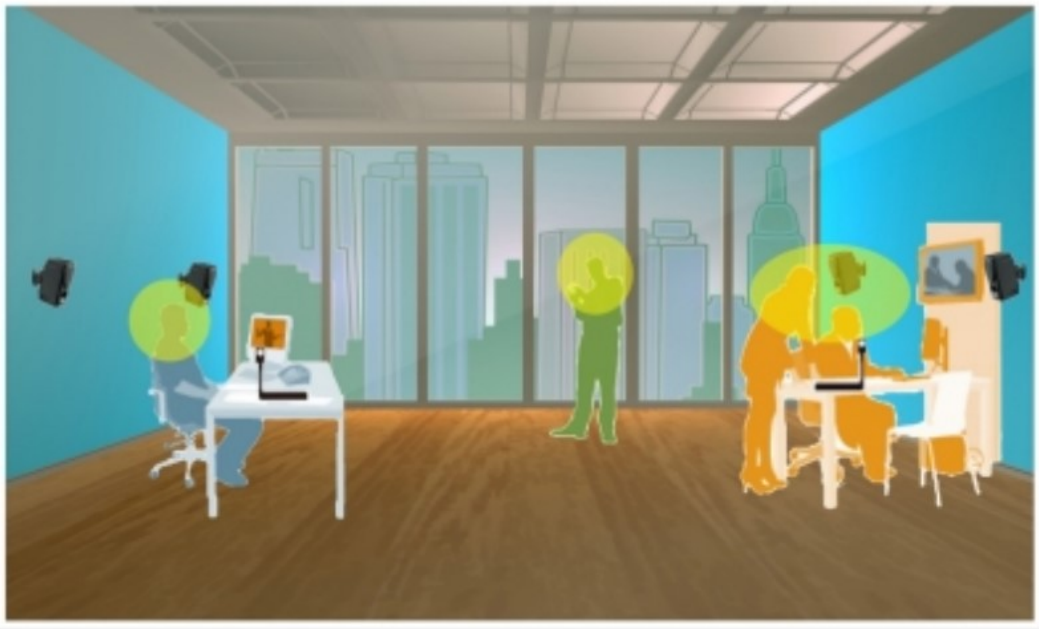

Fig. 1.2. Example of a personalized multi-channel ANC in an office [42].

Fig. 1.2 shows an example of multiple listeners experiencing ANC in a room. The thesis will then investigate the ANC system's mobile and stationary performance using globally and locally controlled quiet zones with the help of integrating wireless communication to allow mobility and eliminate the use of cables.

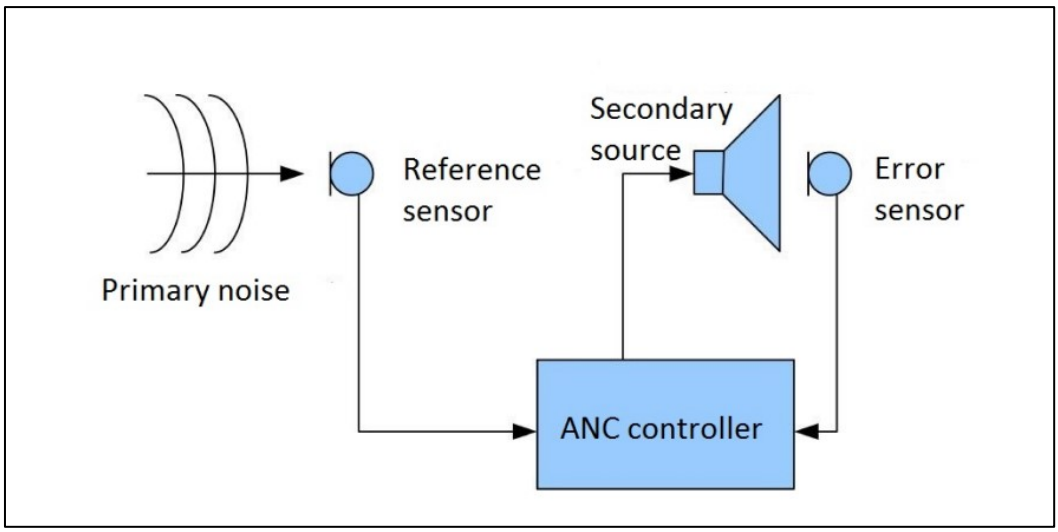

Fig. 1.3. Schematic of a simple adaptive feedforward ANC system [43].

Fig. 1.3 shows a Feed-forward control system which includes an error sensor and a reference sensor. ANC systems that only include error sensors are called ANC feedback systems. Some ANC applications have a combination of both feed-forward and feed-back structures. The conventional algorithms implemented for ANC systems are mainly based on the least-mean-square (LMS) algorithm. It has many versions, such as normalized LMS, recursive LMS and adjoint LMS [30]. There is also a practical version that has been used for decades called the Filtered-x LMS (FxLMS), which accounts for the effects of the secondary path, including delay.

1.6 Thesis Outline

Chapter 2: Literature Review

- The chapter reviews FIR filter implementations, which is the ANC system's core subject. After that, an introduction to adaptive filters is covered in section **2.1.2**, followed by the Mean-square error (MSE) derivations and the Least-mean square (LMS) algorithm. The Filtered-x algorithm is covered after. Finally, the chapter reviews the existing wireless ANC systems and their limitations.

Chapter 3: Numerical Analysis of Wireless ANC System

- The chapter implements a wireless ANC system numerical model in Simulink. This is mainly to investigate the effect of wireless transceivers on the ANC system's performance. The investigated parameters are the sampling rate, bit rate and the frequency channel of the transceivers.

Chapter 4: Validation of a wireless ANC in an air duct

- This chapter presents the validation of the functionality of the proposed transceivers for the ANC system. This is done by investigating several configurations to show the impact of adding transceivers to the ANC system.

Chapter 5: In-ear microphone experiments

- This chapter mainly investigates stationary and mobile cases when using an in-ear microphone. First, the mobile experiments involve head rotations or walking while ANC is performed. Next, the effect of loudspeaker placement is investigated to observe the noise control performance of the ANC system and record it. After that, the effect of online system identification is studied for both

stationary and mobile cases. Finally, speech interference is investigated to see its' effects on ANC performance.

- A summary of the experiments is discussed at the end of the chapter.

Chapter 6: Conclusion and Future work

- The chapter summarizes and concludes the work done through the thesis. Suggestion for future work is also included.

Chapter 2: Literature Review and Background Theory

Overview: This chapter provides a comprehensive review of the implementation of FIR Filters, adaptive algorithms, single-channel and multi-channel algorithms and control configurations. It reviews global and local ANC systems and existing wireless-based ANC systems.

2.1 FIR Filter and ANC Adaptive Algorithms

Filters are important data processing tools for signal handling and modification, such that one can change an input signal, process it, remove noise (Low pass filter, for example), and process it to obtain the desired output. In signal processing, analog and digital filters are considered the main types of filters. Components like capacitors, resistors and inductors are the main components that make analog filters [44]. Digital filters, on the other hand, are only implemented for systems that handle digital signal processing where the filter is embedded in a processor chip in a DSP. The filters can attenuate or add limited gain at specific frequencies and can add phase delay. In addition, digital filters are easier to modify and more flexible since software can change the properties of a digital filter, such as the number of coefficients or weights of the filter [44, 45].

Digital filters can easily implement adaptive filters compared to analog filters and can achieve desired output by manipulating and changing system parameters in real-time. Adaptive filters are often associated with an optimization algorithm [46], and the filter is considered a linear system that has a transfer function. The filter also has a set of changing parameters that control the transfer function [46]. For example, a closed-

loop adaptive filter updates the transfer function by computing the error, which is an example of the LMS method. An optimization algorithm includes a cost function in an adaptive filter, which determines the best performance for such applications by adjusting filter weights [45, 46]. The algorithm and digital filters embedded within the DSP in an ANC system influence the performance, such as computational efficiency and accuracy. This section will review FIR filters and conventional algorithms used in ANC.

2.1.1 Finite Impulse Response (FIR) Filter

Finite Impulse Response (FIR) filters can be used to estimate the secondary path(s) in an ANC system. That is the frequency response(s) between the secondary loudspeaker(s) and the error microphone(s) [45]. FIR filters are digital filters that decay to zero, unlike Infinite Impulse Response (IIR) filters which may not decay to zero since the output is used as feedback [47]. FIR filters are designed to be simple, linear, and mostly stable filters that can be used for modern ANC applications [45, 47]. The algorithm is efficiently implemented in software using FIR filters compared to IIR filters [47] as the controller. FIR filters may require a higher order to have the desired accuracy and may introduce additional delays compared to IIR filters. The delays may affect ANC performance if they are significant. However, in this thesis, only tonal noise will be controlled, and as a result, the effect of delays is not an issue for stationary noise conditions.

A block diagram of a digital filter is shown in Figure 2.1 for a linear system in which the system's output $y(k)$ is bounded for a given bounded input $x(k)$.

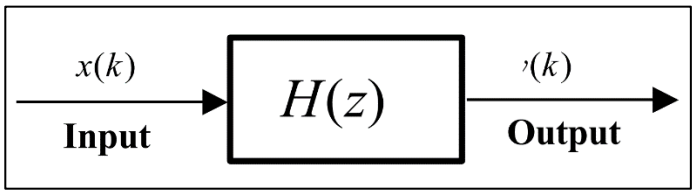

Fig. 2.1. Block diagram of a linear digital filter H(z)

The output $y(k)$ is affected by the current and past values of the input, such that the input can be written as $x(k), x(k-1), ...$

$$y(k) = H[x(k), x(k-1), ...] \tag{2.1}$$

$H(z)$ is a linear function that obeys the principle of superposition. As a result, the expression can be re-written in the form of a linear summation given by

$$y(k) = \sum_{i=0}^{\infty} h_i(k)x(k-i) \tag{2.2}$$

Equation (2.2) describes the discrete-time convolution of $x(k)$ with the sequence $h_i\ (k)$ at the time step k. In practice, the output of the digital filter is truncated in the summing equation and $h_i(k)$ is written as $w_i(k)$ as the filter notation is referred to as the Wiener FIR filter. The output equation becomes

$$y(k) = \sum_{i=0}^{L-1} w_i(k)x(k-i) \tag{2.3}$$

L represents the order of the FIR filter, and i is the filter coefficient at input sample k at a time. The filter coefficients and input signal can be written in vector form as

$$w(k) = [w_0(k)\ \ w_1(k) \dots \dots\ w_{L-1}(k)]^T \in R^{L\times 1}$$

$$x(k) = [x(k)\ \ x(k-1) \dots \dots\ x(k-L+1)]^T \in R^{L\times 1}$$

where T superscript represents the transpose of a vector. Hence, the output $y(k)$ after

filtering can be expressed in vector form as

$$y(k) = w^T(k) * x(k) = x^T(k) * w(k) \tag{2.4}$$

In equation (2.4), * denotes a linear convolution. Similarly, in a block diagram, the FIR Wiener filter is a digital filter that estimates $x(k)$ signal and yield $y(k)$ as the optimal solution:

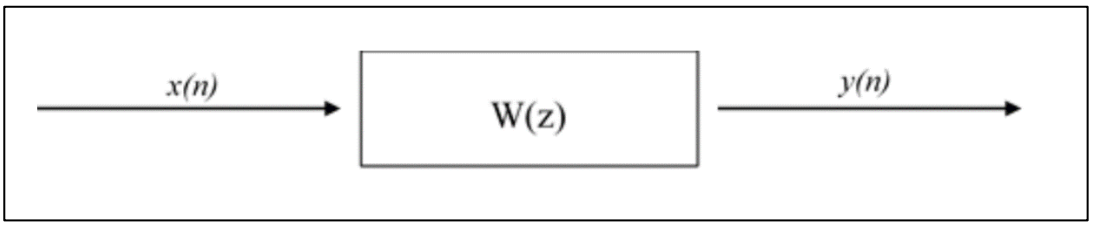

Fig. 2.2. The wiener solution using the Wiener filter.

The FIR filter can be represented as a block diagram as a weighted sum of finite numbers for past input samples, as shown in **Fig.** 2.3**.**

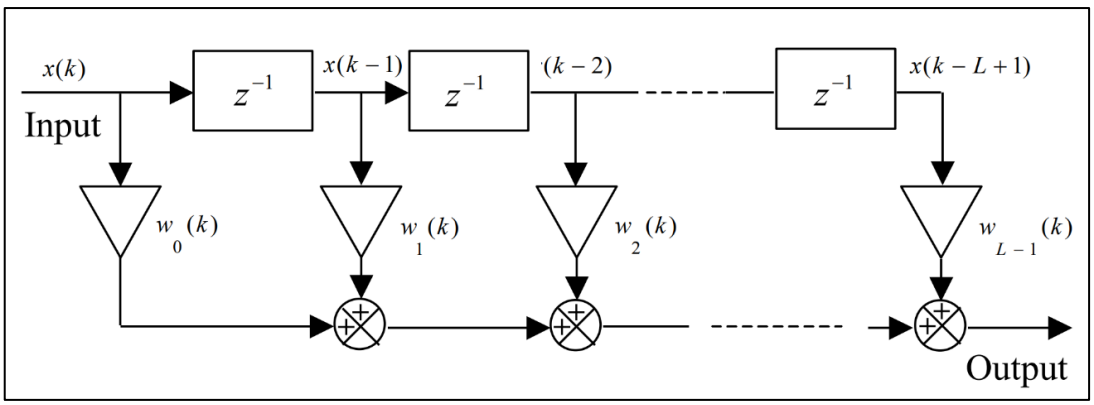

Fig. 2.3. Finite weighted sum of an FIR Filter [48]

The transfer function of the FIR filter can be expressed as [47],

$$W(z) = \frac{Y(z)}{X(z)} = w_0 + w_1 z^{-1} + w_2 z^{-2} + \ldots\ldots + w_{L-1}\, z^{-(L-1)} \tag{2.5}$$

where X(z) and Y(z) are the z-transforms of the input and output sequences x(k) and y(k), respectively. Alternatively, it can be expressed in summation form with order *L* as:

$$W(z) = \sum_{k=0}^{L-1} w_k \, z^{-k} \tag{2.6}$$

where w_k are the Wiener filter coefficients, and the Wiener Filter $W(z)$ is the z-transform of w(k). The z-transform translates discrete-time signals to a transfer function, which is a complex function that has its own plane that is called the z-plane. In order to obtain the frequency response of the filter, we can apply Fourier transform by substituting $z = e^{j\omega T}$,

$$W(j\omega) = \sum_{k=0}^{L-1} w_k \, e^{-j\omega Tk} \tag{2.7}$$

2.1.2 Adaptive FIR Filter

Adaptive filters can modify their performance characteristics in real-time to achieve the desired adaptive goal by setting predefined objectives through the performance cost function. The most common adaptive FIR filters used in active control systems are based on the LMS (least mean square), as they are simple to design and implement. Two components are needed to implement an adaptive filter. The first component is a digital filter (an FIR filter, for example), and the second is an adaptive algorithm block. The algorithm mainly adjusts the coefficients of an FIR filter in real-time to meet the desired objective, which in ANC's case is the minimization of the acoustic error at a specific location. Figure 2.4 represents the block diagram of an adaptive

filter.

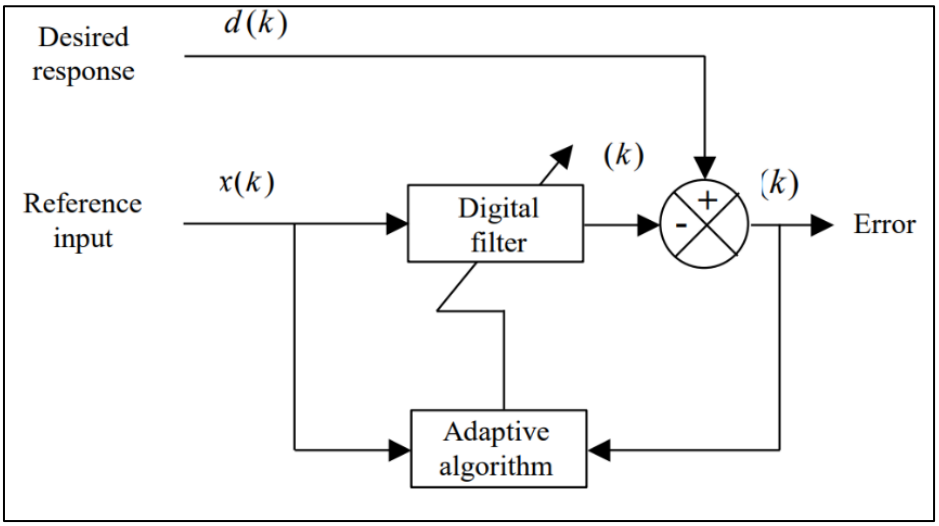

Fig. 2.4. block diagram of FIR filter implementation

In order for the FIR filter to meet the desired output, the adaptive filter adjusts the coefficients by minimizing the mean square error $e(k)$. The error $e(k)$ can be obtained by applying the difference equation between the desired response signal $d(k)$ and the output of the FIR filter in Equation (2.4). This leads to the equation

$$e(k) = d(k) - y(k) = d(k) - w^T(k)\, x(k) \tag{2.8}$$

To minimize the mean-square error (MSE) of the function, the optimum weight vector must be determined. Usually, the input signals are assumed to be statistically stationary for simplicity to ease the mathematical analysis. The following section will outline the means of finding the optimized weight vector to minimize the error of the performance surface.

2.1.3 Mean Square Error (MSE) derivations

A performance criterion, such as the mean squared error is selected for the adaptive filter. This is the optimal solution for a Wiener filter and is called the mean-square error (MSE) criterion that will make the adaptive algorithm update filter coefficients to achieve the goal of that criterion. The MSE error can be obtained through the equation

$$\xi(k) = E[e^2(k)] \tag{2.9}$$

where E is the expected value of the squared error. The equation can be expanded in the form:

$$\xi(k) = E\left[\left(\boldsymbol{d}(k) - \boldsymbol{w}^T(k)\boldsymbol{x}(k)\right)^2\right]$$

$$\xi(k) = E[\boldsymbol{d}^2(k)] - 2\boldsymbol{p}^T w(k) + w^T(k)\boldsymbol{R}w(k) \tag{2.10}$$

where **p** is the cross-correlation vector and **R** is the autocorrelation matrix [47, 49]. Both can be defined by:

$$\mathbf{p} = \mathrm{E}[\boldsymbol{d}(k)\boldsymbol{x}(k)] \tag{2.11}$$

$$= [\boldsymbol{r_{dx}}(0)\, \boldsymbol{r_{dx}}(1) \ldots \boldsymbol{r_{dx}}(L-1)]^T$$

Where the cross-correlation function between $d(k)$ and $x(k)$ is expressed as:

$$\boldsymbol{r_{dx}}(n) = \mathrm{E}[\boldsymbol{d}(k)\boldsymbol{x}(k-n)] \tag{2.12}$$

The auto-correlation Toeplitz matrix is expressed as:

$$\boldsymbol{R} = E[\boldsymbol{x}(k)\boldsymbol{x}^T(k)]$$

$$= \begin{bmatrix} r_{xx}(0) & r_{xx}(1) & \cdots & r_{xx}(L-1) \\ r_{xx}(1) & r_{xx}(0) & \cdots & r_{xx}(L-2) \\ \vdots & \vdots & \ddots & \vdots \\ r_{xx}(L-1) & r_{xx}(L-2) & \cdots & r_{xx}(0) \end{bmatrix} \quad (2.13)$$

The auto-correlation function of $x(k)$ is expressed as:

$$\boldsymbol{r_{xx}}(n) = E[\boldsymbol{x}(k)x(k-n)] \quad (2.14)$$

There are necessary conditions for the autocorrelation matrix, as follow:

1- The autocorrelation matrix $\boldsymbol{R}$ must be symmetric such that $\boldsymbol{R}^T = \boldsymbol{R}$, assuming that $r_{xx}(n)$ is a real, non-complex signal that makes $\boldsymbol{R}$ a real-valued matrix.

2- $\boldsymbol{R}$ must be a Toeplitz matrix such that the element parallel to the main diagonal is equal.

3- The eigenvalues of $\boldsymbol{R}$ are real and non-negative.

4- The conjugate transpose of the matrix must equal itself, which makes it a Hermitian Toeplitz matrix [50].

Equation (2.10) is a quadratic function of the filter coefficients w(k). Differentiating the equation with respect to the weight vector gives the theoretical optimum weight vector, which is called the Wiener-Hopf equation [48, 49]:

$$\mathbf{R}\mathbf{w^o} = \mathbf{p} \quad (2.15)$$

Using equations ((2.15)and (2.10)) the minimum MSE is given by

$$\xi_{min} = \mathrm{E}[\boldsymbol{d^2}(k)] - p^T w^o \quad (2.16)$$

The MSE equation can then be expressed as

$$\xi(k) = \xi_{min} + [\boldsymbol{w}(\boldsymbol{k}) - \boldsymbol{w^o}]^T \boldsymbol{R}[\boldsymbol{w}(\boldsymbol{k}) - \boldsymbol{w^o}] \quad (2.17)$$

This equation indicates that the performance surface has a single minimum at $\mathbf{w} = \mathbf{w^o}$, where the value of the error function is $\xi(k) = \xi_{min}$. It is, therefore, possible to search the quadratic performance surface for the minimum and obtain the optimum vector $\mathbf{w^o}$**.**

Several gradient-based methods exist to find the optimum. These are discussed briefly in **Appendix A.1**. The next section outlines the most popular algorithms; the LMS and the FxLMS.

2.1.4 Least Mean-Square (LMS) Algorithm

The LMS method is similar to the steepest descent method outlined in **Appendix A.1.2**. Except that the MSE is estimated using the instantaneous error instead of the expected error. The equation for the new error is given by

$$\hat{\boldsymbol{\xi}}(k) = \boldsymbol{e^2}(k) \tag{2.22}$$

The instantaneous gradient is then given by

$$\nabla\hat{\boldsymbol{\xi}}(k) = 2[\nabla \boldsymbol{e}(k)]\boldsymbol{e}(k) \tag{2.23}$$

Using the equation $e(k) = d(k) - w^T(k)\, x(k)$, and knowing that the gradient of the error is

$$\nabla \boldsymbol{e}(k) = \ -\boldsymbol{x}(k)$$

The instantaneous gradient becomes

$$\nabla\hat{\boldsymbol{\xi}}(k) = -2\boldsymbol{e}(k)\boldsymbol{x}(k) \tag{2.24}$$

Using equation (2.20) found in Appendix **A.1**, the new adaptation algorithm for the LMS method becomes

$$\boldsymbol{w}(k+1) = \boldsymbol{w}(k) + 2\boldsymbol{\mu}\mathbf{e}(k)\boldsymbol{x}(k) \tag{2.25}$$

This approach is also considered a stochastic gradient algorithm, called the LMS algorithm. It does not require differentiation, averaging or squaring and only uses the error vector and the input signal, making it a simple algorithm to implement in practice. Hence its widespread use.

In equation (2.25), the coefficients of the filter $\boldsymbol{w}(k)$ iteratively updates based on the input signal $\boldsymbol{x}(k)$ and the error signal $\boldsymbol{e}(k)$. The convergence rate of the adaptive

process is influenced by the step size or convergence factor $\boldsymbol{\mu}$. Using performance analysis of the LMS algorithm provides the upper and lower bounds for convergence of the step-size μ given as [48]

$$0 < \boldsymbol{\mu} < \frac{1}{\boldsymbol{\lambda}_{max}} \tag{2.26}$$

$\boldsymbol{\lambda}_{max}$ is the maximum eigenvalue of the auto-correlation matrix $\boldsymbol{R}$ [47-49]. Since it is difficult to obtain $\boldsymbol{\lambda}_{max}$ in actual applications, the limits of the convergence factor are usually set as

$$0 < \boldsymbol{\mu} < \frac{1}{\boldsymbol{LP_x}} \tag{2.27}$$

where $\boldsymbol{P_x} = E[\boldsymbol{x}^2(k)]$ is denoted as the power of the signal $\boldsymbol{x}(k)$, and $\boldsymbol{L}$ is the order of the filter. After the convergence of the filter coefficients, theoretically, there is a residual error for the LMS algorithm. The residual error is also called excess MSE. Using performance analysis on the LMS algorithm, the excess error can be given as

$$\xi_{exc} = \mu L P_x \xi_{min} \tag{2.28}$$

The excess error after convergence is directly proportional to the step-size factor μ and filter order. Assuming that the filter order and the input noise power are constant, the step-size will influence the residual error such that if the step-size is set to a high value, the performance will be worse after convergence, but the convergence rate will be fast enough. Then there is a trade-off between residual error and the convergence rate. In practical applications, the step size is tuned based on the stability requirements of the active noise control.

A typical block diagram of the use of the LMS algorithm is shown in **Fig.** 2.5.

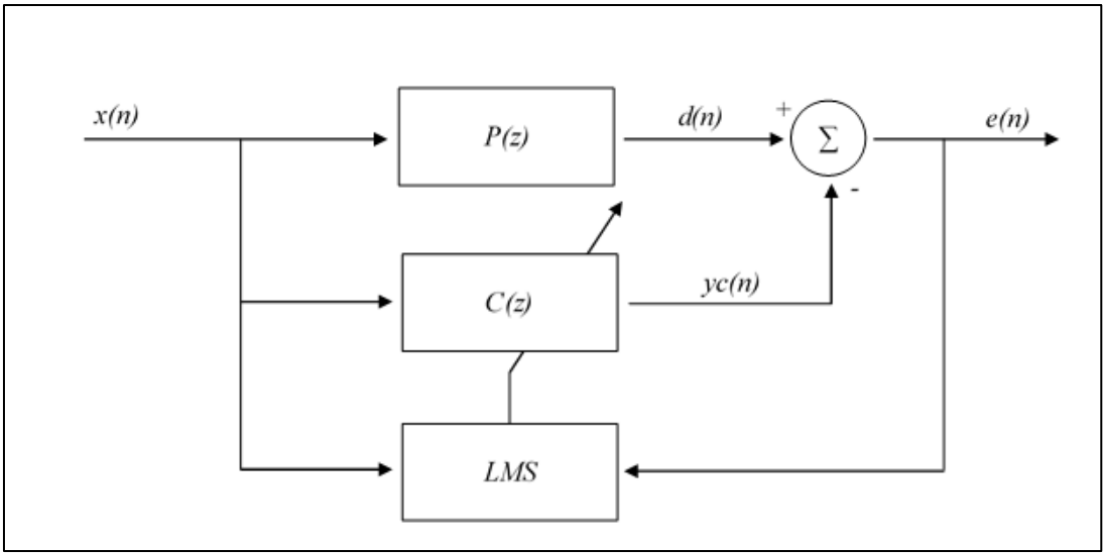

Fig. 2.5. Schematic of LMS block diagram

$e(n)$ is the error signal that needs to be minimized, $d(n)$ is the disturbance noise, and P(z) is the primary path of that disturbance, yc(n) is the destructive output signal of the digital FIR filter $C(z)$. Both $C(z)$ and the LMS algorithm form an adaptive filter together that is computed from the input reference signal $x(n)$ [45, 49]. In this figure, it should be noted that there is no existence of any path assumed after the control filter. In practice, however, such a secondary path exists and can destabilize the adaptive algorithm. The FxLMS algorithm can then be applied as discussed next.

2.1.5 Filtered-x LMS (FxLMS) Algorithm

Although the primary path can be modelled by the LMS algorithm, but it does not model the secondary path [48, 49]. The stability of the ANC system mainly depends on the secondary-path transfer function $h_s(k)$ [30]. In the LMS algorithm diagram, the reference and error signals are therefore not aligned in the time domain [51]. It is possible to avoid secondary path considerations by using the Infinite Impulse Response (IIR) or a high-order FIR filter [15, 45]. However, using IIR filters can often cause instability and using high-order FIR filters can introduce an additional unnecessary delay to the ANC System [44, 45]. Thus, it is necessary to compensate for the secondary path in ANC Systems [45, 49] for stable operation. A practical solution is to introduce an identical filter to the secondary path to filter the reference signal before the adaptive algorithm. This is called the FxLMS algorithm. The only difference between the LMS and the FxLMS algorithm is the addition of the FIR filters in representing a model of the secondary path to filter the reference signal. This is necessary to ensure time adjustment and stability of the adaptive algorithm.

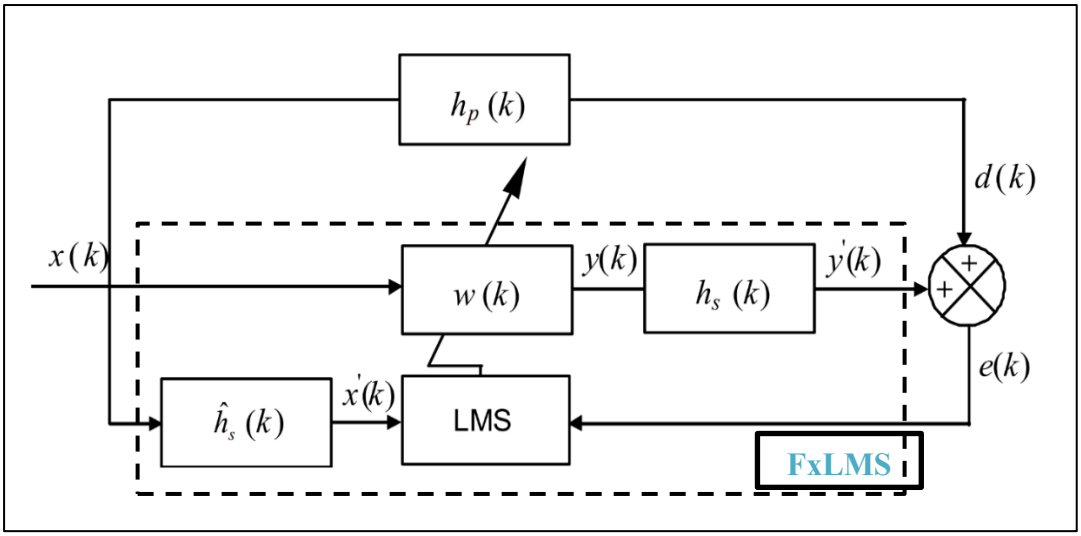

Fig. 2.6. Schematic of FxLMS block diagram.

The secondary path includes the acoustic path (physical path) and the electrical delay as well. The latter accounts for the analog and digital components in the system, such as digital-to-analog converters (DAC), analog-to-digital converters (ADC), FIR digital filters and amplifiers [30, 45]. Using the FxLMS, the stability and performance of the ANC system can be negatively impacted if the secondary path estimate is inaccurate [45, 46, 49].

The Filtered-x method is mainly applied in an ANC system to compensate for the influences of the secondary path on the ANC stability. The input signal $x(k)$ is passed through an FIR filter $\hat{h}_s(k)$ that is identical to the actual secondary path $h_s(k)$. The filtered reference signal $\boldsymbol{x}'(k)$ can be expressed as

$$\boldsymbol{x}'(k) = \boldsymbol{x}(k) * \widehat{\boldsymbol{h}}_{\boldsymbol{s}}(k) \tag{2.30}$$

Therefore, the update equation of the FxLMS algorithm can be written as

$$\boldsymbol{w}(k+1) = \boldsymbol{w}(k) - 2\boldsymbol{\mu}\mathbf{e}(k)\,\widehat{\boldsymbol{h}}_{\boldsymbol{s}}(k)\,\boldsymbol{x}(k) \tag{2.31}$$

Alternatively, can be expressed as

$$\boldsymbol{w}(k+1) = \boldsymbol{w}(k) - 2\boldsymbol{\mu}\mathbf{e}(k)\boldsymbol{x}'(k) \tag{2.32}$$

Performance analysis of the FxLMS algorithm gives the upper and lower bounds of the step-size μ as

$$0 < \mu < \frac{1}{(\boldsymbol{L}+\boldsymbol{\Delta})\boldsymbol{P'}_{\boldsymbol{x}}} \tag{2.33}$$

Where $\boldsymbol{P'}_{\boldsymbol{x}} = E[\boldsymbol{x}'^2(k)]$ is denoted as the power of the filtered input signal $\boldsymbol{x}'(k)$ and $\boldsymbol{\Delta}$ is the number of sample delay in the secondary path. $\widehat{\boldsymbol{h}}_{\boldsymbol{s}}(k)$ is considered the impulse response of the secondary path estimate [15, 45].

The filtered-x algorithm is very tolerant of errors in estimating the secondary path $\widehat{\boldsymbol{h}}_{\boldsymbol{s}}(k)$. The secondary path can be estimated by an offline modelling method applied during the ANC system's initial training period before applying control [30]. Adaptive online system identification (secondary path modelling can also be applied [52, 53]. With slow adaptation, the algorithm can handle phase errors between the initially estimated path and the actual path up to 90 degrees. For faster adaptation, a 50 degrees phase error can be tolerated, and the adaptive filter can converge and effectively attenuate the noise [54]. The FxLMS has many variants that have shown improvement in ANC performance and have been published. Common variant algorithms are Filtered-x normalized LMS (Fx-NLMS) [55] and the Leaky FxLMS [56, 57]. Figure 2.7 shows a typical example of an FxLMS-based algorithm ANC. The multi-channel extension of an FxLMS-based ANC system is briefly discussed in **Appendix A.2**.

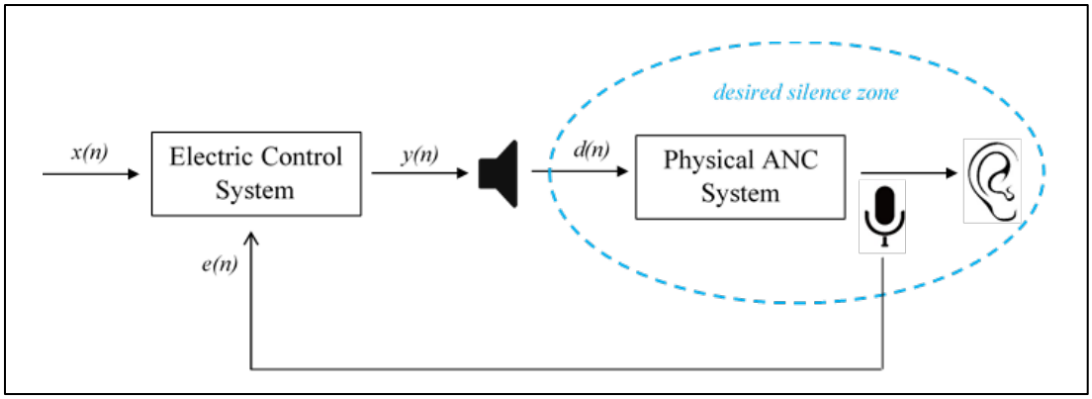

Fig. 2.7. Schematic of the secondary path of the FxLMS algorithm-based ANC System [58]

2.2 Implementation of wireless spatial ANC System

2.2.1 Previous Work Conducted on Wireless ANC Systems

One major limitation in implementing ANC systems is the significant amount of cabling often required to connect various parts in multichannel systems. This can be bulky, costly, and prohibitive. One possible solution is to use wireless transceivers in active noise control. Until now, only a limited number of research has been reported on the subject of wireless ANC. Sujbert and co-workers [59] worked on wireless sensing in ANC, which involved several microphones detecting the noise and sending the signal to a Digital Signal Processor (DSP) through a wireless setup using Berkeley MICAZ motes. As the sampling frequency is reduced, the delay between sampling and sending increases slowly but continuously, resulting in an increasing phase error in the secondary path model. The results showed that a system with only a stationary wireless error microphone performs similarly to a corresponding wired system. Research by Michalczyk and Czyz [60] demonstrated the movement of the quiet (noise control) zone around a moving error microphone. The study revealed the relationship between the convergence factor and the attenuation level for different moving microphone speeds. However, the ANC system was wired. Kajikawa and Nomura [61] further investigated the effect of movable error microphones for multi-channel ANC. They implemented a Simultaneous Perturbation algorithm where the adaptive filter coefficients are updated by two error signals showing that the system was stable, and attenuation was obtained for systems with varying secondary paths. These papers also used a wired system. The most recent work by Paurobally et al. [62] presented for the first time the results obtained by using two transceivers in partially wireless adaptive feedforward ANC setups and a completely wireless setup for single-

frequency noise control. The schematics of the two setups are depicted in Figure 2.13. The results between the wired and wireless systems were compared in terms of system delay and accuracy by using two types of transceivers.

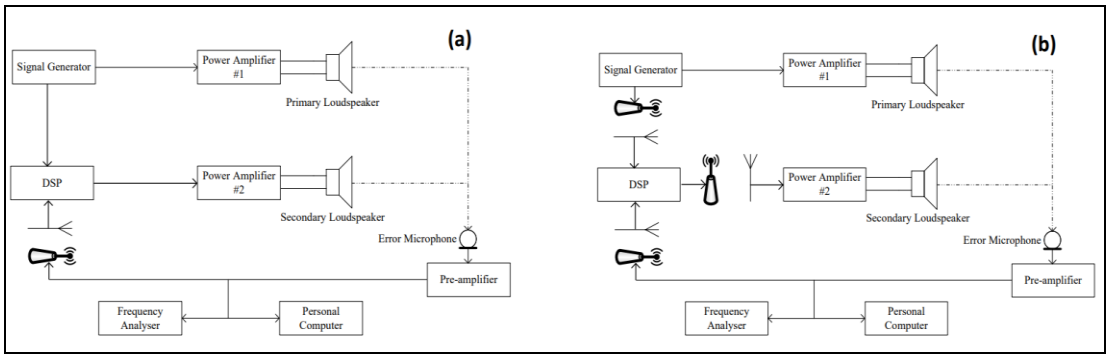

Fig. 2.8. Schematics of the (a)Mic-DSP partially and (b)complete wireless systems [62]

For single frequency noise control, the wireless systems performed very well, although the wired system was slightly better. A COP SECURITY analogue transceiver, despite having a larger static error, delivered higher performance due to having a smaller time delay compared to the NRF24Z1 digital transceiver, which had a larger time delay. There was static error mainly from the transmitters, and this caused some low-level background random noise. The results from the complete wireless system were similar to the partially wireless systems, and the study concluded that any fully wireless ANC system performs as well as its worst wireless link or path. The results are summarized in **Fig.** 2.9 with the black line of primary interest here.

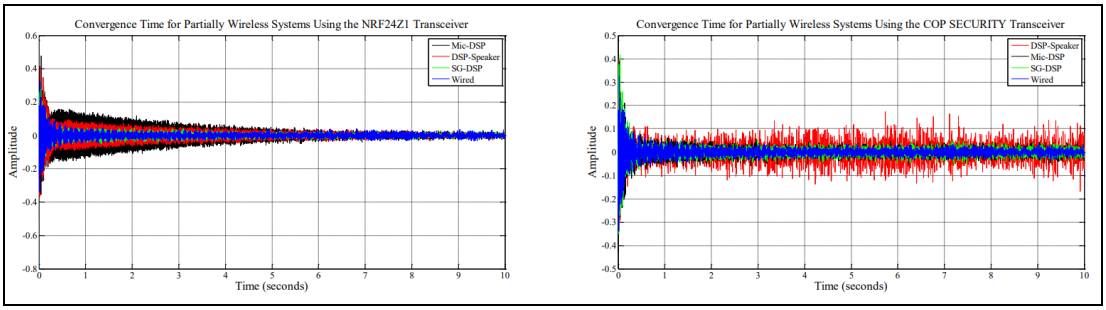

Fig. 2.9: Convergence for partially wireless systems using two transceivers [62]

A moving error microphone was also tested using the setup shown in **Fig.** 2.10 and **Fig.** 2.11 to investigate how the single-channel fully wireless system performs. This is important in the application of wireless ANC in a headset. The results depicted in **Fig.** 2.12 and **Fig.** 2.13, from a moving error microphone in a wireless ANC system, show that the system can adapt to changes in the secondary path and good noise reduction is obtained when the error microphone moves at 2.5 m/s. As the microphone moves, the secondary path changes and the FxLMS algorithm updates the controller filter coefficients. For a larger controller step size of 1.0, the filter coefficients are updated fast enough to cancel the noise. The quiet zone moves along with the error microphone. When the controller step size is small, the FX-LMS algorithm update is too slow, and the performance is reduced. The convergence coefficient selection becomes important, and a compromise between convergence speed, stability and maximum noise reduction exists. Although the results were for a single-channel system, they show that wireless ANC has the potential to provide good performance comparable to wired systems, especially when dealing with slowly varying low-frequency tonal noise and when the error does not move too fast.

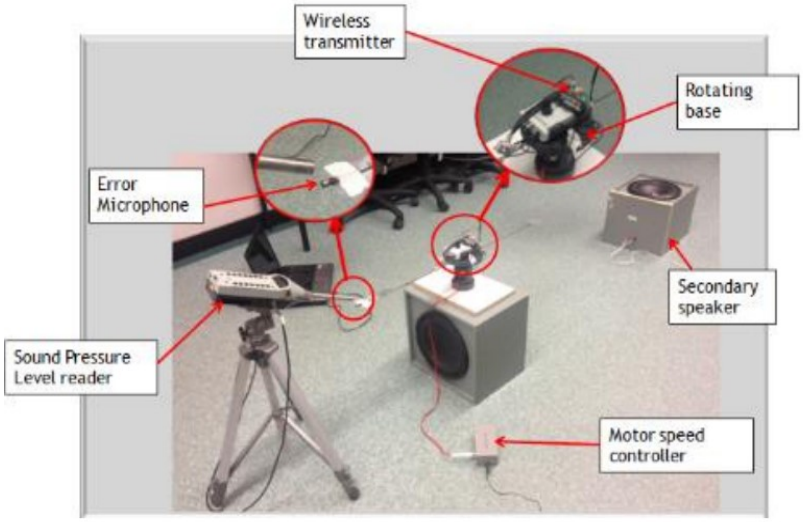

Fig. 2.10: Rotating microphone experimental set up [62]

2.2.2 Addressed research gap from previous work on wireless ANC

The few papers that previously investigated wireless ANC were mostly focused on controlling noise for stationary purposes. One paper [62] investigated wireless ANC with limited mobility experiments, such as spatial noise control on a rotating arm. In the thesis, dual-channel wireless ANC experiments were also investigated for stationary experiments to extend previous work. For such cases, single-channel and dual-channel wireless ANC were tested in a spacious environment to replicate practical working conditions in industrial applications such as walking with a wireless ANC in a workshop, where there is stationary noise for example.

2.2.3 Contributed work to wireless ANC in this thesis

The contributed work to the research gap in this thesis consists of the following:

- Investigating single-channel Wireless ANC using Simulink. This is done by obtaining the Impulse response of the transceivers experimentally and adding them to the ANC structure in the Simulink model to see the effects of a few parameters on ANC performance. After properly tuning the transceivers by studying the optimal parameters of the transceiver, a validation experiment is carried out to compare single-channel fully wired performance with single-channel partially (wired reference) wireless performance.

- A single-channel partially wireless in-ear ANC system was developed and tested for stationary and mobile cases, where the spatial experiment is selected to match the practical experience in an industrial environment. This was performed without and with online system identification (to keep the secondary path tracked in real time). Moreover, the control loudspeaker locations are experimented with for two cases. Firstly, one loudspeaker is placed close to the noise source (which can achieve an effect of global noise control). Secondly, the control loudspeaker is separated far from the noise source (which can introduce an effect of local noise control).

- A dual-error partially wireless ANC was similarly tested for the same cases mentioned in the second point of the contribution above.

2.2.4 Comparison to previous wireless ANC work

The thesis intends to present results of research carried out for Wireless ANC using wireless in-ear microphones and including mobility applications. The results obtained cannot be compared to other research due to the difficulty of replicating other authors' works and also for reasons such as those listed below:

- There are very few research work that deals with wireless ANC in some form. These are however not similar or comparable to the work presented in this thesis.
- Tonal noise was used since the FxLMS algorithm works best for slowly varying tonal noise levels. A 124 Hz tonal noise was used corresponding to the air duct's resonant frequency. As such comparison to other work is not relevant. The same frequency of 124 Hz was used throughout the research to be consistent and for relative performance comparison purposes.
- Replication of work requires microphones and loudspeakers with similar properties, such as frequency response. If the work is to be compared, the same microphones and loudspeakers have to be used. This is not practically feasible.
- Replication of spatial setup: The working environment in which the experiment was carried out cannot be replicated easily due to pre-existing geometry and size that cannot be duplicated.
- For the papers reviewed in this chapter, limited mobility experiment was performed such as wireless ANC using a rotating arm. In this thesis, the mobility experiment was extended by using a wireless in-ear microphone and walking in one direction with a range of about 7 meters from the noise source. The

movement of the user is bi-directional to make the experiment simple and close to practical application.

- No fully wireless ANC systems as presented in this thesis (even for the single-channel case), including in-ear microphones and loudspeakers have been studied before. This is the first time such work is undertaken and results of a practical system are provided.

2.3 Factors that can affect spatial wireless ANC Performance

There are a few factors that can affect the performance of a wireless ANC system. These need to be understood and dealt with before implementation. This section gives a brief review of some factors to be considered from existing work.

2.3.1 Effect of Mobility of error microphone on ANC Performance

Previous work has shown that the mobility of error microphones can impact the performance of the ANC System [62]. A microphone was attached to an extended arm that rotates around a point, as shown in Fig. 2.10. An issue of inconsistent attenuation was observed when the step size of the controller was large. This is due to the filter coefficients of the FxLMS changing fast enough to cause fast attenuation in the error signal. As the error signal changes periodically from low to high, without control, the ANC system follows the same trend. This is because the adaptation is fast enough. If the step size is smaller, the DSP will not be fast enough to update the coefficients, which results in a constant but less impressive attenuation level. Even if the error microphone is placed far away, the attenuation is still present, and inconsistent attenuation is also noted [62]. A different author had a similar experience with the mobility of an error microphone. It is observed that the attenuation was considered acceptable by tweaking the step size of the adaptive controller through each experiment but is still considered ineffective for higher rotational velocities [60]. Another study shared that the mobility of the error microphone can also impact the performance of a multi-channel ANC system [61].

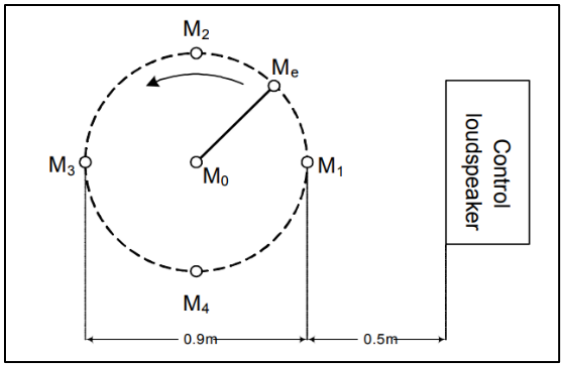

Fig. 2.11: Rotating Error Microphone [60].

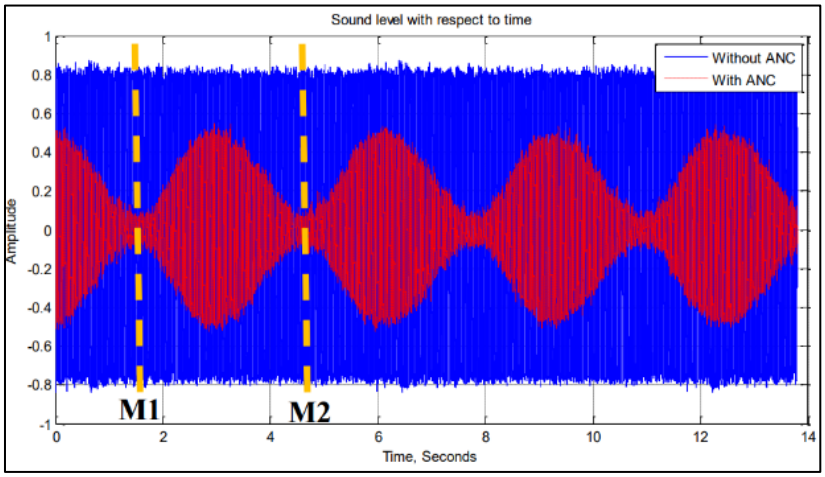

Fig. 2.12: Error Signal with Step-size of 1 at 1.03 m/s [62].

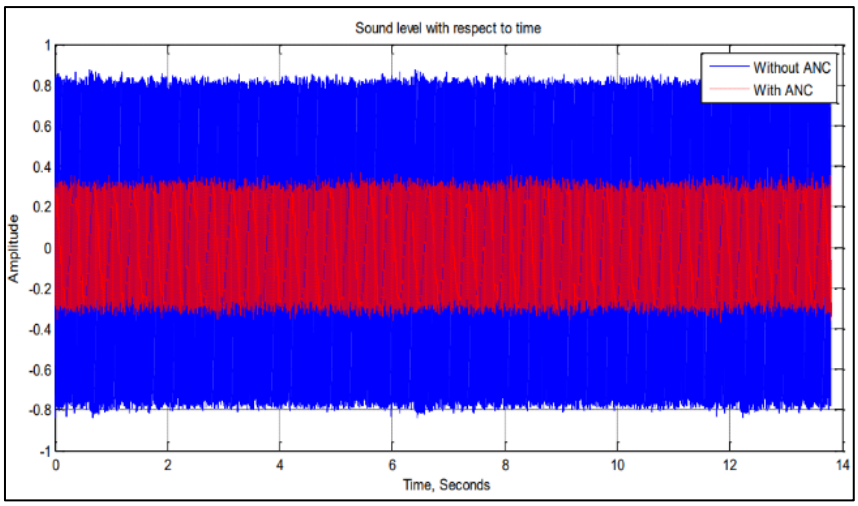

Fig. 2.13: Error Signal with Step-size of 0.1 at 1.03 m/s [62].

2.3.2 Effect of Wireless Reference Signal on ANC Performance

Shen et al. [63] have implemented an ANC system that uses a Feed-forward wireless signal concept. This was done to obtain the reference signal to achieve better results using wireless transmission. It was also observed that inverse-channel estimation produced through the DSP algorithm had fewer problems when the lookahead signal was present. This is because the noise source positions are estimated in the enclosed space, and this makes the acoustic channel stable and, thus, achieves better attenuation [63]. The effect of mobility of reference signals was not studied, but it was mentioned that the performance is at its peak for stationary applications.

2.3.3 Single and Multi-channel ANC performance

Few published works have mentioned that wireless multi-channel ANC Systems were studied. A paper studied the feasibility of deployment of Wireless Sensor Networks for ANC inside a vehicle cabin [64]. A different paper studied multi-channel wireless ANC for infant incubators and has provided simulation results [65-67]. The target control volume here is the infant incubator enclosure. The paper concluded that using dual channel ANC, external and internal noises can be significantly reduced with the help of integrating wireless communications.

2.3.4 Effect of transceivers on wireless ANC performance

In all wireless transceivers, some delays exist. These can impact an ANC system if the disturbance has changing characteristics. However, if the delay is insignificant and the noise is assumed stationary or slowly changing, the ANC system will perform well in cancelling tonal noise.

In signal processing, digital transceivers require analog-to-digital (ADC) and Digital to analog (DAC) converters. They require filters to make the received signal as identical as possible to the original signal. Applying these processes causes a delay to the transmission, which can cause additional delay to the secondary path in the wireless ANC system. These should be minimized.

In a multi-channel wireless ANC, the use of an array of transceivers is needed. In case there are many transceivers used in a room, there might be chances of interference between these transceivers. There also could be external interference, such as interference between the transceivers and a wireless router placed in a room. A way

to avoid interference is to select a transceiver with wider operating bandwidth or narrow center frequency that can reduce the interference and employ more transmission channels.

2.4 Configurations of the Wireless ANC System

The ANC system can be setup with different configurations depending on the number of error channels, control channels and reference channels. In this research, a fully wireless dual-error ANC will be the main objective. Initially, a single-channel partially wireless ANC system, as shown in **Fig.** 2.14 is developed and finally extended to a fully wireless dual-channel system.

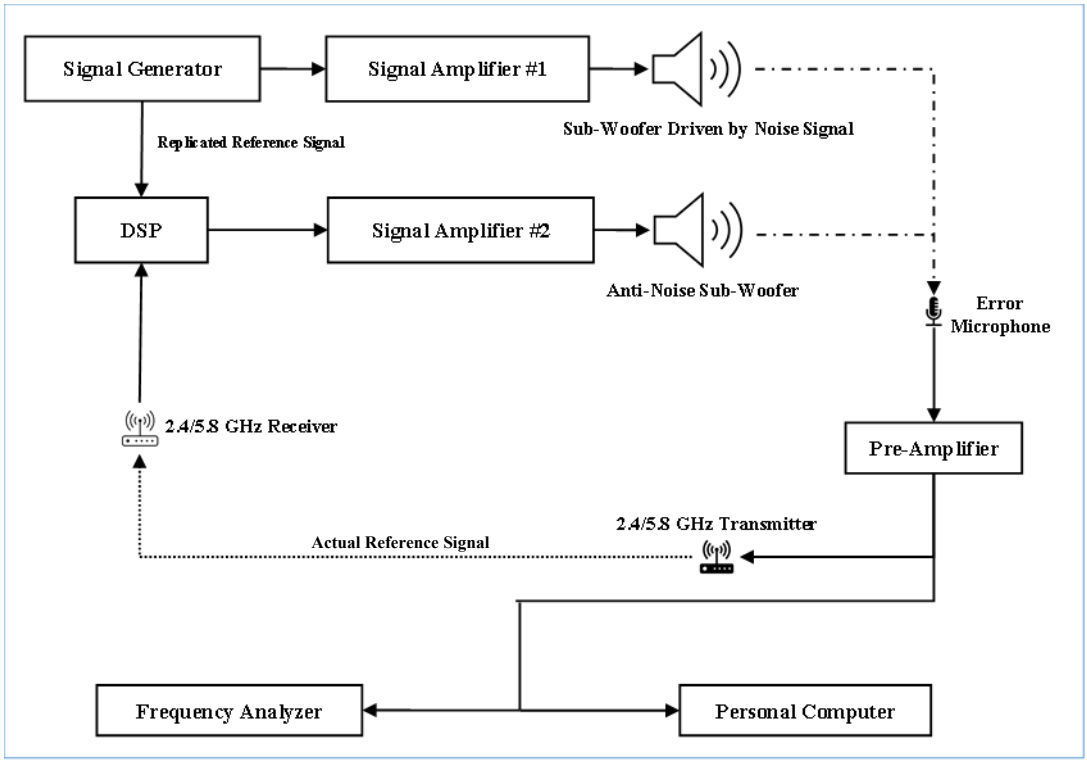

Fig. 2.14. Configuration #1 Single-Channel Partially Wireless ANC System.

This configuration basically represents a simple ANC system that consists of a signal

generator connected to a loudspeaker that represents the primary noise. This reference signal from the generator is also connected to one input channel of the Digital Signal Processor (DSP) Board. The error microphone captures the acoustic noise and is transmitted through wireless means to another input channel of the DSP. This is to generate the coefficients of the adaptive control filter for the anti-noise signal. This signal is then sent to the secondary control loudspeaker.

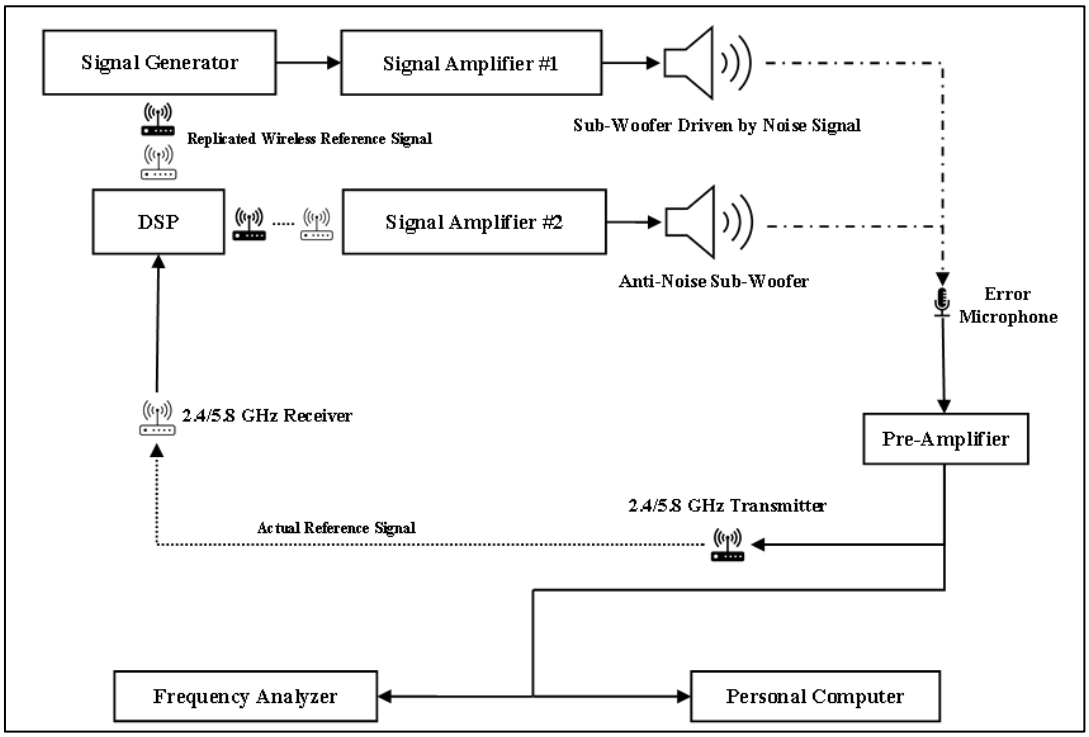

Fig. 2.15. Configuration #2 Single-Channel Fully Wireless ANC System.

The second possible configuration is similar to configuration #1 except that the signal generator, error signal and signal amplifier connections are upgraded to wireless connections, as shown in **Fig.** 2.15.

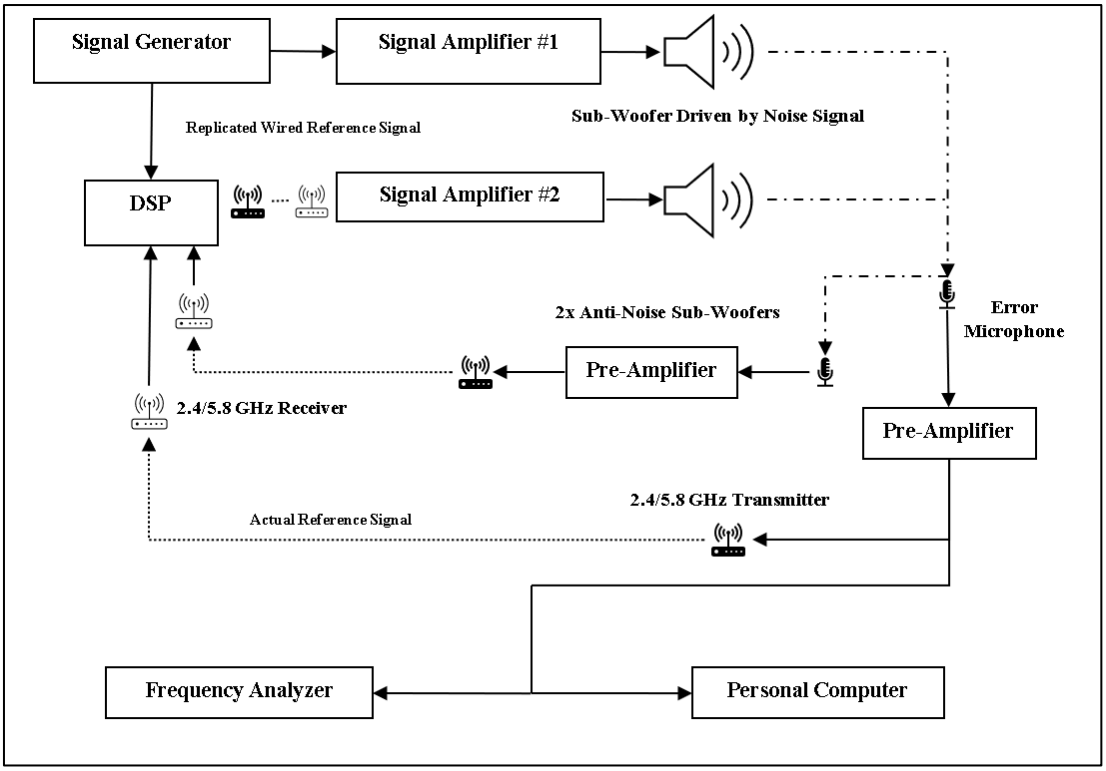

Fig. 2.16. Configuration #3 Dual-error channel partially wireless ANC System.

The third configuration represents a dual-error channel with a single-control, wireless ANC system. The setup allows the control loudspeaker to attenuate the noise at the two error microphones simultaneously. This configuration was used for in-ear experiments. The reason is to minimize the cost by reducing the loudspeakers used for ANC. Also, it can be used due to the closely spaced in-ear microphones.

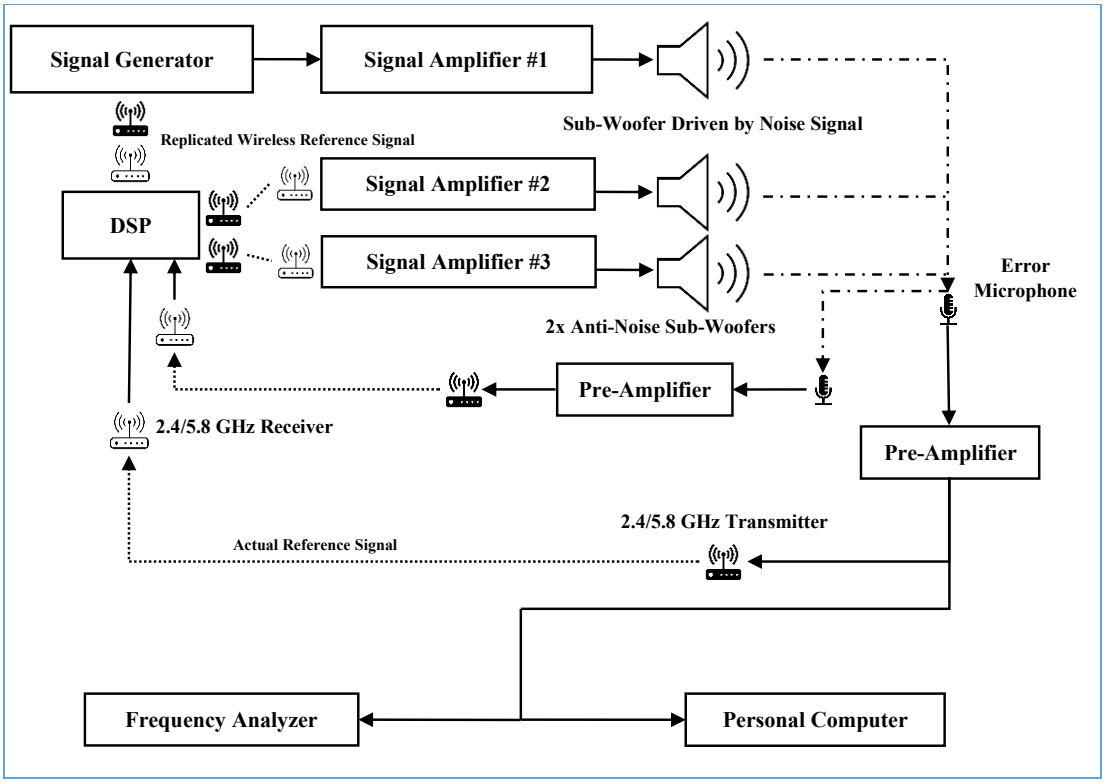

Fig. 2.17. Configuration #4 Dual-Channel Fully Wireless ANC System.

The last configuration, as shown in **Fig.** 2.17 represents a dual-channel wireless ANC system for a single listener. The configuration allows the DSP to treat the noise signals coming from two different microphones, such as two ears independently, as well each signal has its control actuator (e.g., two microphones, two anti-noise speakers).

In this thesis, the investigation of several configurations was carried out for a single listener. **Table 2.1** and **Table 2.2** provide a way to designate the setups used in the ANC structure investigated. For example, a fully wired single-channel system has a setup ID of 1.1.1.

Table 2.1: Single Channel Setups and their IDs

	Error Channels	Control Channels	Reference Channels	Setup ID
Type of Connection and Number of Channels	Wired, 1	Wired, 1	Wired, 1	1.1.1
	Wireless, 1	Wired, 1	Wired, 1	W.1.1
	Wired, 1	Wireless, 1	Wired, 1	1.W.1
	Wireless, 1	Wireless, 1	Wired, 1	W.W.1

Table 2.2: Dual Channel Setups and their IDs

	Error Channels	Control Channels	Reference Channels	Setup ID
Type of Connection and Number of Channels	Wired, 2	Wired, 2	Wired, 1	2.2.1
	Wireless, 2	Wired, 2	Wired, 1	2W.2.1
	Wired, 2	Wireless, 2	Wired, 1	2.2W.1
	Wireless, 2	Wireless, 2	Wired, 1	2W.2W.1

2.5 Identification of ANC performance variables

The performance of an ANC system relies on many variables. These are identified as dependent and independent variables, as depicted in **Fig.** 2.18.

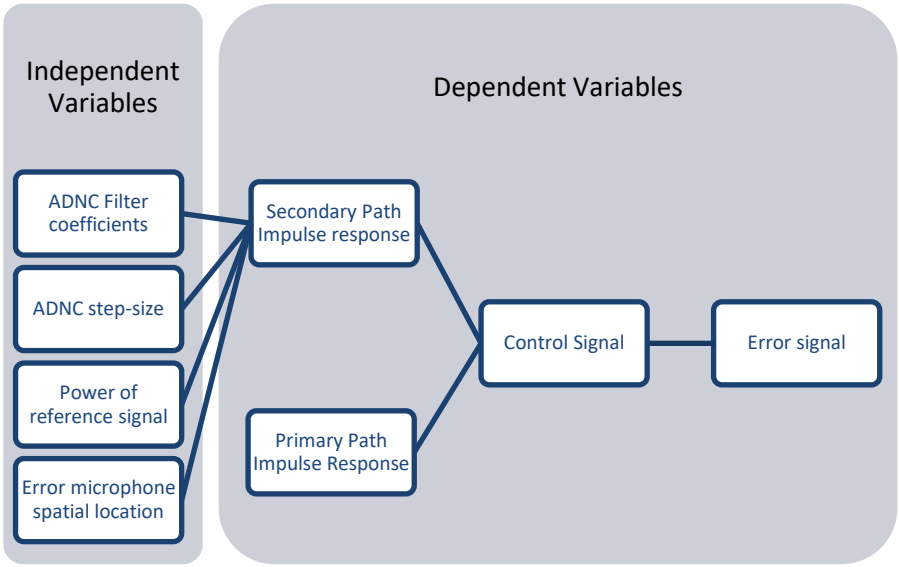

Fig. 2.18. The hierarchical relationship between the identified variables.

The main dependent variable is the error signal, which ultimately aims to reduce the acoustic pressure at the microphone location. The secondary path impulse response, which captures the room acoustic conditions, needs to include the wireless transceivers since these can introduce a slight delay and amplitude changes.

2.6 Chapter Summary

This chapter gave brief literature and background review of ANC, including realizable wireless ANC systems. It is found that ANC is well established to control low-frequency noise effectively based on sound theoretical development. In a bid to make ANC more practical, wireless systems are being developed. Limited published work indicates that a partially wireless system, such as a wireless error microphone, can perform similarly to a wired system. An attempt at a fully wireless ANC was also undertaken with encouraging results. It was also shown in previous work that if the error microphone is moving, it is possible to still get noise reduction with proper selection of the convergence factor $\boldsymbol{\mu}$. These previous works motivated the content of the research proposed in this thesis. Some possible wireless ANC performance factors and their effects have been summarized in **Table 2.3.**

Table 2.3: Identified parameters and their potential effects on ANC performance

Parameters	Residual error / Steady-state attenuation	Response Time
Microphones Frequency Response		
Loudspeaker Frequency Response		
Transceivers Frequency Response	✓	✓
Secondary acoustical path (stationary/dynamic)		
Room Enclosure Conditions		
Number of Control Channels	✓	✓
Number of Error Channels	✓	✓
Number of Reference Channels		
Characteristic Delay of Transceivers	✓	✓
Type of Control Algorithm	✓	✓
Mobility of error microphone	✓	✓

Several parameters can affect the performance of a wireless ANC system. Some are shown in **Table 2.3** with a potential effect on the performance.

The main problem statement can be summarized as follows: How the Wireless ANC Performance can be implemented? And what parameters can cause a significant change in the performance? From the problem statement, the research questions can be divided into further questions, which can be listed as follows:

1. How significant is the **impact of using transceivers** on ANC performance?
2. What is the **impact of dual-error ANC channels** (using single reference, single control channels) on wireless ANC performance?
3. What is the **impact of online system identification** on the wireless ANC performance in mobile applications?
4. What is the **impact of secondary loudspeaker placement** on the wireless ANC Performance in terms of responsiveness and tonal noise reduction in mobile applications?
5. How significant is the **impact of speech interference** on the wireless ANC Performance in terms of responsiveness and tonal noise reduction in mobile applications?

In this thesis, numerical and experimental work will be presented to provide some understanding and try to answer these questions.

Chapter 3: Numerical Analysis of Wireless ANC System

3.1 Impact of Transceiver's properties on ANC System

In this chapter, a model used for numerical simulation of the wireless ANC for the single-channel case is developed. This section studies the impact of transceiver characteristic properties on ANC performance. Some of the main characteristics of the transceiver are sample rate, bit rate and operating channel frequency. The simulation was carried out to study the effect of these variables. For example, the sample rate (S.R) used may impact the transceiver's impulse response, potentially degrading the performance of the ANC system. This chapter, therefore, discusses how significant the impact can be expected by changing some parameters in the simulations.

From the simulation carried out, the results indicate that:

1- Changing the sampling rate of the Arduino board can significantly impact the ANC performance. Decreasing the sampling rate can cause a delay in the control response.
2- Changing the bitrate of the NRF transceiver does not have a significant impact on the ANC performance.
3- Changing the operating frequency channel of the NRF transceiver is expected to have no or minimal effect on ANC performance due to similarities in impulse responses.

3.1.1 Implementation of Wireless ANC System in Simulink

A typical single-channel Fx-LMS control system was implemented in Matlab Simulink, as depicted in **Fig.** 3.1.

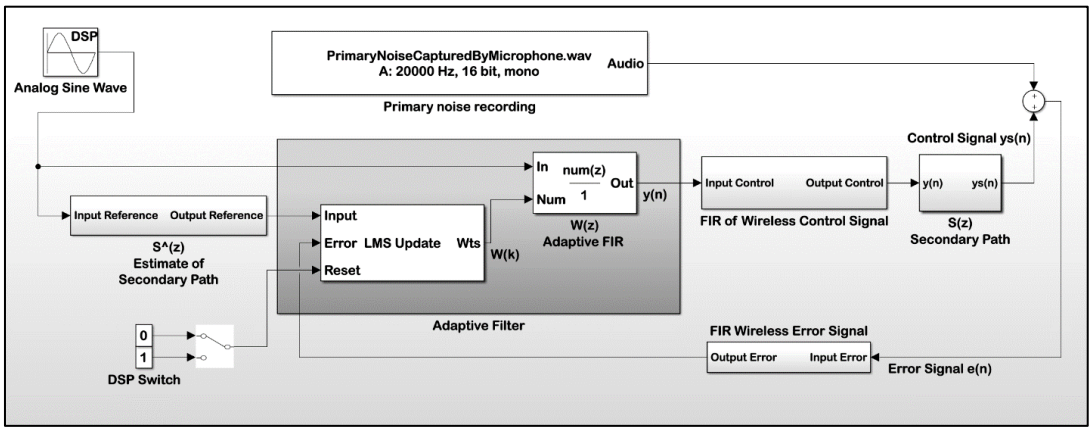

Fig. 3.1.Schematic of partially wireless single-channel Feedforward ANC Using an Fx-LMS algorithm

In **Fig.** 3.1, an analog sine wave is passed to the secondary path estimate representing the reference signal. Next, the filtered signal is passed to the adaptive filter block, which consists of the LMS algorithm and the Adaptive FIR filter. That reference is then passed to an FIR filter that represents the transceiver's response. The signal is then sent to the microphone using the actual secondary path FIR filter model. Finally, the error is passed to an identical transceiver FIR filter to be sent to the DSP input. A recording of the primary noise represents the actual primary path noise recorded from the experiment.

3.1.2 Acquired FIR coefficients from experiment vs MATLAB's Computed Coefficients from measured signals.

In an ANC practical implementation, system identification is needed to get the FIR coefficients of the system's secondary path model. Using the System Identification Toolbox in MATLAB, the Impulse response of the secondary path was obtained as a plot and compared with the acquired FIR coefficients from actual experimental measurement.

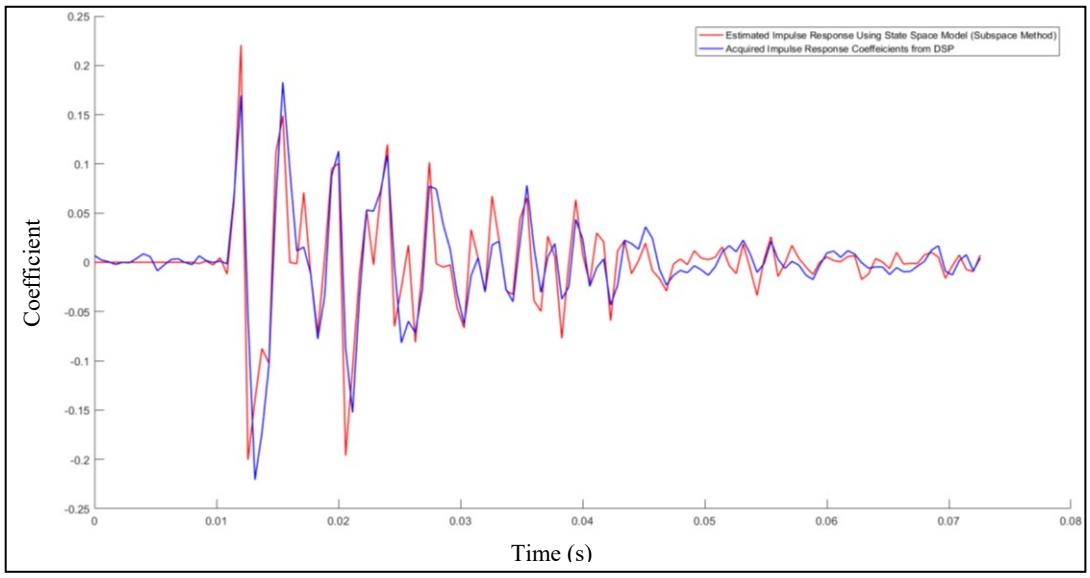

Fig. 3.2. Actual FIR Coefficients compared with Computed FIR Coefficients.

Fig. 3.2 shows the experimental impulse response (and hence FIR coefficients) versus the ones obtained from the simulation. The initial part of the response shows that the system had an overall total electroacoustic delay of about 21 samples when a sampling frequency of 1750 Hz was used to acquire and output all signals. The order of the magnitude of the delay is about 10 ms. The impulse response can now be used to study the performance of ANC system including wireless transceivers for different parameters.

3.1.3 Impact of audio sampling rate on ANC performance

The Arduino microcontroller board has an adjustable sampling rate for audio processing. Changing the sample rates causes a significant change in the ANC performance. The frequency and phase responses of a transceiver pair were computed using Simulink's built-in function "transfer function estimator". The function requires an input and an output to perform average-based frequency and phase response calculations. The frequency and phase responses were calculated for 15 seconds. In **Fig.** 3.3, noises can be spotted at the 8kHz signal. These are artefacts from the loss in transmission at some sampling frequency. The 35kHz has slightly less noise.

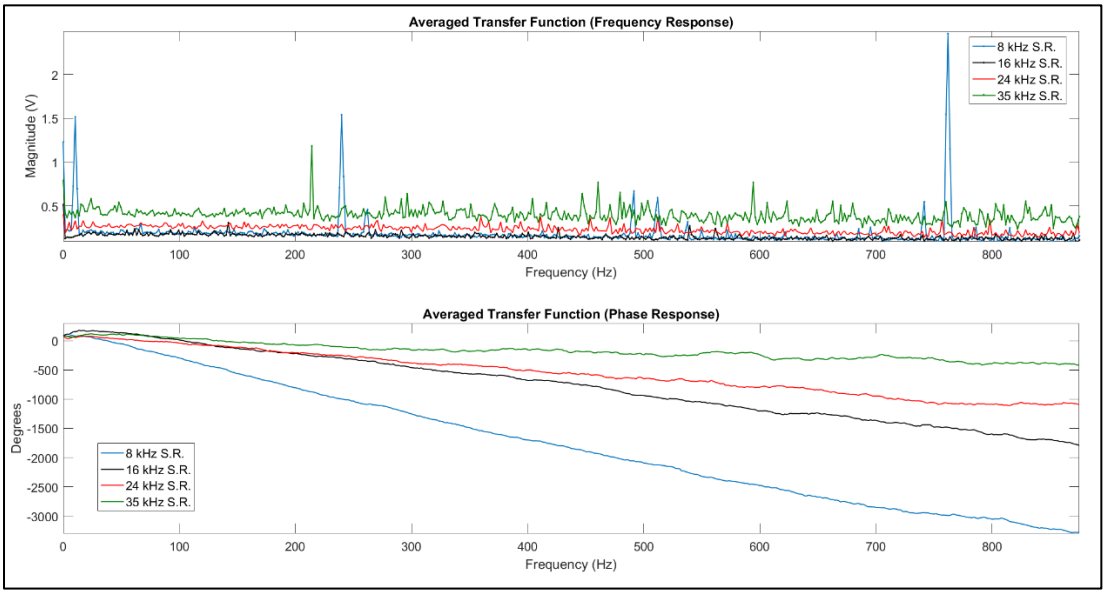

Fig. 3.3. Average Frequency and Phase Response of transceivers at different sample rates.

The impulse responses for each sampling rate used above were computed using the LMS method in Simulink for **15 seconds** duration with order **128 coefficients** and 1750Hz modelling sample rate. These are shown in **Fig.** 3.4. The four sample rates

used are 35 kHz, 24 kHz, 16 kHz, and 8 kHz. These sample rates have an overall delay of around 7, 10, 15, and 29 samples. That corresponds to about 4, 6, 8, and 16 ms, respectively.

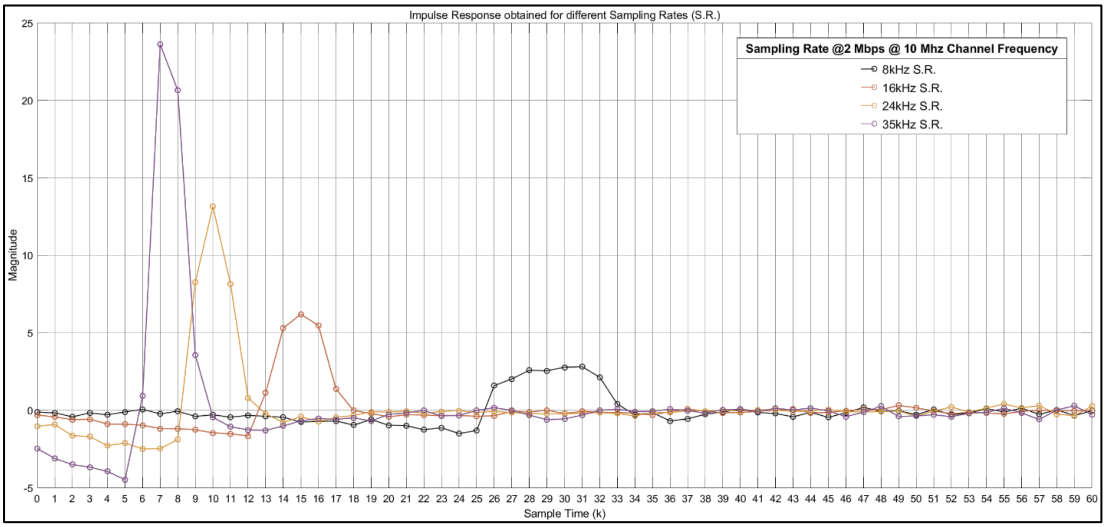

Fig. 3.4. Impulse Response of transceivers obtained at different sampling rates.

It can be observed that the delay in the system increases when the sampling time of the Arduino microcontroller decreases. It is also noted that decreasing the sample rates reduces the magnitude of the impulse responses. This indicates that the transceiver's frequency response magnitude is decreased when this occurs and is also apparent in **Fig.** 3.3.

Using the FIR coefficients obtained in **Fig.** 3.4, a single-channel wireless ANC simulation was carried out for the four sample rates. After carefully optimizing the step sizes for each sample rate, the results are plotted as shown in **Fig.** 3.5. The error signal is plotted on the left side, and the control signal is plotted on the right side of the figure.

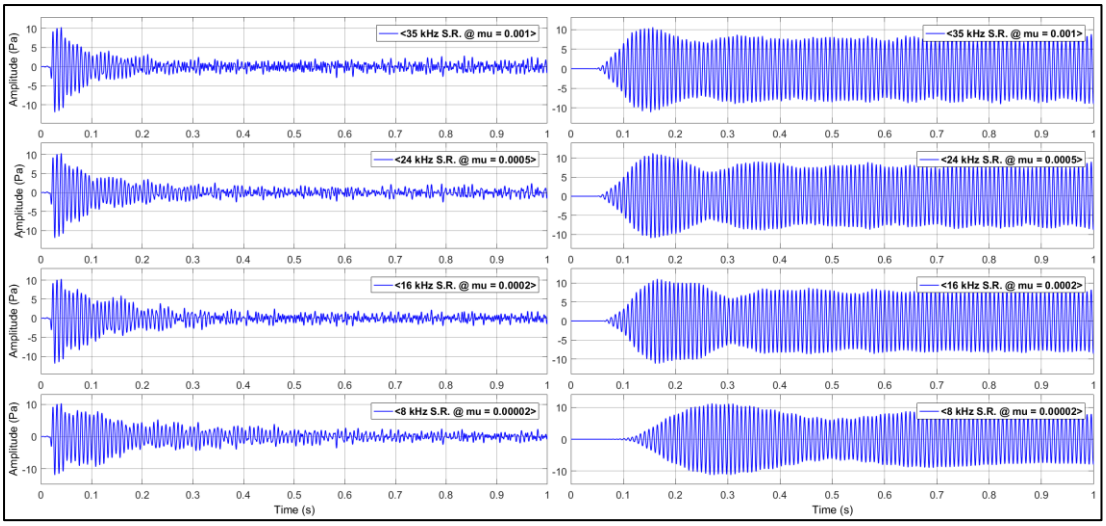

Fig. 3.5. Time-domain signals using the computed FIR weights of **Fig.** 3.4.

The time-domain signals are slightly affected by the change in the sample rates, where the control response is slightly delayed by about 50 ms using the 8 kHz sample rate. It is also seen that the convergence rate is slightly affected, and the error signal settled down to a minimum. FFT analysis was performed after a steady state was reached. The result is plotted in **Fig.** 3.6.

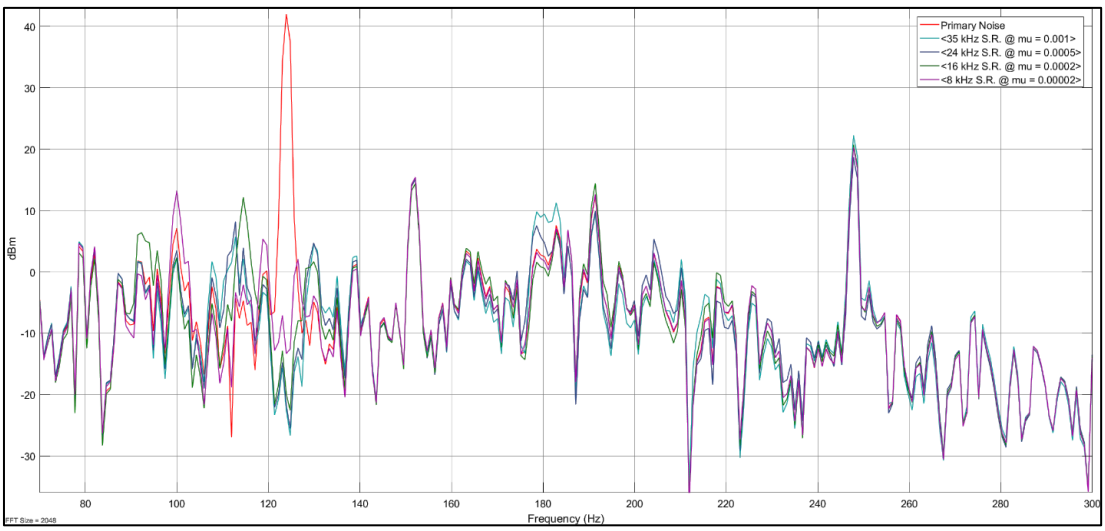

Fig. 3.6. FFT Analysis of the ANC Simulation obtained at the final sample.

All sample rates perform good noise reduction of the single frequency noise.

However, the 8kHz sample rate leads to a slightly reduced noise reduction compared to the remaining sample rates. This is seen in Fig. 3.5 in the error signal. It seems that there is an additional delay in the control signal that causes a slight deterioration in noise control performance.

3.1.4 Impact of transceiver's bitrate on ANC Performance

The bitrate, in this case, is the ability of a transceiver transmitting data signals in bits (ones and zeros) in a unit of time. Changing the bitrate for the transceiver may cause a change in the ANC performance. The frequency and phase responses were computed similarly to those in **section 3.1.3**. In **Fig**. 3.7 and **Fig.** 3.8, it appears that as the bitrate decreases, the amplitude of the response remains similar. Some high amplitude noises can be noted in **Fig.** 3.8. These are artefacts from the loss in transmission at some bitrate and sampling frequency.

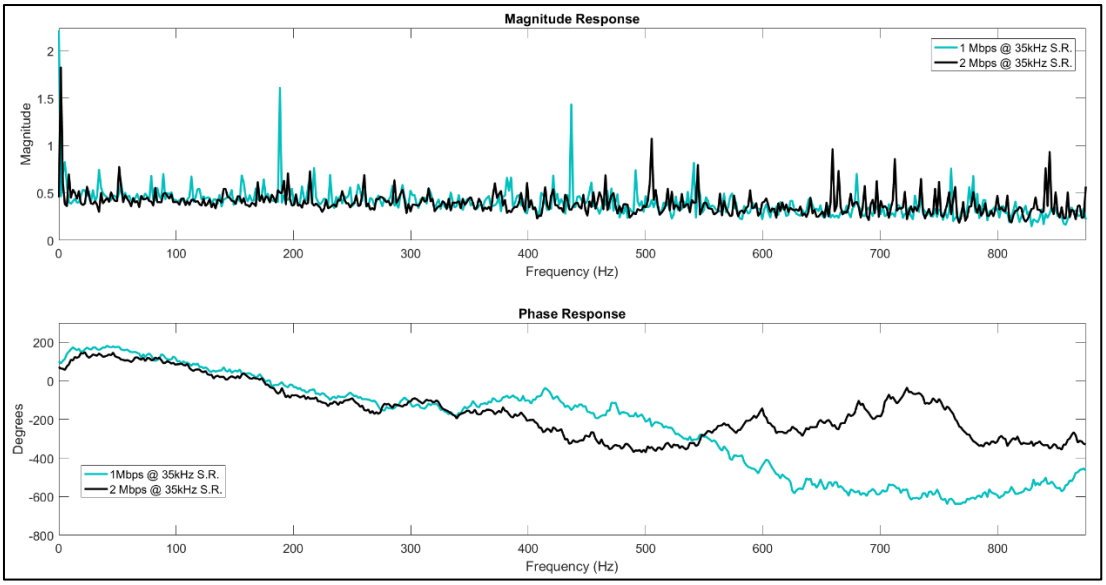

Fig. 3.7. Magnitude and phase response of transceivers obtained at different bit rates at 35 kHz S.R.

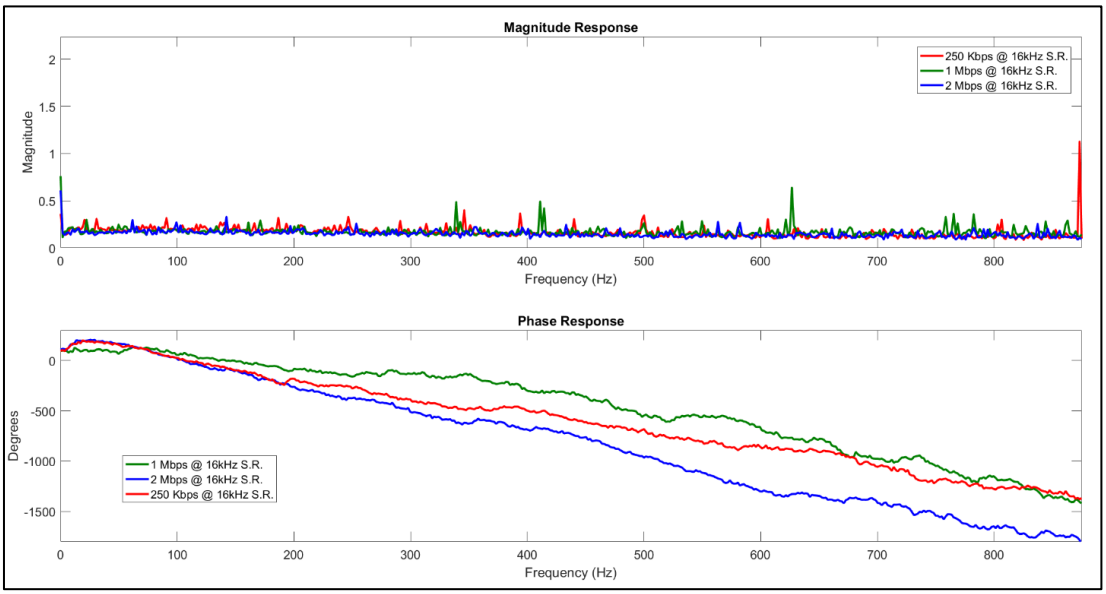

Fig. 3.8. Magnitude and phase response of transceivers obtained at different bit rates at 16 kHz S.R.

The impulse responses for each bitrate used were computed using the same method as in section **3.1.3**. The impulse responses were computed at two different audio sampling rates, which are **35kHz** and **16kHz**.

Fig. 3.9 shows the impulse responses for the three bitrates of **2Mbps**, **1Mbps,** and **250Kbps** used. The signals with a high sample rate (**35kHz**) have the same sample delay of about 7 samples. The signals with lower sample rate (**16kHz**) have around 15 sample delay except for the signal with **1Mbps** bitrate, which has 8 sample delay. It appears that the effect of the transceiver's bitrate is not significant in terms of delay compared to the audio sampling frequency. This is also true for the magnitude.

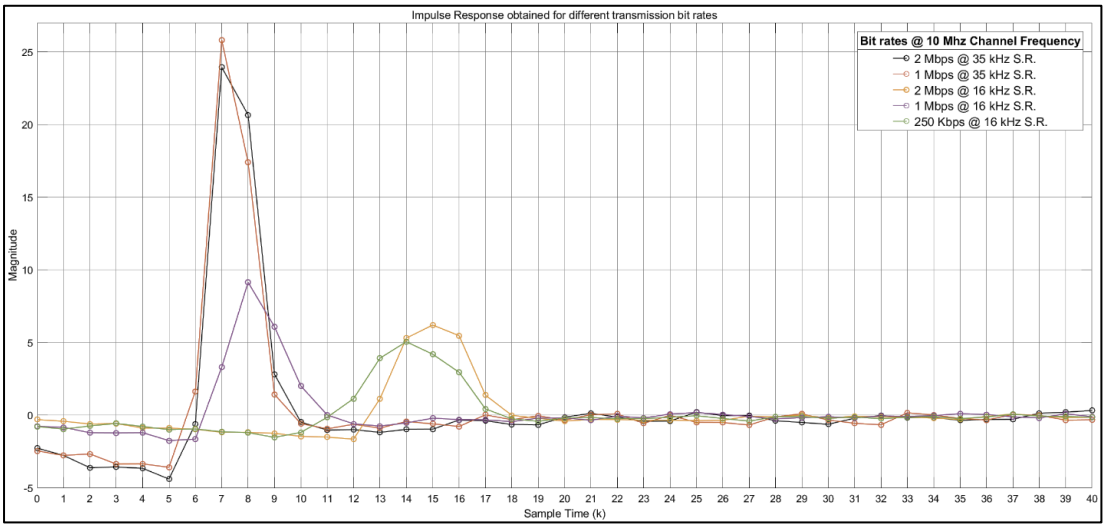

Fig. 3.9. Impulse Response of transceivers obtained at different bit rates.

Using the FIR coefficients obtained from the impulse response shown in **Fig.** 3.9, a single-channel wireless ANC simulation was performed for different bitrates. The results are shown in **Fig.** 3.10 for the **35 kHz** sample rate and **Fig.** 3.11 for the **16 kHz** sample rate.

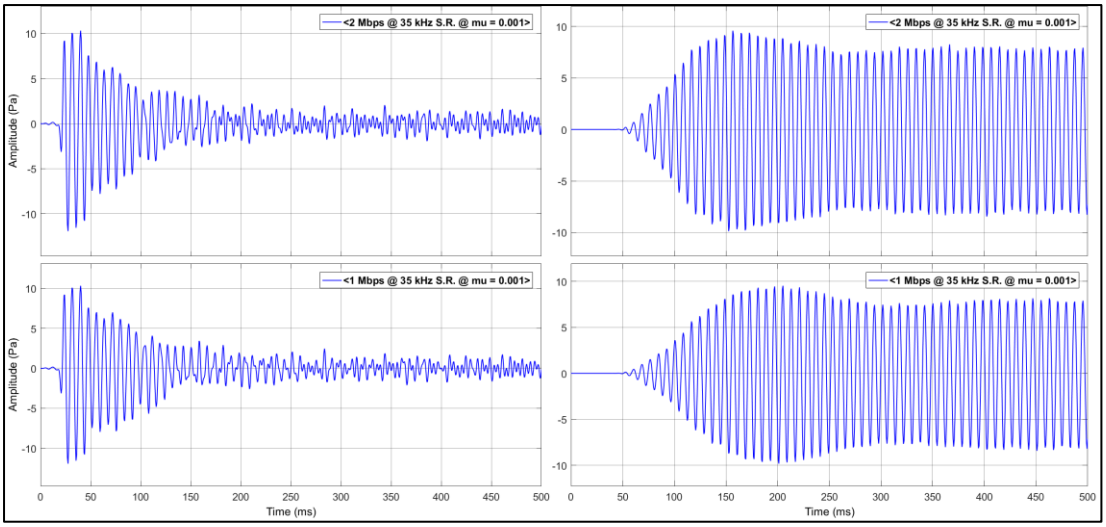

Fig. 3.10. Time-domain signals using the computed FIR weights @ 35kHz sampling rate.

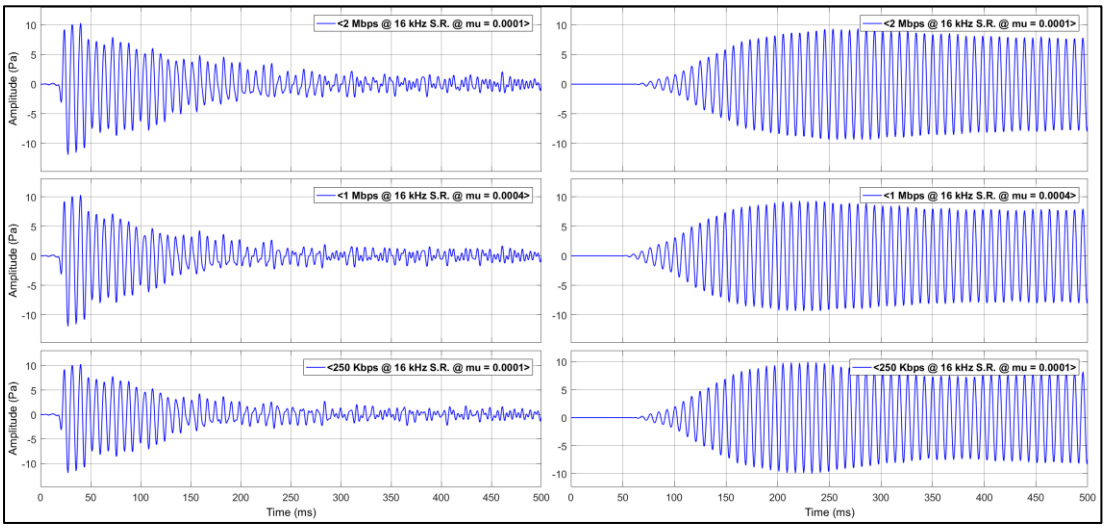

Fig. 3.11. Time-domain signals using the computed FIR weights @ 16kHz sampling rate.

It is noticed that the time-domain signals are not affected significantly by the change in the bitrates. The results show similar convergence. The delays are very similar, and hence the noise control results are similar too.

FFT analysis was done for different bitrates at two sampling frequencies. The results are plotted in **Fig.** 3.12.

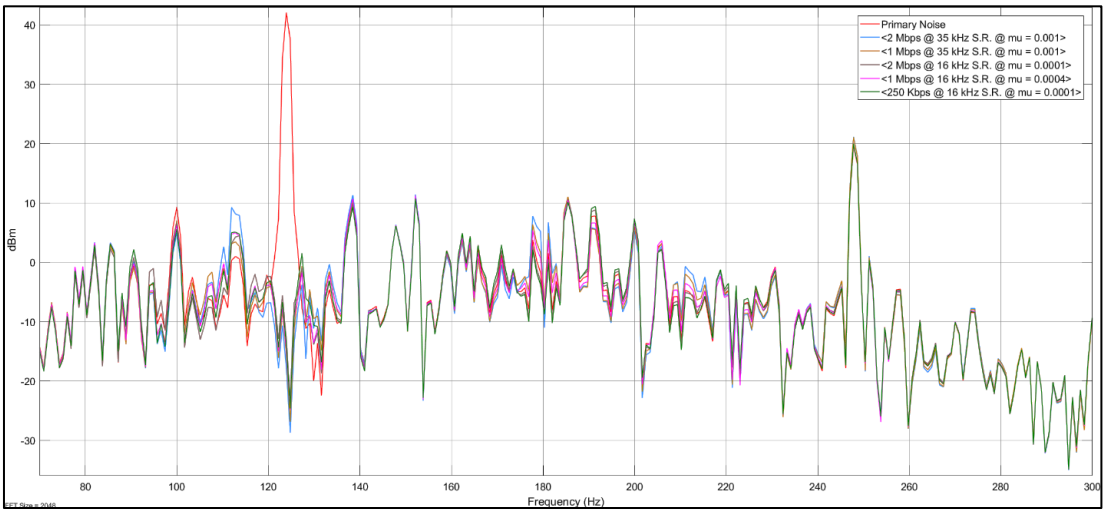

Fig. 3.12. FFT Analysis of the ANC Simulation obtained at the final sample.

The performance of each case is similar as far as noise reduction of the single-frequency noise is concerned. The average noise reduction is between **25 dB** and **28 dB**.

3.1.5 Impact of Channel Frequency on ANC Performance

The transceivers were tested using four different frequency channels (10, 20, 30 and 40Mhz). The frequency and phase responses are plotted in **Fig.** 3.13. For these cases, the magnitude response is similar for each case. These show slight dependence at frequencies about 500 Hz mainly. The lower frequency channel exhibits slightly more delay above 500 Hz. Some high magnitude noises are visible, as previously. These are artefacts from the loss in transmission at some sampling and channel frequency.

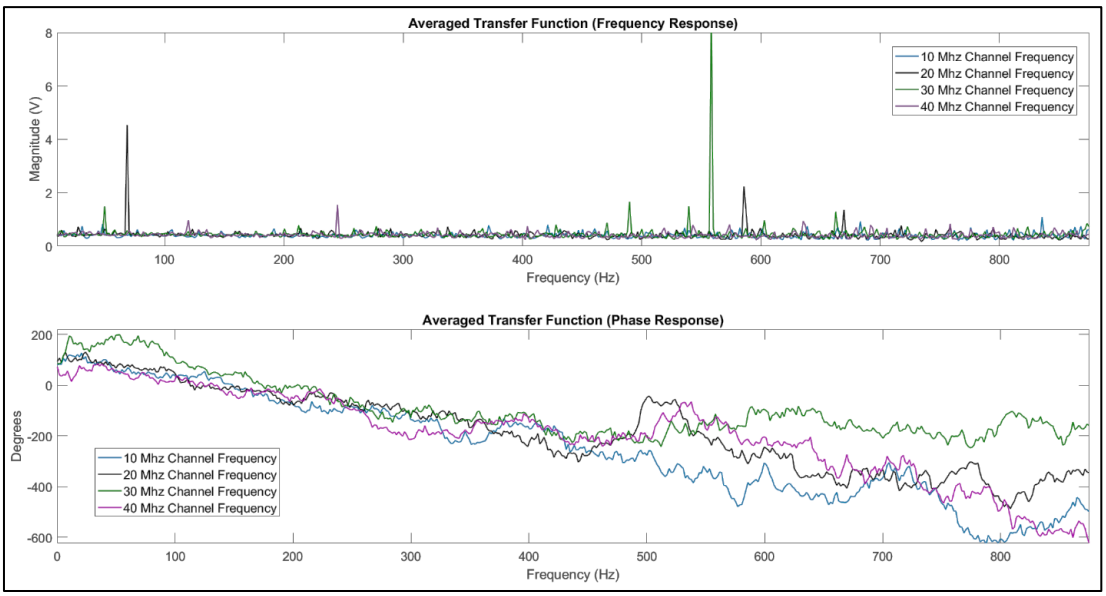

Fig. 3.13. Average Frequency and Phase Response of transceivers obtained at different channel frequencies.

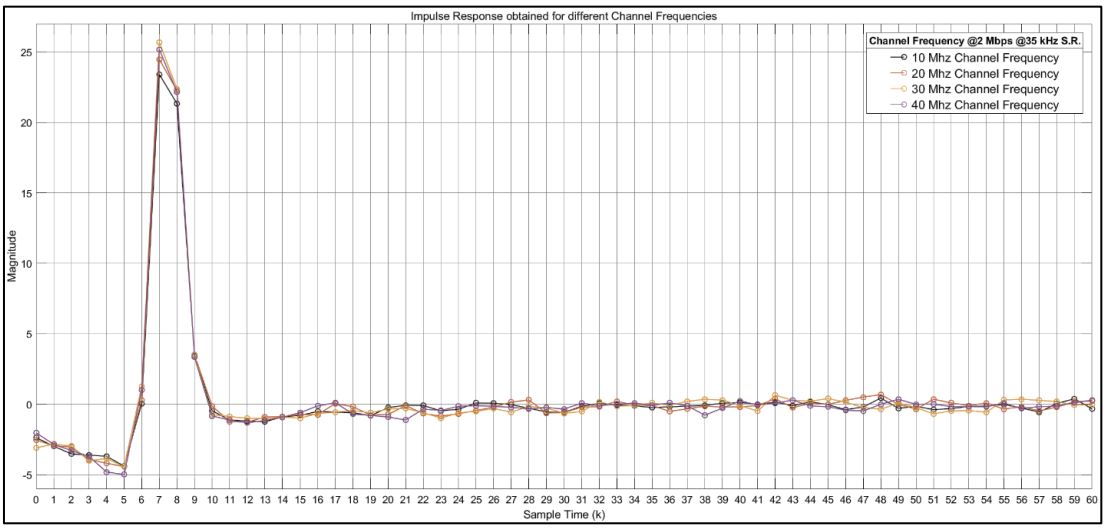

Fig. 3.14. Impulse Response of transceivers obtained at different channel frequencies.

The impulse responses were also computed for different channel frequencies. These did not show significant changes. Therefore, the ANC performance for these cases is expected to be similar without significant differences.

3.2 Effect of noise in the reference signal on wireless ANC performance

Integrating wireless transceivers with the reference signal used for the ANC may introduce noise to the generated signal. The coherence level between the reference and error signals may slightly drop based on the signal-to-noise ratio (SNR) of the noisy signal captured through wireless transmission. For that case, a separate simulation was performed to see the effect of a noisy reference signal on the ANC performance. **Fig. 3.15** shows the reference signal with different SNRs due to added Gaussian white noise (AWGN). A **60 dB, 20 dB, 10 dB** and **7.5 dB** SNRs were selected for this case. **60 dB** SNR refers to a clean or less noisy signal, and the **7.5 dB** SNR is the noisiest signal among them.

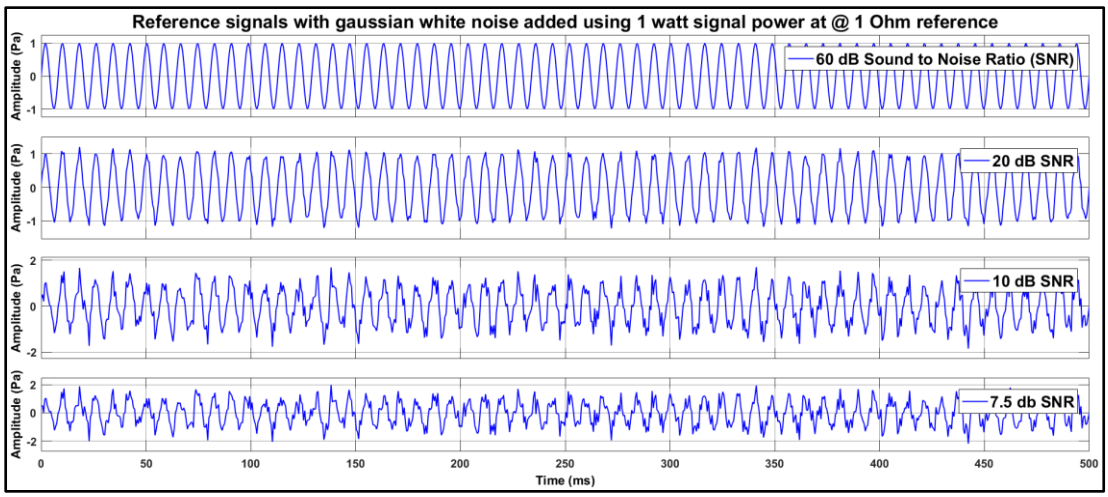

Fig. 3.15. Reference signal with AWGN giving different SNRs.

Fig. 3.16 shows time-domain simulation results for each SNR accounting for the white noise. With a clean reference signal, the ANC control performance is not affected much. The last two (error and control) time-domain signals show that the ANC performance is degraded for lower SNRs. That is, due to the added noise in the reference signal, which reduces the coherence level between the reference and error signals. Adjusting the SNR of the reference signal to less than **7.5 dB** causes a divergence in the control, due to the low coherence level and an increase in the reference signal power due to the added white noise.

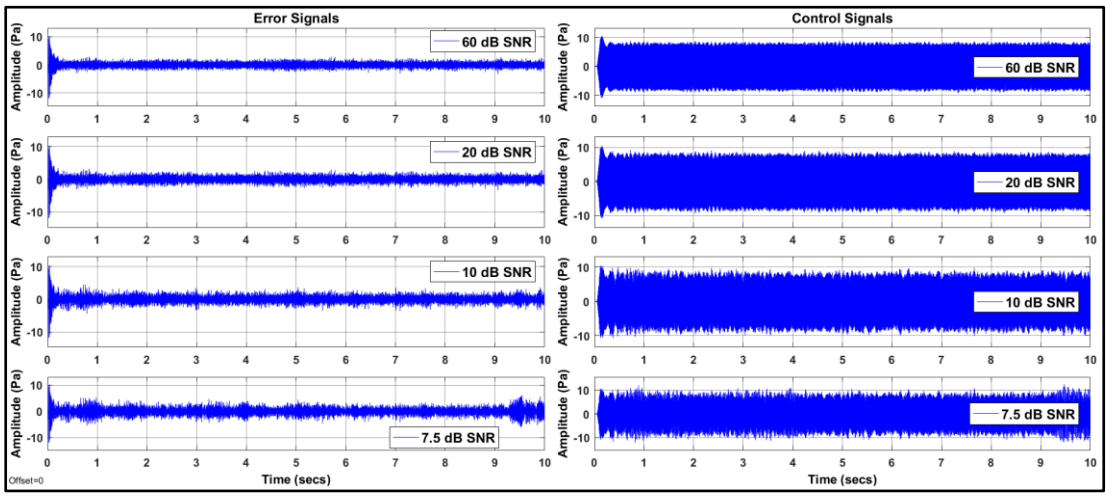

Fig. 3.16. Simulation Results at different SNRs.

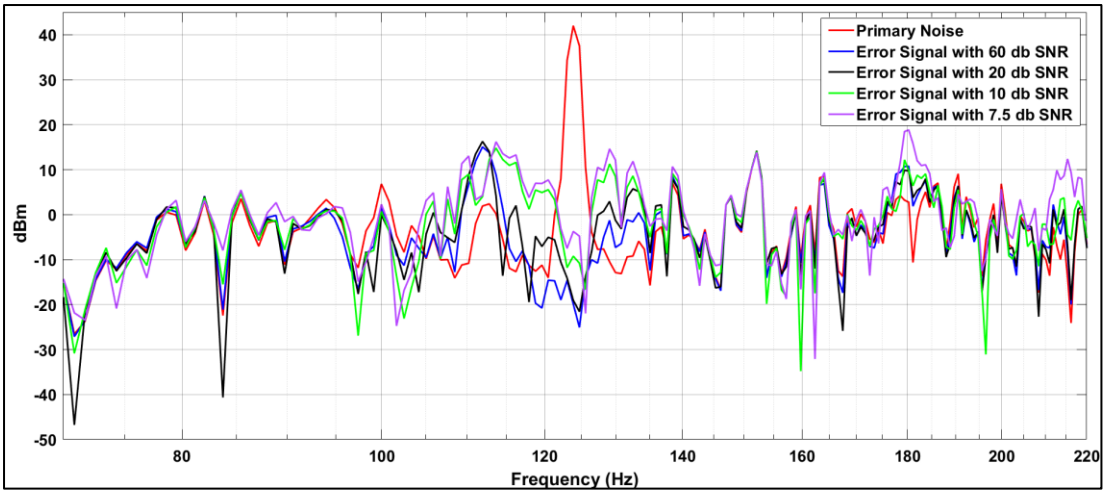

Fig. 3.17. ANC Performance simulations with varying noisy reference signals corresponding to different signal-to-noise ratios (SNR).

Fig. 3.17 shows the ANC Performance using frequency spectrum analysis for both uncontrolled and controlled noises and for each SNR. **70 dB** reduction is obtained with a reference signal that has **60 dB SNR**. The least reduction is about **45 dB**, where the reference signal has **7.5 dB SNR** (About **25 dB** less reduction). This is due to the coherence level between the reference and the error signal being reduced by the addition of white noise to the reference signal. The next chapter is the validation of the functionality of the NRF transceivers applied in an air duct using experiments for the developed wireless ANC systems.

Chapter 4: Validation of a Wireless ANC in an Air Duct

In this chapter, experiments have been carried out for different ANC setups. All experiments were run safely inside a laboratory environment. In order to verify the proper working of the wireless transceivers, a single-channel partially wireless ANC system for the control of tonal noise in a duct was used. The system was implemented with the reference signal connected to the DSP via a cable instead of a wireless connection. A schematic of the partially wireless setup **'W.W.1'** for this purpose is shown in **Fig.** 4.2. for the air duct test rig depicted in **Fig.** 4.1. Two loudspeakers are used as the primary noise and secondary noise sources. A Sony ECM-TL3 in-ear microphone, as shown in **Fig.** 4.5, is placed at the exit end of the air duct connected to a transmitter. A receiver outputs the error signal to the DSP, as shown in **Fig.** 4.3. A Tektronix function generator is used to drive a primary loudspeaker system with a low-frequency tonal noise inside the duct. The frequency generated was 124 Hz and corresponded to an acoustic resonance of the air duct. A Dewesoft Sirius multi-channel DAQ system captured the noise levels in real-time from the in-ear microphone and signals generated by the DSP, as shown in **Fig.** 4.4. These are used for postprocessing and aiding with the analysis of the ANC performance. The results of using the wireless transceivers are given in section **4.1**. The selection and setup of the ANC system components are located in **Appendix B**.

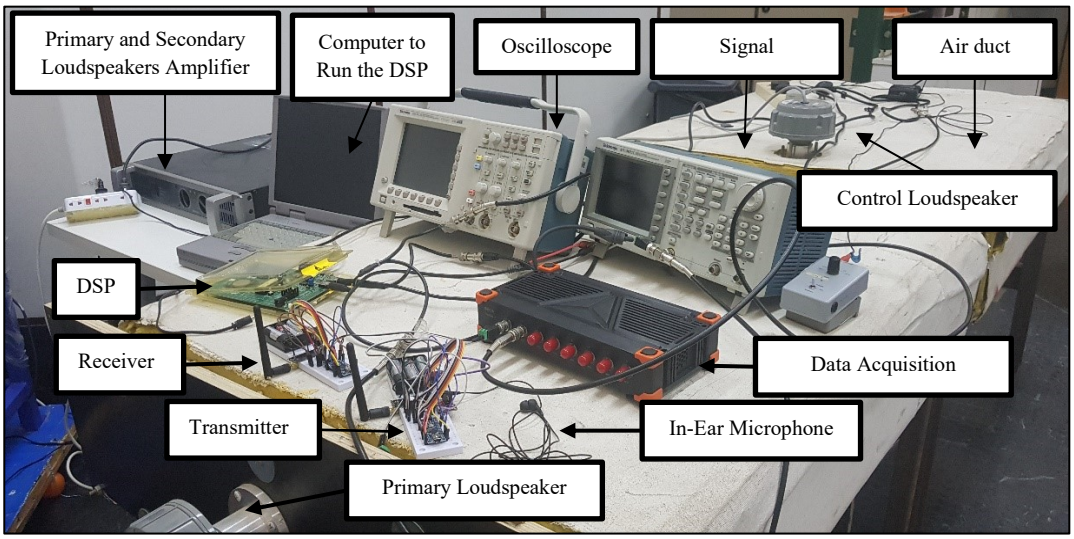

Fig. 4.1. Air duct ANC experiment testing showing all components.

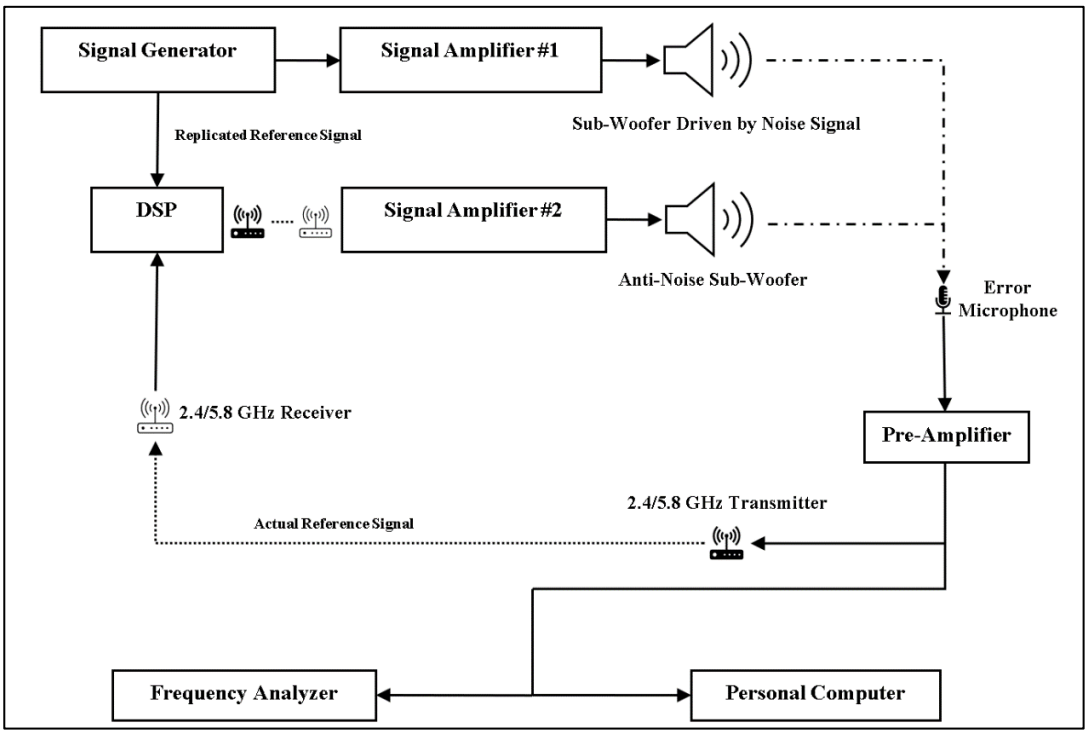

Fig. 4.2. Partially wireless setup W.W.1 single channel ANC (wired reference signal)

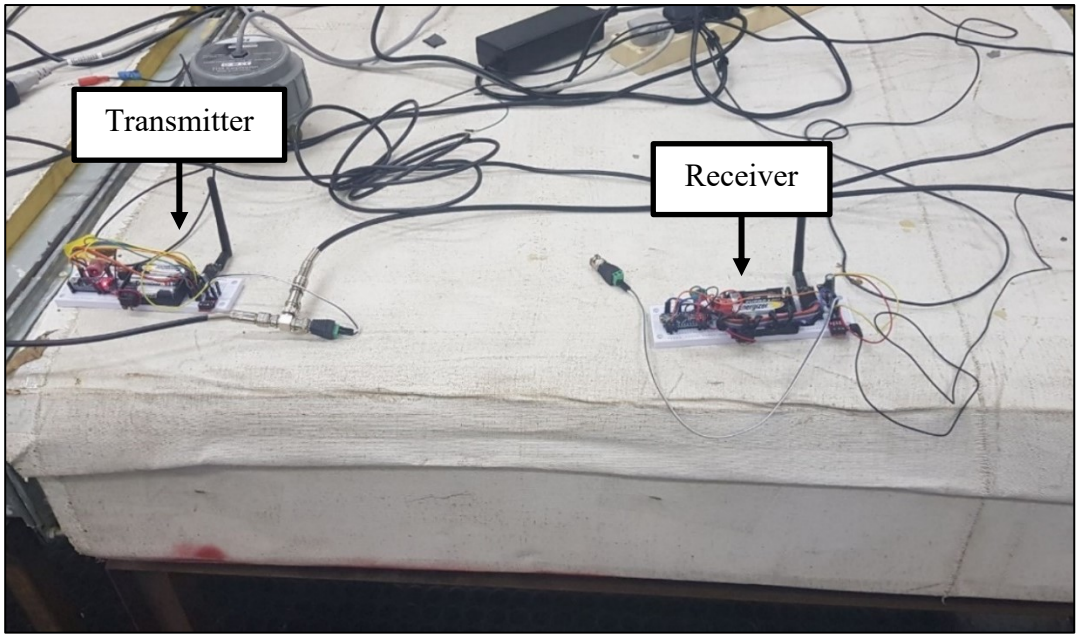

Fig. 4.3. Transmitter and Receiver placed on the Air-Duct Model.

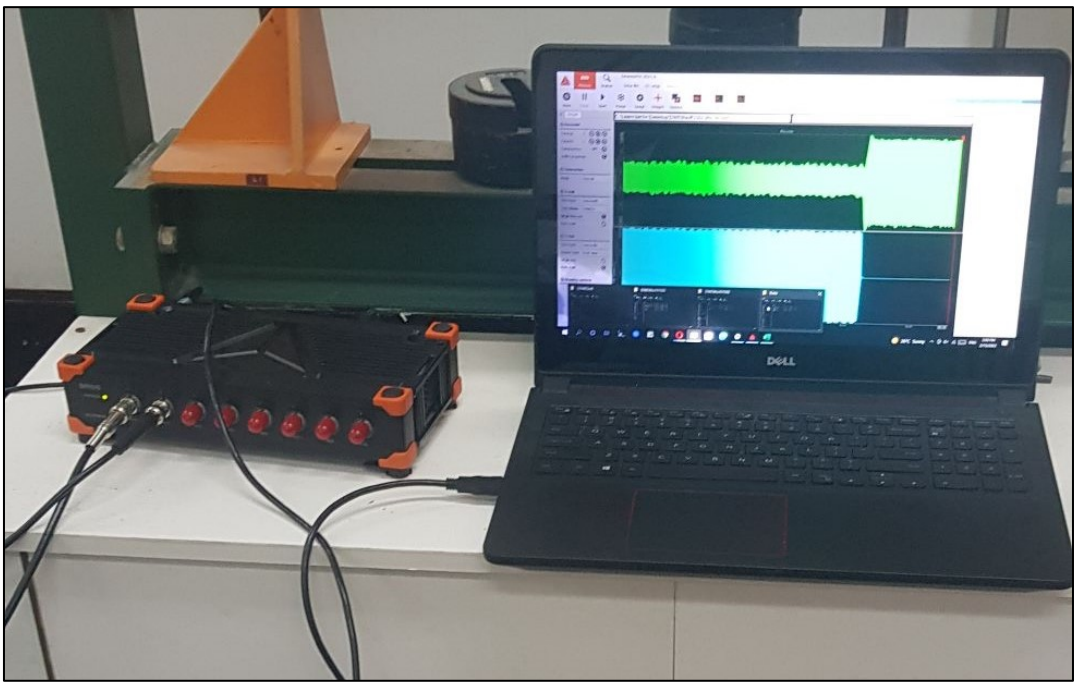

Fig. 4.4. DAQ Setup and recording in the lab using a laptop for postprocessing.

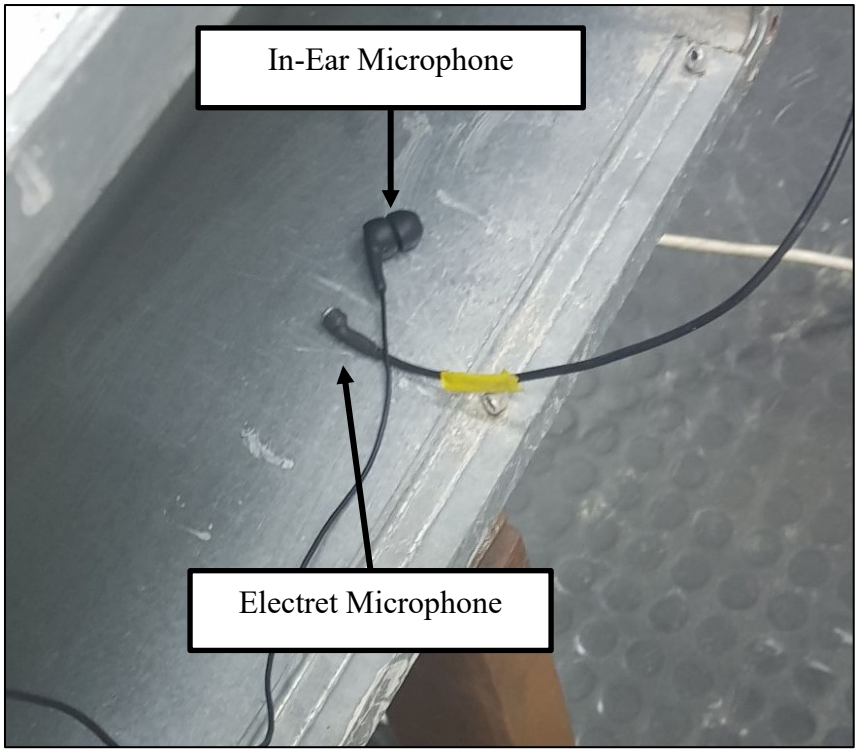

Fig. 4.5. In-Ear Microphone placed at the Duct Opening for validation experiment.

4.1 Results of Wireless ANC in Air Duct with Low-Frequency Noise Source

4.1.1 Setup 1.1.1 (Fully Wired ANC Setup).

The first experiment is for the wired ANC setup. The Fx-LMS algorithm with online system identification is employed as the control algorithm. A single-channel system implies a 1 error, 1 control and 1 reference ANC system designated as **setup 1.1.1**. The wired system was optimized using trial and error by adjusting the convergence coefficient μ. For example, the $\boldsymbol{\mu}$ is adjusted first until the system divergences and then reduced for fast convergence. This $\boldsymbol{\mu}$ is taken as the optimum value. **Fig.** 4.6 shows good convergence using coefficient μ=0.005. If the latter is increased to 0.02, the system stability is compromised. Increasing $\boldsymbol{\mu}$ to larger than 0.02 will cause the system to diverge.

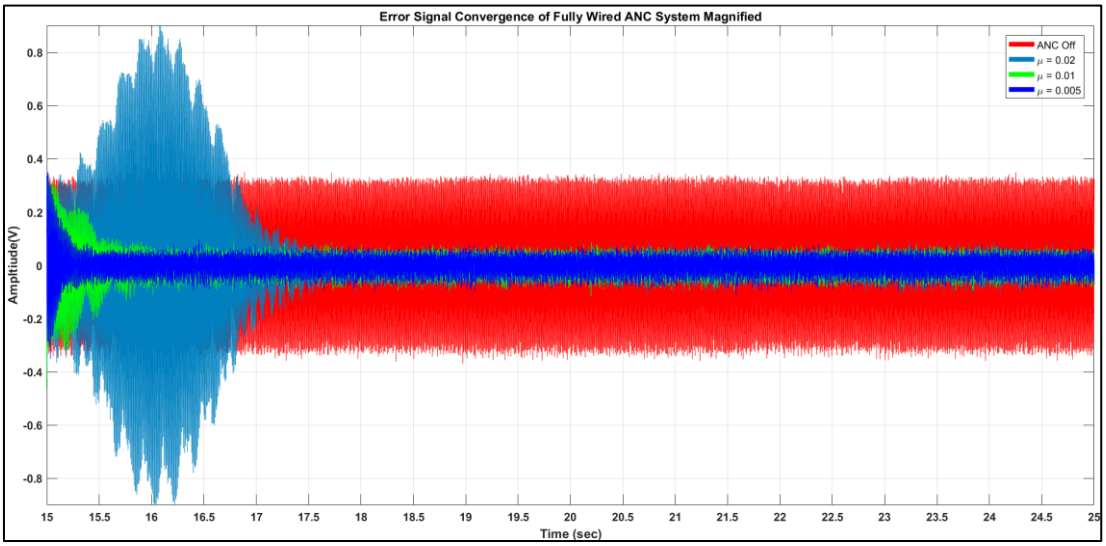

Fig. 4.6. Convergence plot for setup 1.1.1 (Air Duct Experiment) for uncontrolled and controlled cases for different $\boldsymbol{\mu}$.

It is clear that the controller convergence coefficient $\boldsymbol{\mu}$ needs to be appropriately

selected for smooth and fast convergence.

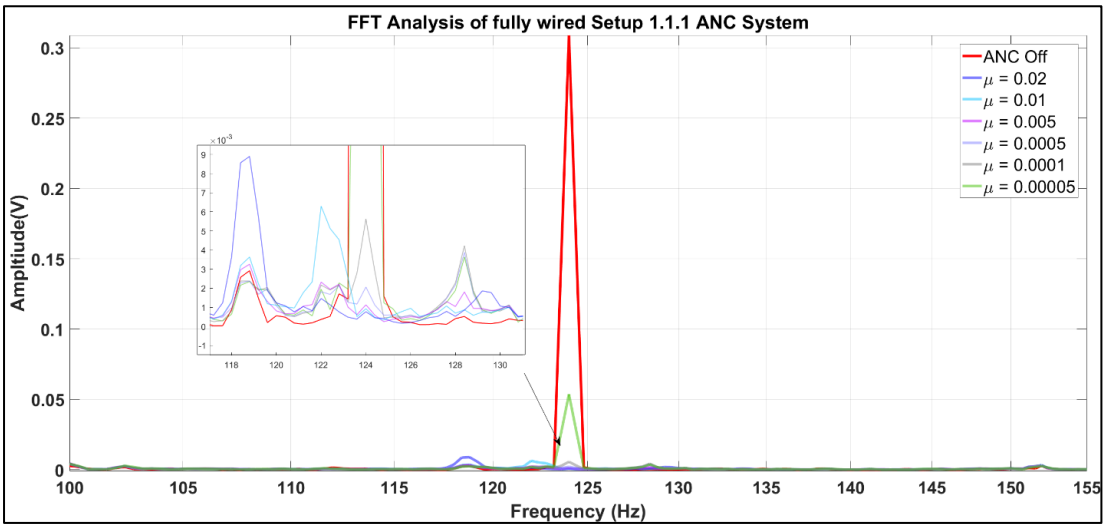

Fig. 4.7. FFT Analysis for Setup 1.1.1 (Air Duct Experiment) showing the importance of selecting appropriate $\boldsymbol{\mu}$.

As shown in **Fig.** 4.6, a step size of 0.005 has a fast and stable response for the fully wired setup. Also, it has good attenuation performance judging from the FFT analysis shown in **Fig.** 4.7

4.1.2 Setup W.1.1 (Wireless Error Signal ANC Setup, wired reference signal).

In the second configuration tested, the error signal picked by the microphone transmitted by wireless connection is designated as **setup W.1.1**. The ANC's step size was adjusted optimally, starting from a divergent step size. **Fig.** 4.8 shows the performance for various $\boldsymbol{\mu}$. Good convergence is obtained by using a step size $\boldsymbol{\mu}$ = 0.05 in this case. Having a higher step size than the optimal step size can introduce instability, on the other hand, whereas having a smaller step size will lead to a slower

response for a slightly smaller error.

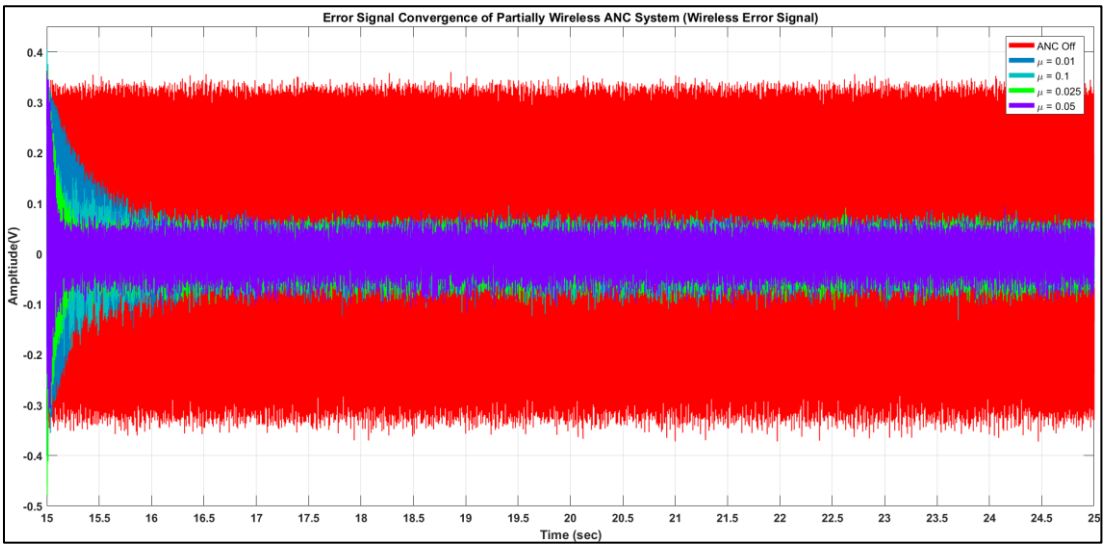

Fig. 4.8. Convergence plot for setup W.1.1 (Air Duct Experiment) for various $\boldsymbol{\mu}$

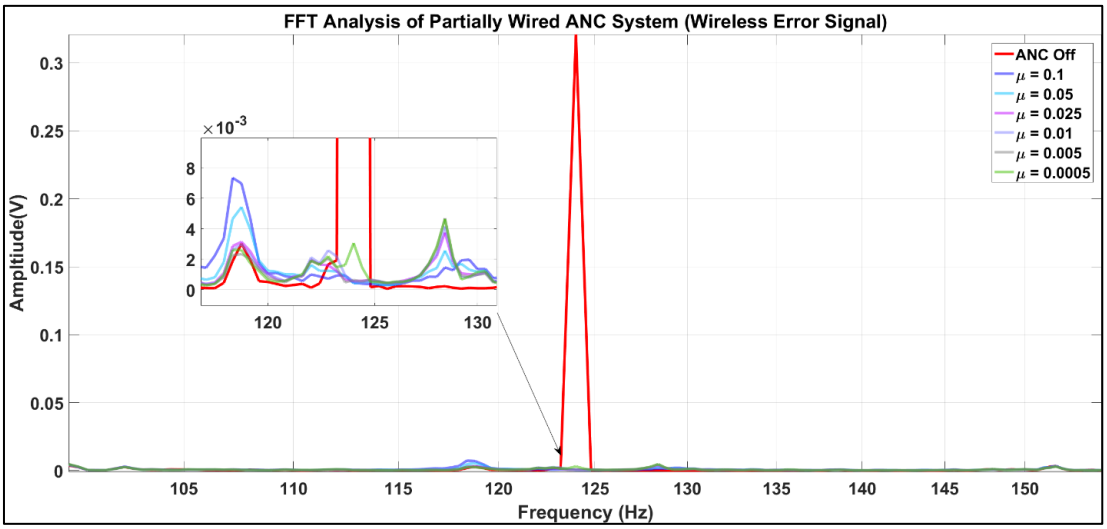

Fig. 4.9. FFT Analysis for Setup W.1.1 (Air Duct Experiment) for various values of $\boldsymbol{\mu}$

As shown in **Fig.** 4.8, a step size of 0.05 has a fast response and is stable for the wireless error signal setup. It also has good attenuation performance judging from the FFT analysis shown in **Fig.** 4.9.

4.1.3 Setup 1.W.1 (Wireless Control Signal ANC Setup, using wired error and wired reference).

The third configuration tested is similar to **section 4.1.2**, except that the control signal is only changed to wireless connection and designated as **setup 1.W.1**.

Fig. 4.10 shows the system's performance for various $\boldsymbol{\mu}$. It shows that good convergence is obtained by using an optimal step size μ = 0.1 in this case. The different $\boldsymbol{\mu}$ is due to the loss in gain in the wireless connection.

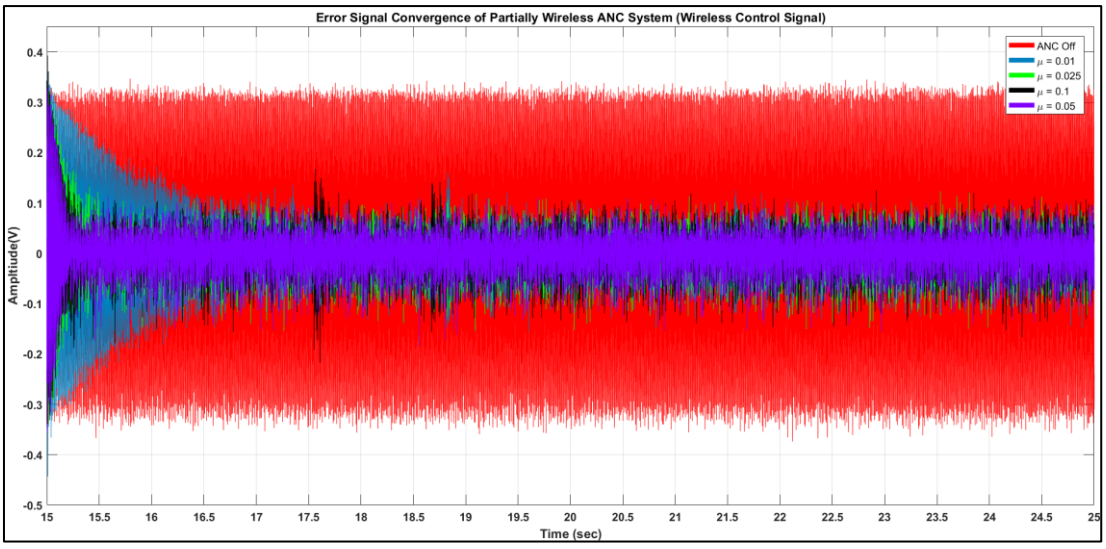

Fig. 4.10. Convergence plot for setup 1.W.1 (Air Duct Experiment) for various values of $\boldsymbol{\mu}$

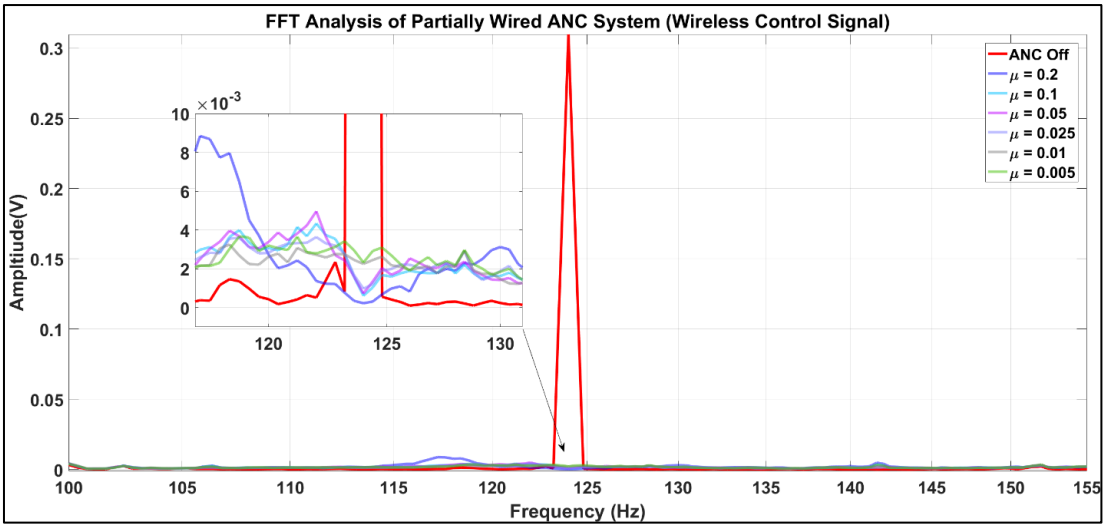

Fig. 4.11. FFT Analysis for Setup 1.W.1 (Air Duct Experiment) for various values of $\boldsymbol{\mu}$ showing importance of proper $\boldsymbol{\mu}$.

Fig. 4.10 shows that a step size of 0.1 has a fast and stable response for the wireless control signal setup. It also has a good attenuation performance judging from the FFT analysis shown in **Fig.** 4.11. Additional experiments show that the system diverges if the step size is larger than 0.2.

4.1.4 Setup W.W.1 (Partially Wireless ANC Setup, wired control channel).

The fourth configuration tested was the partially wireless ANC system of **setup W.W.1.** It is optimized for the best convergence rate, similar to previous cases. The convergence coefficient μ=0.2 gives the best performance for this case, as depicted in **Fig.** 4.12. It is noted that the value of μ does not necessarily need to be the same for the different systems due to the difference in voltage levels for each setup, especially when the wireless connection is added.

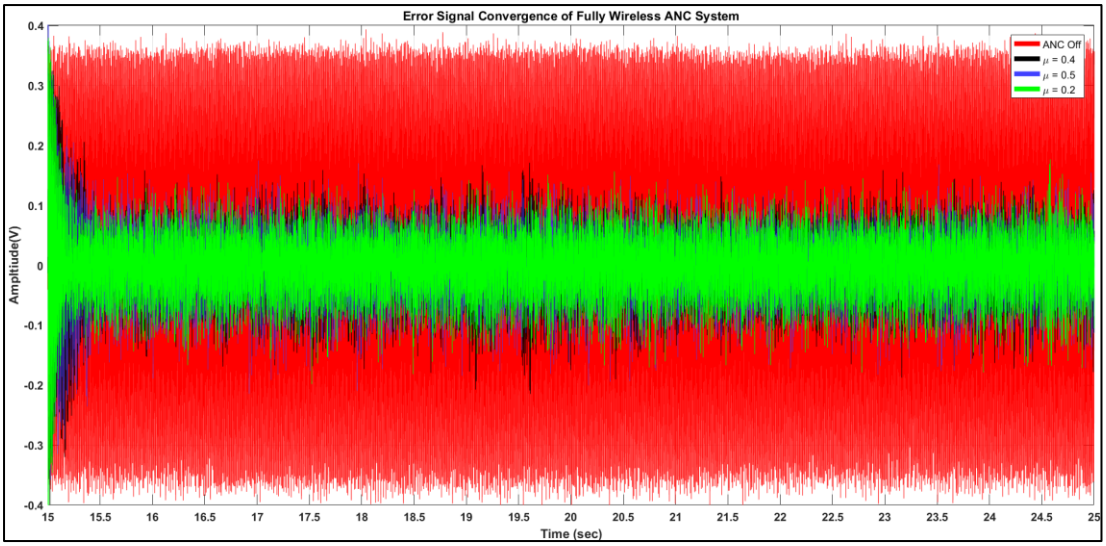

Fig. 4.12. Convergence plot for setup W.W.1 (Air Duct Experiment) for various values of $\boldsymbol{\mu}$

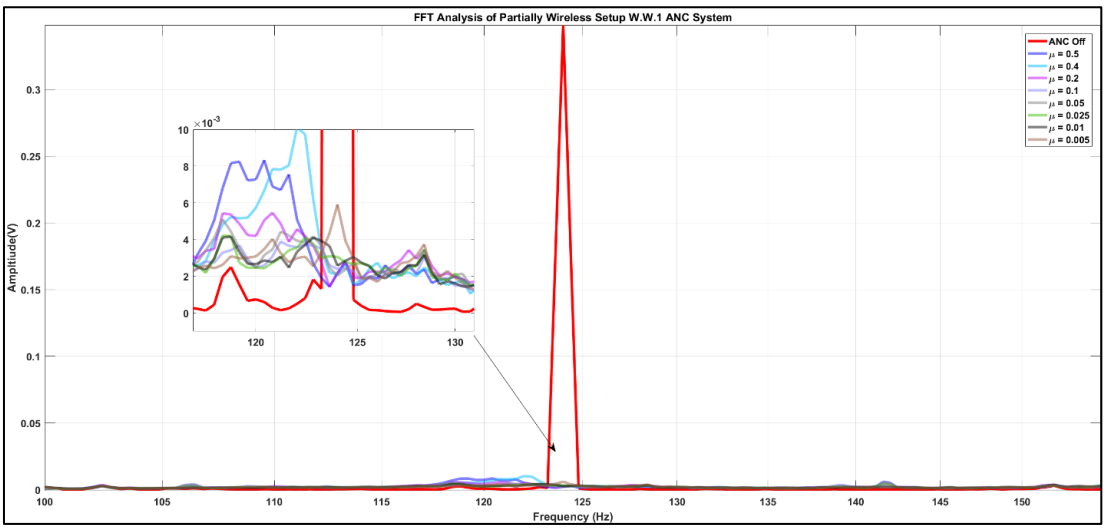

Fig. 4.13. FFT Analysis for Setup W.W.1 (Air Duct Experiment) for various values of $\boldsymbol{\mu}$

Fig. 4.12 shows that a step size of 0.2 has a fast response compared to step sizes of 0.5 and 0.4 and is considered stable for partially wireless configuration Setup **W.W.1**. It also has good performance judging by the FFT Analysis applied in **Fig.** 4.13.

4.1.5 Summary of results for each setup and value of optimal step-sizes

Table 4.1 shows the convergence time for each step size of the four setups.

Table 4.1. Convergence Time for each controller step-size **μ** (in seconds).

Setup ID		1.1.1	W.1.1	1.W.1	W.W.1
Controller Coefficients μ	0.6	Diverging	Diverging	Diverging	Unstable
	0.5	Diverging	Diverging	Diverging	2.5955
	0.4	Diverging	Diverging	Diverging	0.502
	0.2	Diverging	Diverging	(Unstable)	0.3178
	0.1	Diverging	1.2309	0.3540	1.0273
	0.05	Diverging	0.1497	0. 3855	0.9639
	0.025	Un-used	0.4076	0.6244	3.3894
	0.02	2.718	Un-used	Un-used	Un-used
	0.01	1.219	1.0265	4.2415	8.1066
	0.005	0.406	1.7512	4.0968	20.617
	0.001	Un-used	Un-used	Did not Record	Did not Converge

Setup ID		1.1.1	W.1.1	1.W.1	W.W.1
Controller Coefficients μ	0.0005	1.905	17.248	Did not Converge	Un-used
	0.0001	29.511	Did not Converge	Un-used	Un-used
	0.00005	55.191	Un-used	Un-used	Un-used

The error signal is assumed to have converged if the reduced signal level is greater or equal to 95% reduced of the original signal. This table allows the convergence factor to be selected for the fastest response under stable operating conditions. It also shows that the optimum value of $\boldsymbol{\mu}$ depends on the setup used and is not common to all.

Table 4.2. Noise reduction and response time for optimal step-sizes

Setup ID	1.1.1	W.1.1	1.W.1	W.W.1
Approximated tonal noise reduction (dB)	48.19	49.83	51.71	42.58
Approximated total acoustic noise reduction (dB)	12.87	14.26	11.18	11.80
Optimal Response time (ms)	406	150	354	318

The noise reduction performance for each setup is shown in **Table 4.2**. It is noted that the tonal noise reduction is larger than 42 **dB** for all cases and is significant and comparable to the wired case. The wireless configurations performed similarly very well. When both error and control signals were wireless, the attenuation was around

42 **dB**. The total acoustic noise reduction is the overall broadband noise reduction after control of the tone. The reduction is less than the tonal noise reduction because there are other significant frequencies over a wide band that is not attenuated, for example, due to online system identification running in the background. This is possible due to a slightly reduced signal-to-noise ratio of the wireless signals, which slightly decreases the coherence between the error signals and the reference signal. As a result, the noise reduction is slightly reduced.

4.1.6 Comparison between Fully Wired and Partially Wireless setup.

A comparison between the fully wired and partially wireless setups based on the best convergence rate for both setups was carried out. The comparison of the wired and wireless control results is illustrated in **Fig.** 4.14. The wireless ANC system performance is comparable to the wired system, and the slight difference is explained already. The result validates that the wireless system works well compared to the wired setup and can be used in other experiments. In particular, in the investigation of the in-ear wireless ANC system.

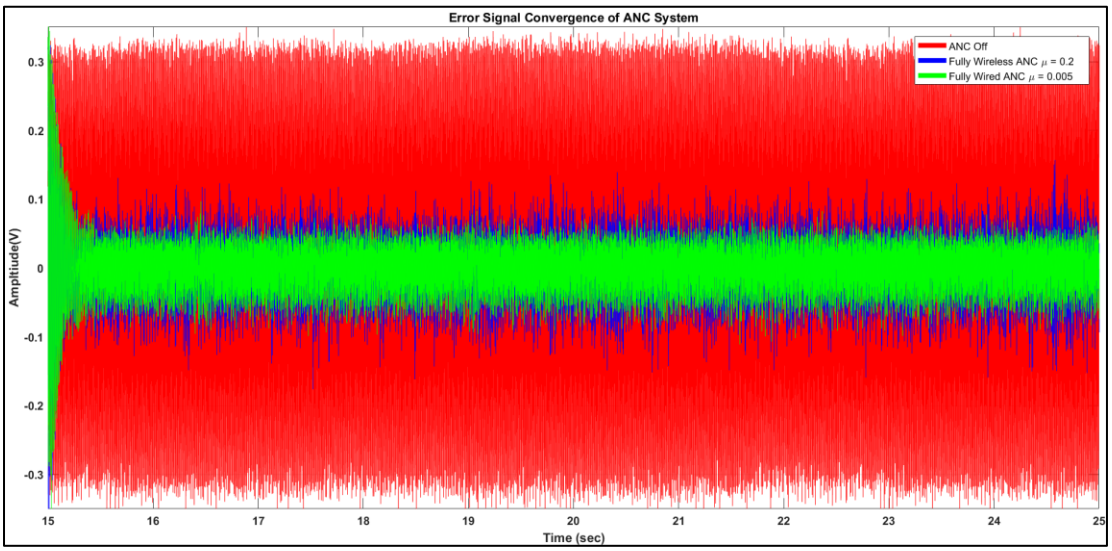

Fig. 4.14. Convergence plots comparing both setups (Air Duct Experiment) wired and partially wireless. This shows the two systems have comparable performance.

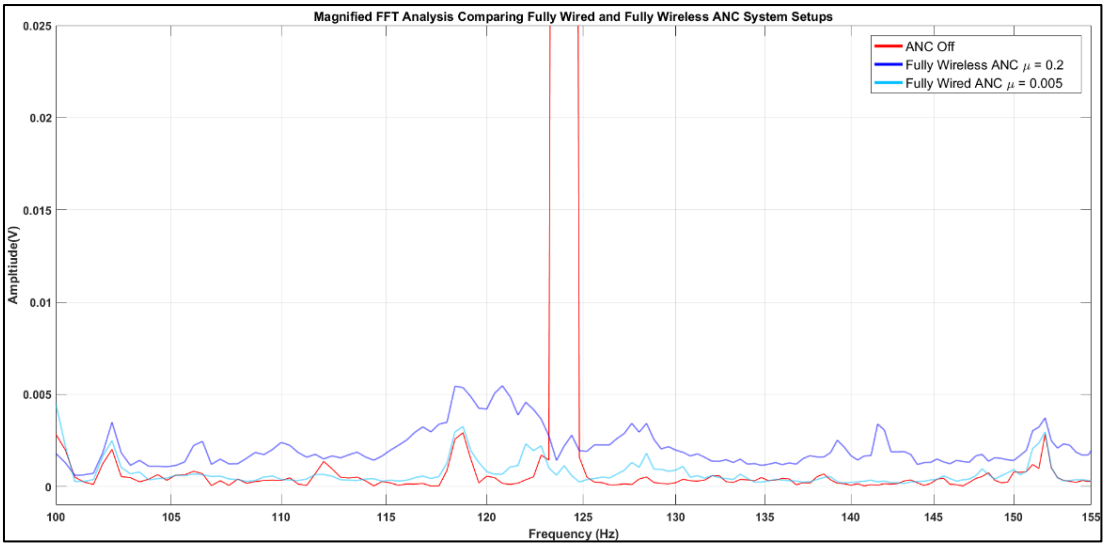

Fig. 4.15. Magnified FFT Analysis comparing both setups (Air Duct Experiment)

The result achieved for the partially wireless setup **(W.W.1)** is considered good compared to the fully wired setup, as shown in **Fig.** 4.15. The two systems have similar convergence behaviour. Note that the wireless setup does not have much impact on ANC performance. The wireless system exhibits slightly more noise than the wired system due to the transmission noise leading to reduced coherence and reduced performance due to the larger delay in the electroacoustic system. However, the noise reduction for the wireless system is still significant at around **42 dB** compared to about **48 dB** with the wired setup. In **Chapter 5**, the results of wireless ANC for the in-ear microphone in single and dual-channel configurations are presented for stationary and mobile cases.

Chapter 5: In-ear microphone experiments

The main purpose of this chapter is to demonstrate the feasibility and performance of the partially wireless ANC system applied to an in-ear microphone for use in an industrial environment. A single-error channel and a dual-error channel system for various setups are studied for stationary and mobile cases. Furthermore, the performance when stationary but with head rotation and when walking at a normal pace with the in-ear microphones are discussed in the mobile cases. For such cases, the experiments can be categorized as follows:

- Stationary in-ear ANC experiments. This corresponds to a scenario in which someone is sitting in an enclosed space such as an office and wearing the in-ear microphone.
- In-ear ANC with steady pace head rotation experiments. An example of this scenario is an individual that is stationary but is constantly changing head directions at a consistent pace.
- In-ear ANC with spatial mobility experiments. An example is if an individual such as a machine operator walks in an enclosed space such as a workshop with a microphone fitted.
- In-ear ANC speech experiments. The speech experiments are performed for all the previous cases mentioned above.

Experiments were carried out for each case discussed. The time-domain signals were recorded, and the corresponding Fast-Fourier Transform (FFT) analysis results show that the ANC system proposed can attenuate tonal noise well in most cases with proper

tuning of the system. Hence, these results show the practical ability of wireless in-ear microphones. **Section 5.8** summarizes and discusses the in-ear ANC results. These results are tabulated in **Appendix D**.

5.1 Design of experiments for wireless in-ear ANC System

5.1.1 Stationary experiments

The first experiment is about using wireless ANC with loudspeakers separated apart, using a single microphone worn by a stationary user. This is depicted in **Fig.** 5.1.

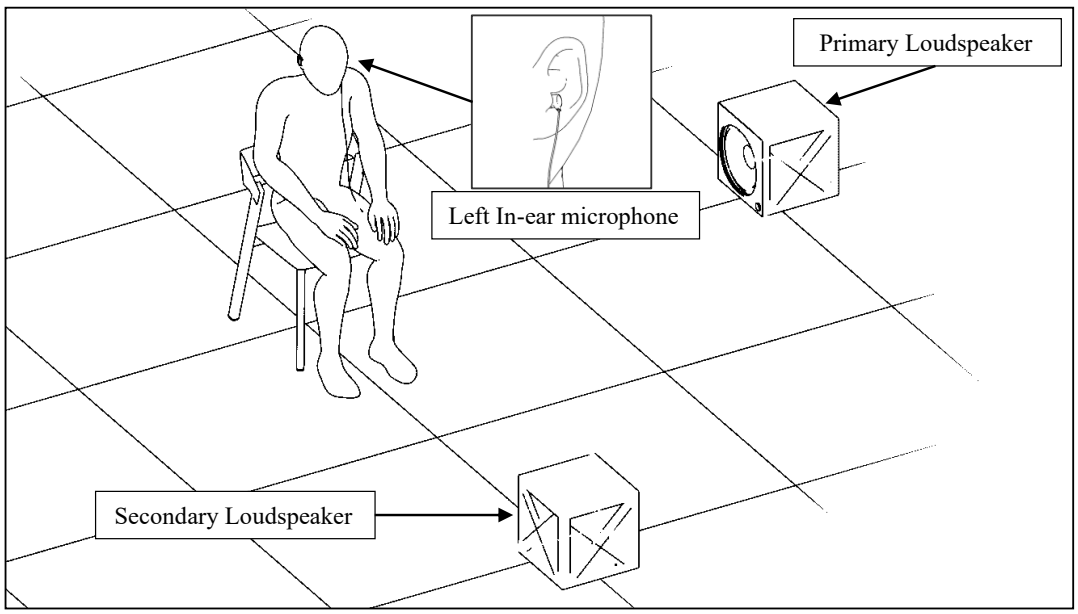

Fig. 5.1. Local noise control - Single Channel In-ear ANC

A similar experiment was carried out by adding an additional microphone to the other ear, which implies a wireless dual-channel ANC with a single control loudspeaker. This is shown in **Fig.** 5.2

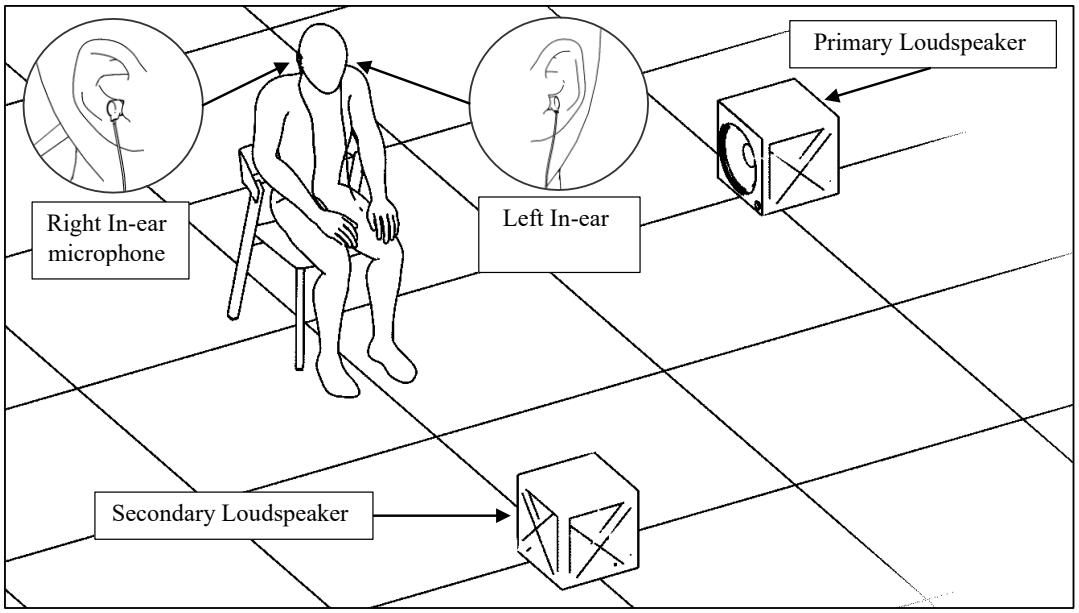

Fig. 5.2. Dual-channel In-ear ANC with loudspeakers separated apart.

For the study of secondary loudspeaker placement location, and to try and achieve global noise reduction, the control loudspeaker was placed nearby the primary noise. This case is depicted in **Fig.** 5.3. The performance was investigated for several cases.

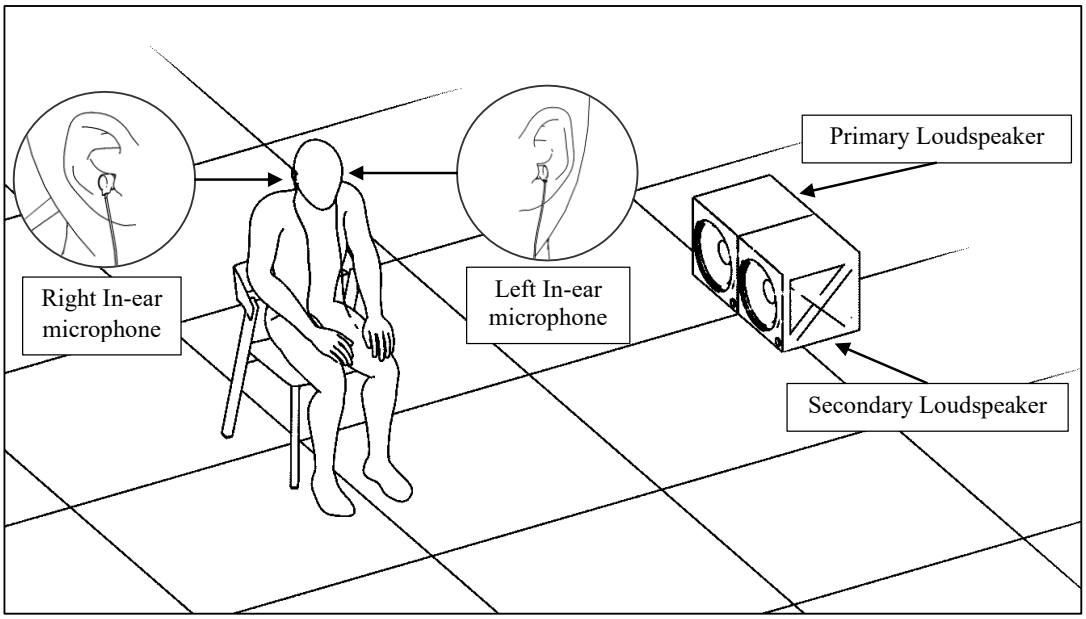

Fig. 5.3. Closely spaced loudspeakers - In-ear Dual Channel ANC

5.1.2 Steady pace head rotation experiment

The case where a user is wearing the in-ear microphone and is rotating the head at a steady pace was investigated for different cases. **Fig.** 5.4 shows a schematic of the experiment for this purpose.

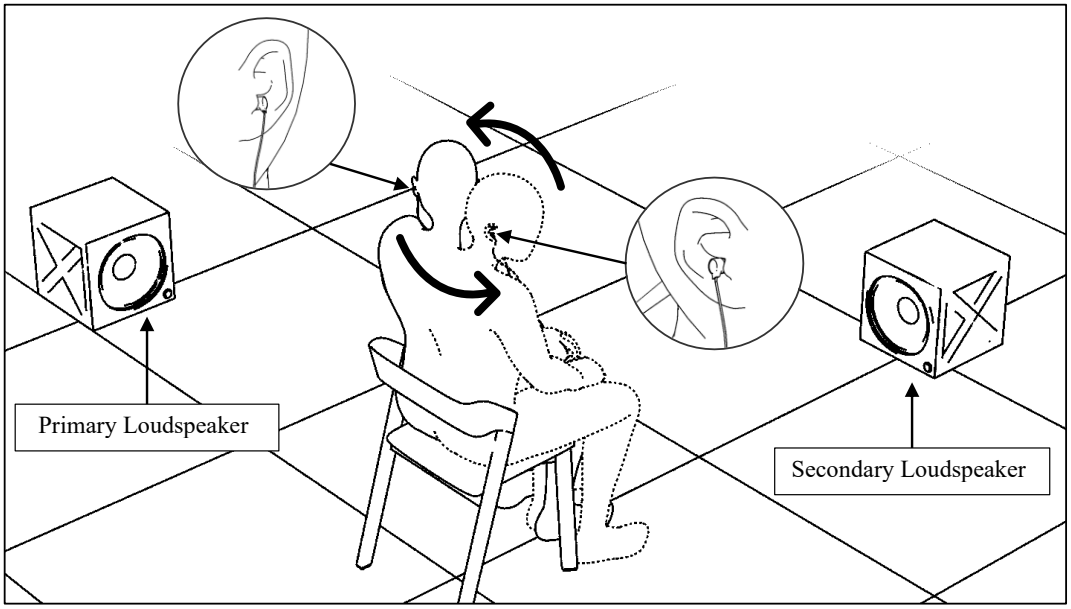

Fig. 5.4. Sketch of head rotation in-ear ANC Experiment

5.1.3 Walking experiment

The case where a user is walking in an enclosed space is also investigated for different cases. **Fig.** 5.5 shows the schematic illustrating this experimental setup.

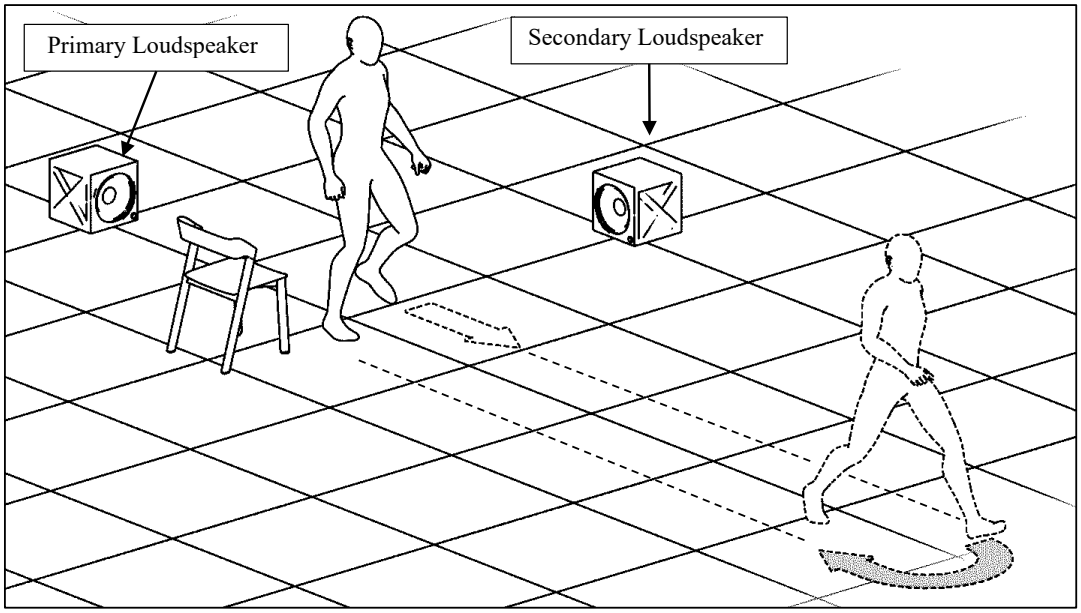

Fig. 5.5. Sketch of spatial mobility of in-ear ANC Experiment

5.2 Stationary in-ear ANC experiments

5.2.1 Local Noise Control

In the first experiment, an in-ear microphone is placed on a stationary chair with an elevation of **72 cm** from the ground, representing a person sitting on a chair. The primary and secondary loudspeakers were placed 1.5m away from the chair, with each loudspeaker directed 90 degrees apart from the chair, as shown in the single-channel setup in **Fig.** 5.6 and the dual-channel setup shown in **Fig.** 5.7.

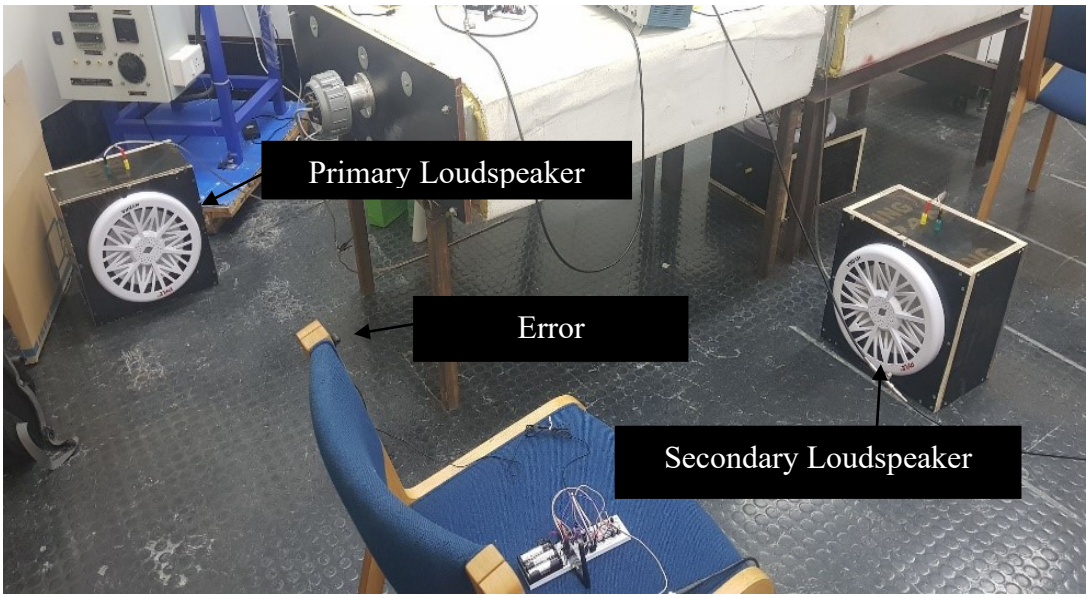

Fig. 5.6. Single channel in-ear microphone experiment setup for stationary case.

The dual-error channel setups **2W.1.1** and **2W.W.1** have the same setup with two wireless in-ear microphones and a wired reference signal in the former, while the latter uses wireless control signal.

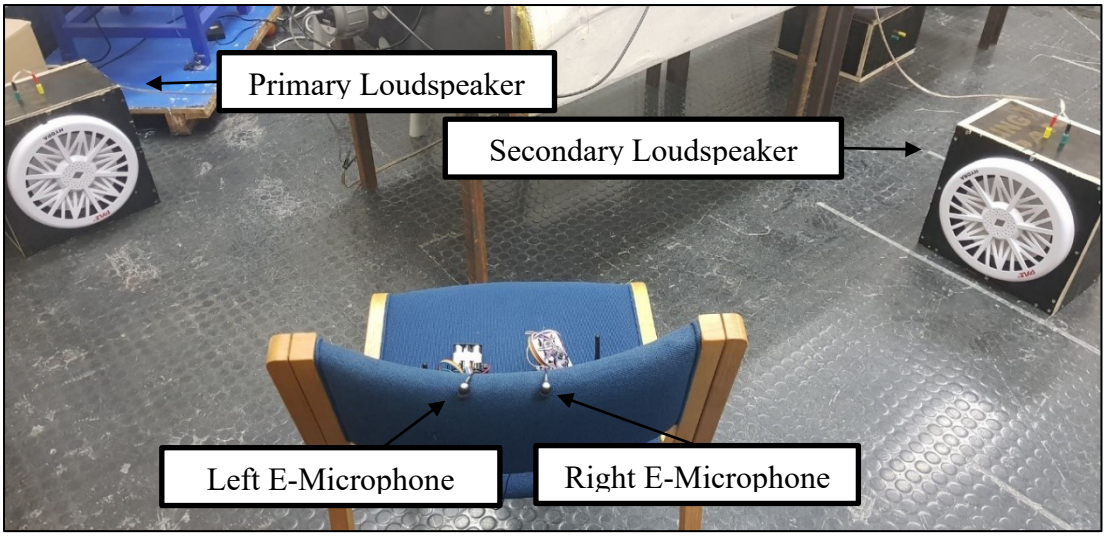

Fig. 5.7. In-ear microphone experiment setup with two error microphones and one secondary loudspeaker.

In the experiments, the control system is run for about one minute after system identification using an input pseudo-random binary sequence **(prbs)** that is carried out for 15 seconds. After system identification, the ANC system starts to control the external noise for one minute duration for data collection purposes. Optimizing of the convergence coefficients has been conducted by trial and error in the experiments. For example, a $\boldsymbol{\mu}$ that leads to instability is first found and then reduced by half to reach an allowable optimal value. This is done **for each experiment** of the ANC setups. The time-domain signals for the **microphone signal** are shown in **green,** and the time-domain signals for the **control signal** are shown in **light blue**, mostly for the single-channel experiments. For the stationary case, the noise control results are provided in the form of time-domain signals without and with the online system identification experiments. The results are discussed in the following sub-sections.

5.2.1.1 Setup W.1.1 (wireless error microphone) using offline system identification

For **setup W.1.1**, where the error microphone signal is transmitted wirelessly, offline secondary path system identification was first carried out for 15 seconds. The time-domain signal before and during the control session is included in **Fig.** 5.8 for $\boldsymbol{\mu}$ = 0.05. The tonal attenuation was measured as **42 dB**, that was obtained from FFT analysis after steady state was reached. The overall attenuation of around **23 dB**, which was the RMS value of the attenuated signal.

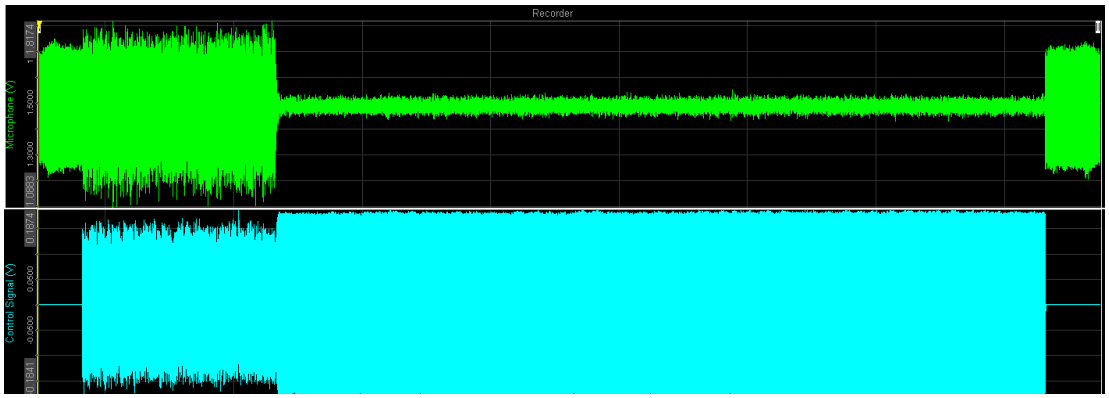

Fig. 5.8. Offline Stationary Experimental ANC, for $\boldsymbol{\mu}$ = 0.05. The green plot shows the error signal and the blue plot the control signal.

5.2.1.2 Setup W.1.1 (wireless error microphone) using online system identification

The effect of having online system identification on noise reduction performance is also studied and discussed for each type of experiment. Here, online system identification refers to the case when background system identification is run

continuously in the background after 15 seconds. This is necessary in cases where the secondary path changes significantly during control. To do this, the **prbs** signal level is reduced to a low level. However, the convergence factor for system identification must be increased proportionally. **Fig.** 5.9 shows that there is no significant difference when compared to the offline system identification experiment. The reason for the slightly less attenuation is because of the background noise emitted by the control loudspeaker and required for the online background system identification. The tonal attenuation for this case is **37 dB,** and the overall attenuation is around **22 dB**. Since both experiments were for a stationary error microphone, the difference between online and offline system identification results are similar. That is, there is no necessity for an online system ID since the secondary path does not change in real time.

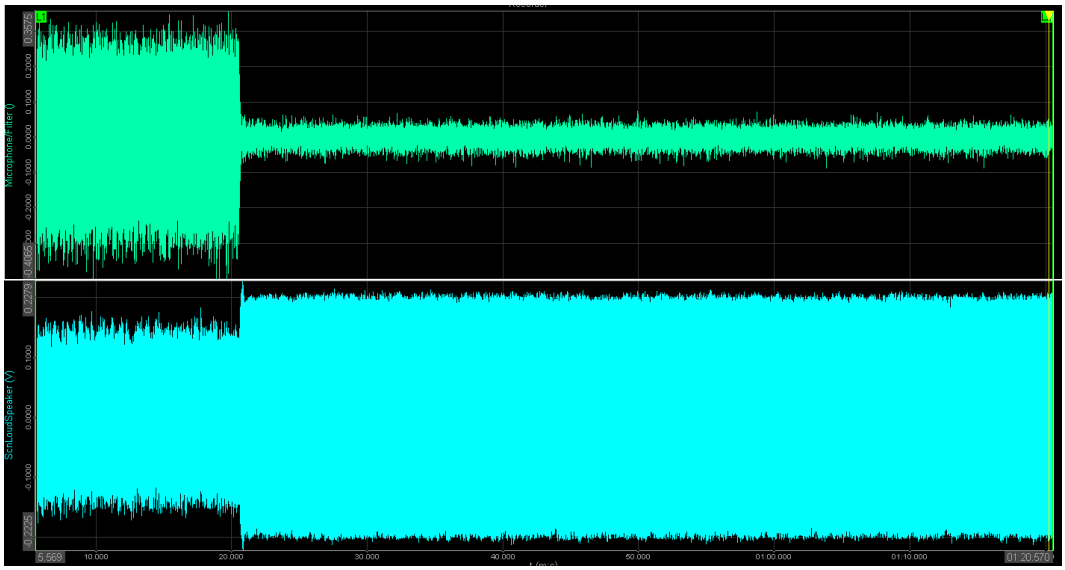

Fig. 5.9. Online Stationary Experimental ANC, for $\boldsymbol{\mu}$ = 0.05.

5.2.1.3 Setup W.W.1 (wireless error, wireless control) using offline system identification

Since this is also a stationary experiment, only offline system identification was used for **setup W.W.1**. The time-domain signal for the error microphone is shown in **Fig.** 5.10. The control signal was not captured in the experiment. The tonal attenuation was obtained as **38 dB**, and the overall attenuation of around **18 dB** was calculated.

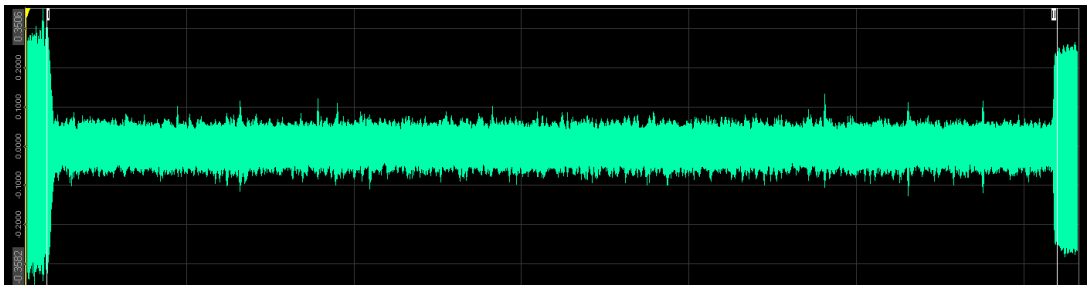

Fig. 5.10. Offline Stationary Experimental ANC, μ = 0.1. This plot shows the error microphone signal before and during control.

5.2.1.4 Setup 2W.1.1 (2 wireless errors, wired control and reference) using online system identification for the stationary case.

The effect of having online system identification on the noise reduction performance is only studied for the two partially wireless setups, **2W.1.1** and **2W.W.1**. The results are depicted in **Fig.** 5.11 and **Fig.** 5.12. When the online system identification is used, the plot for the left ear channel has more attenuation compared to the right ear channel. This is probably due to the left ear microphone being closer to the primary noise during the experiment was running. It can be deduced that the algorithm favours the control of the channel, which has higher tonal noise. It was noticed that the control

did not fully settle to a steady state for both channels because the algorithm is continuously biased to simultaneously control the two error channels using one control channel. Moreover, the difference in secondary path impulse response between the left and right ears will cause the error signals to be controlled at different rates and levels.

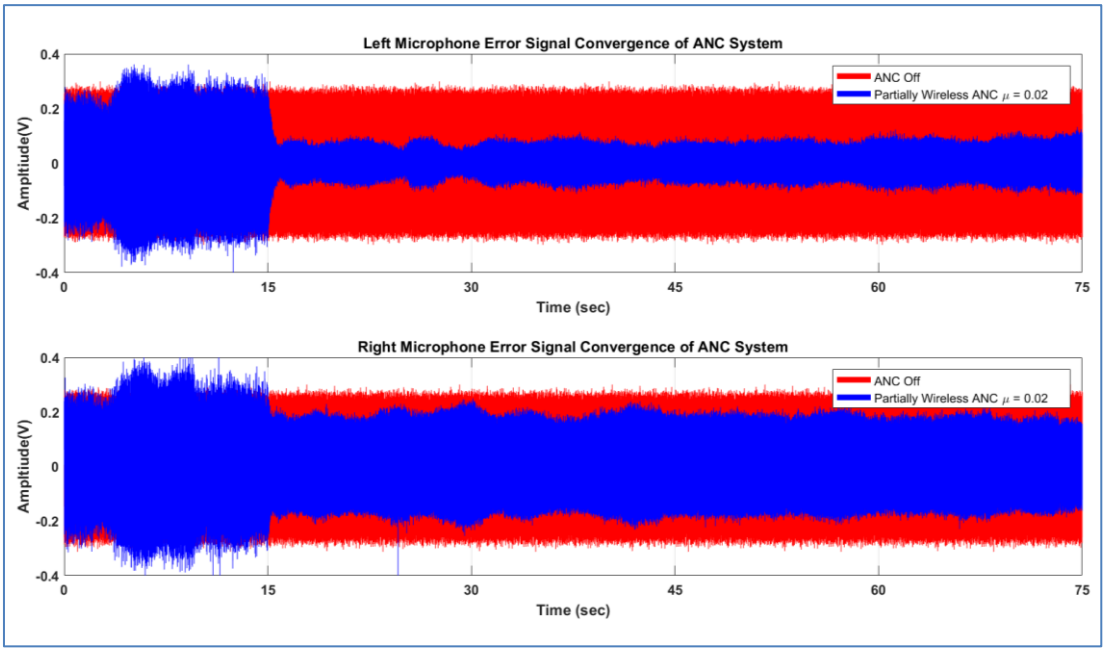

Fig. 5.11. Online Stationary Experimental ANC, μ = 0.02 with 2 wireless error microphones

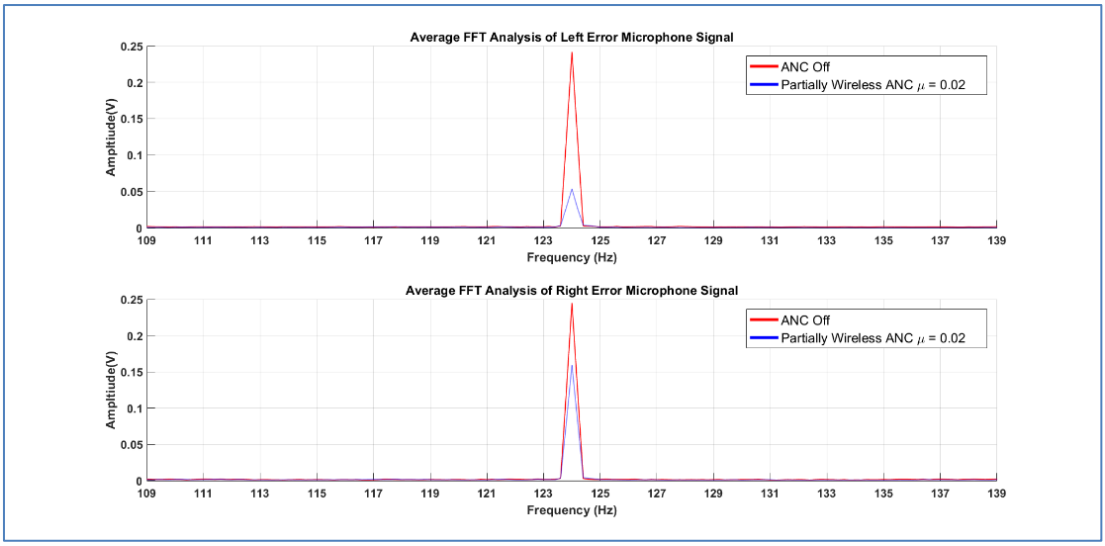

Fig. 5.12. FFT Analysis of Online Stationary Experimental ANC, μ = 0.02 for left and right signals.

Fig. 5.12 shows the average FFT analysis after 5 seconds of convergence. It is clear that the attenuation in the left ear channel is higher than in the right ear for the control of a 124 Hz tonal noise. For both ears, the average tonal attenuation is **8 dB**, and the average total attenuation is around **10 dB**. The individual tonal noise reductions are **13 dB** for the left ear and **3 dB** for the right ear. Despite the differences in each ear, it is clear that ANC using two wireless error microphones can be achieved.

5.2.1.5 Setup 2W.W.1 (two wireless error and one wireless control) using online system identification

When the system is configured as setup **2W.W.1**, the results are similar to the partially wireless experiment setup **2W.1.1**, as shown in **Fig.** 5.13. This is as expected for the same reason that was explained previously. It is noted that the left error channel is attenuated better than the right error channel. For both ears, the average tonal

attenuation is **9 dB,** and the average total attenuation is around **10 dB**. The individual tonal noise reductions are **12 dB** for the left ear and **5 dB** for the right ear. The FFT analysis is shown in **Fig.** 5.14.

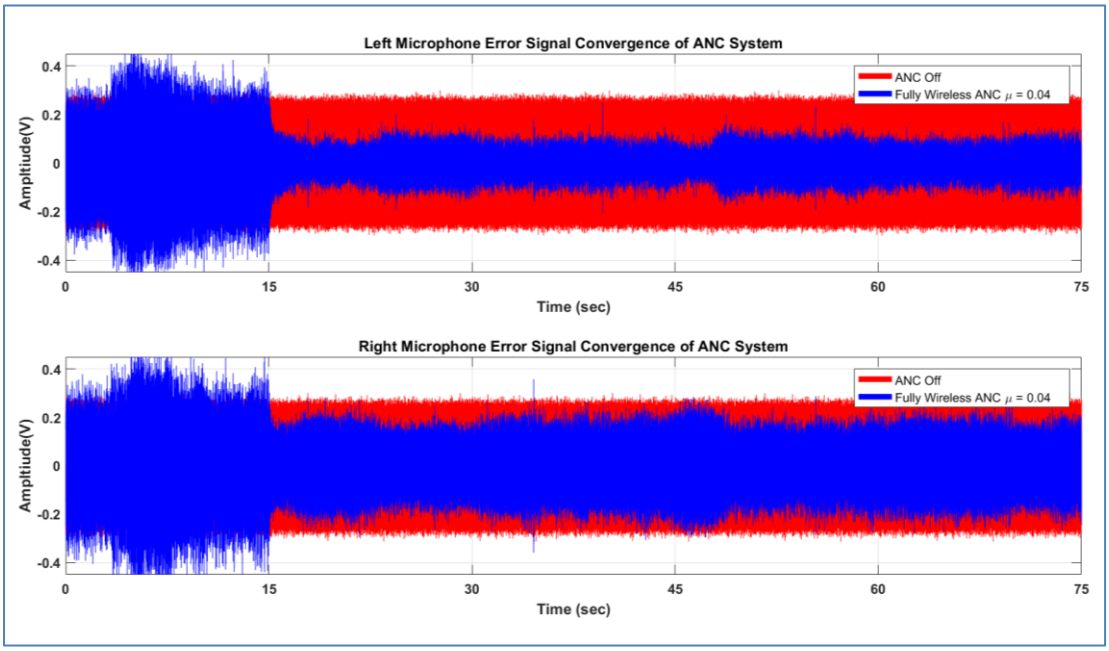

Fig. 5.13. Offline Stationary Experimental ANC, μ = 0.04 for two wireless error and one wireless control signal.

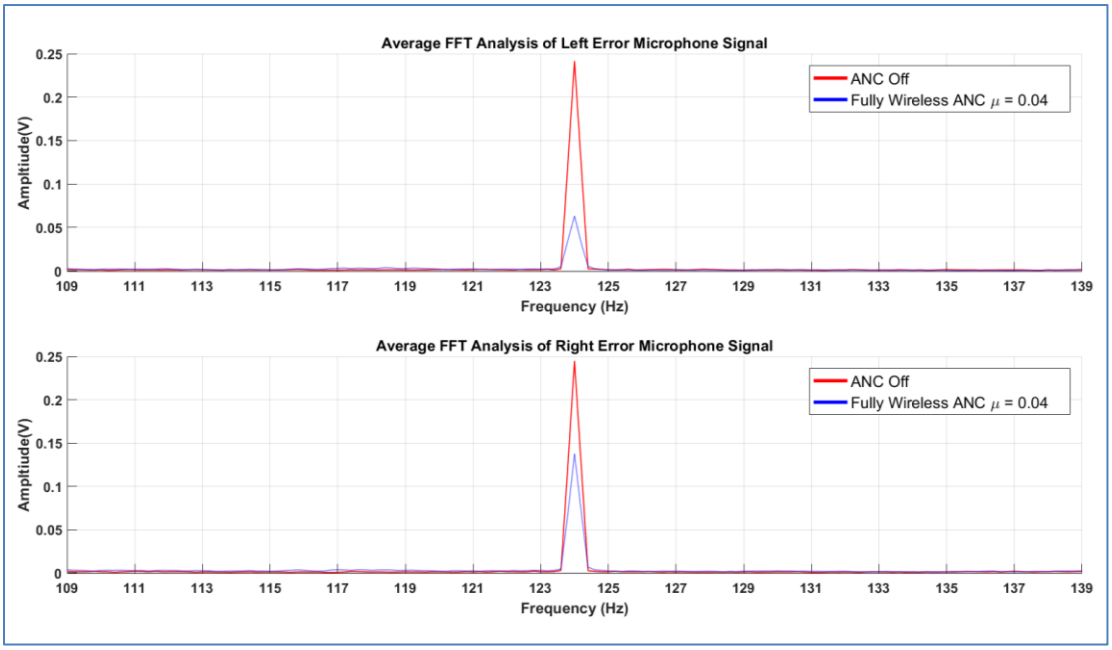

Fig. 5.14. FFT Analysis of Offline Stationary Experimental ANC, $\mu = 0.04$

The results discussed so far are for the loudspeakers separated from each other. It can be deduced that local control was possible at both ears for the wireless configurations. However, the noise control results differ for each ear when using two wireless error microphones and one control loudspeaker. The two channels compete against each other to achieve the best noise reduction. In the next section, the two loudspeakers are placed adjacent to each other, and the performance of the ANC configuration is evaluated.

5.2.2 Active Noise Control using closely spaced loudspeakers

The following sections outline experiments carried out when the primary and secondary loudspeakers are adjacent, as shown in **Fig.** 5.15. In the starting case, the in-ear error microphone is placed on the chair at the same position as before. The loudspeakers are placed 1.5 m away from the chair, as shown in the figure. Similarly, the dual-channel setups **2W.1.1** and **2W.W.1** have the same setup discussed previously with a second in-ear microphone.

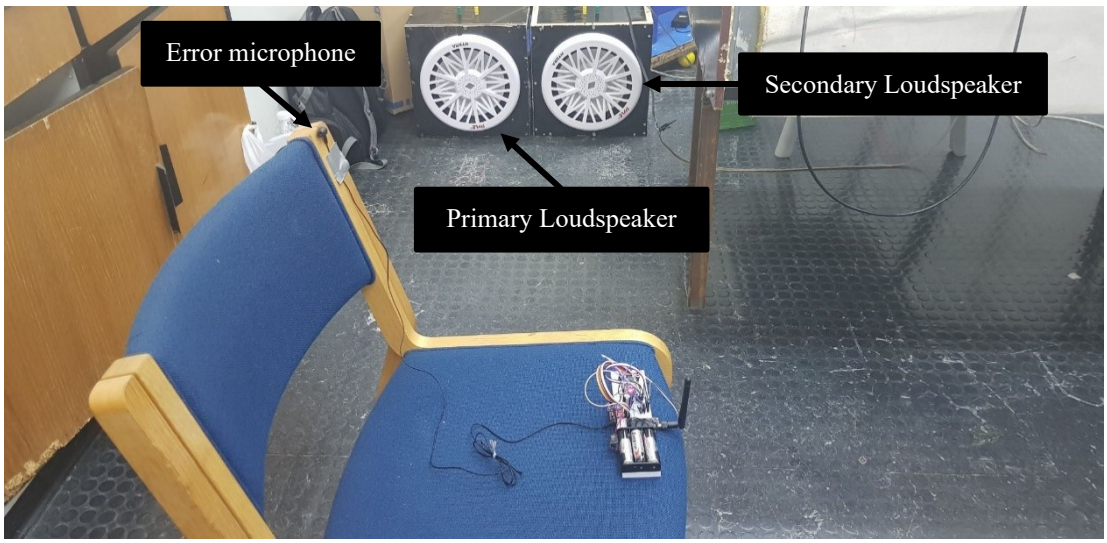

Fig. 5.15. In-ear microphone experiment setup with adjacent placement of loudspeakers.

The experiment is to show the effect of loudspeaker placement on the performance of the ANC system.

5.2.2.1 Setup 2W.1.1 (two wireless errors, wired control, wired reference) using online system identification

The noise reduction when the primary and secondary loudspeakers were placed close together was investigated for setups **2W.1.1** and **2W.W.1**. Online system identification was used to see its effects on the noise reduction for both in-ear microphones compared to the case of loudspeakers separated apart, discussed in sections **5.2.1.4** and **5.2.1.5**. For both ears, the average tonal attenuation is **22 dB,** and the average total attenuation is around **18 dB**. The left ear tonal noise reduction is **26 dB,** and that in the right ear is **18 dB**, as shown in **Fig.** 5.17.

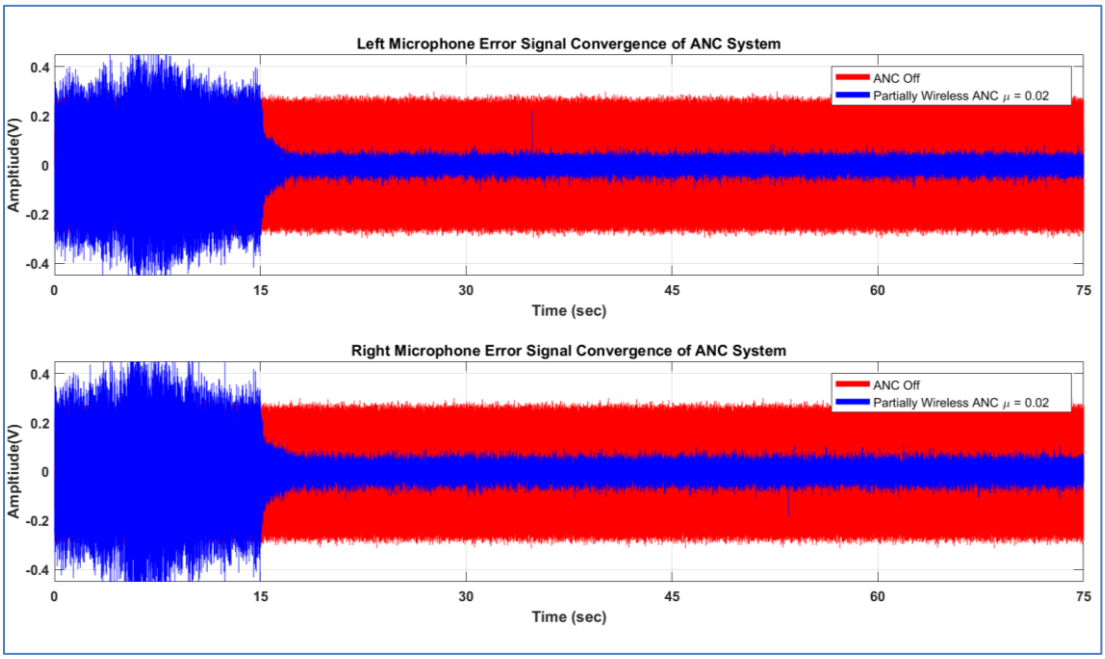

Fig. 5.16. Online Stationary Experimental ANC, μ = 0.02 for closely spaced loudspeakers.

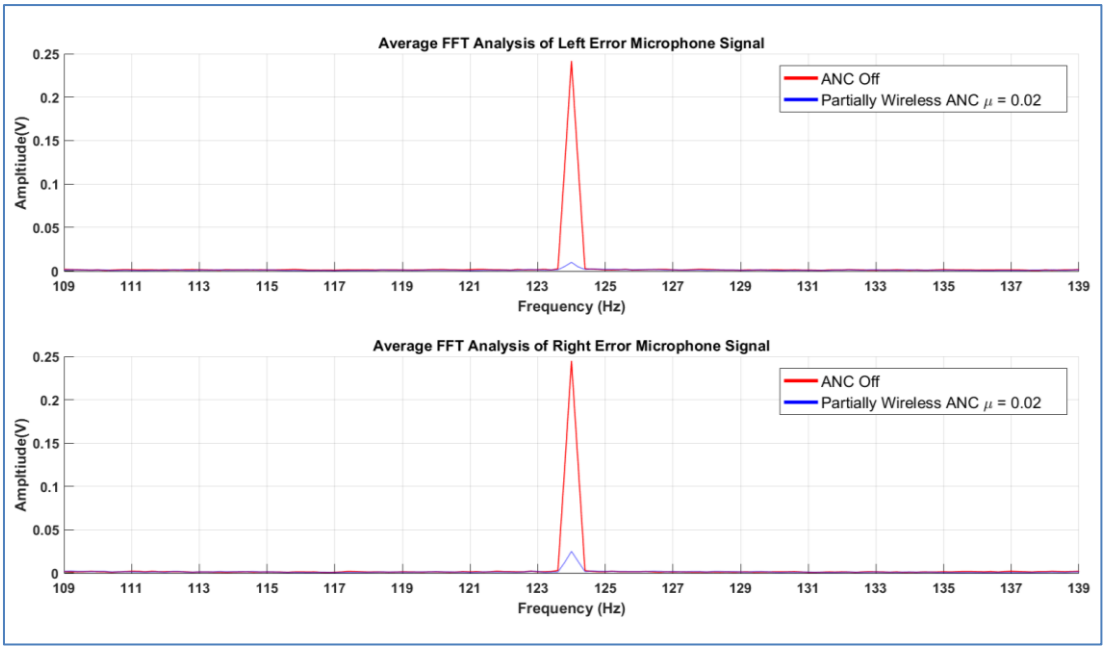

Fig. 5.17. FFT Analysis of Online Stationary Experimental ANC, μ = 0.02 for closely spaced loudspeakers.

The time-domain signals and the FFT analysis shown in **Fig.** 5.16 and **Fig.** 5.17 indicate that the noise reduction has increased for both in-ear microphones compared to section **5.2.1.4**. This is an expected case of global noise control, where the secondary path is almost identical to the primary path. As a result, the attenuations are expected to be the same for both ears. However, the left channel is attenuated slightly more than the right ear. This could be due to the two electroacoustic paths having some slight differences.

5.2.2.2 Setup 2W.W.1 (two wireless, wireless control and wired references) using online system identification

When both error microphones and the control signal are through wireless transmission, the same performance of the last case can be observed in the time-domain signals and the FFT Analysis, as shown in **Fig.** 5.18 and **Fig.** 5.19. For both ears, the average tonal attenuation is **24 dB,** and the average total attenuation is around **20 dB**. The left ear has **28 dB** tonal attenuation, whereas the right ear has an attenuation of **21 dB**.

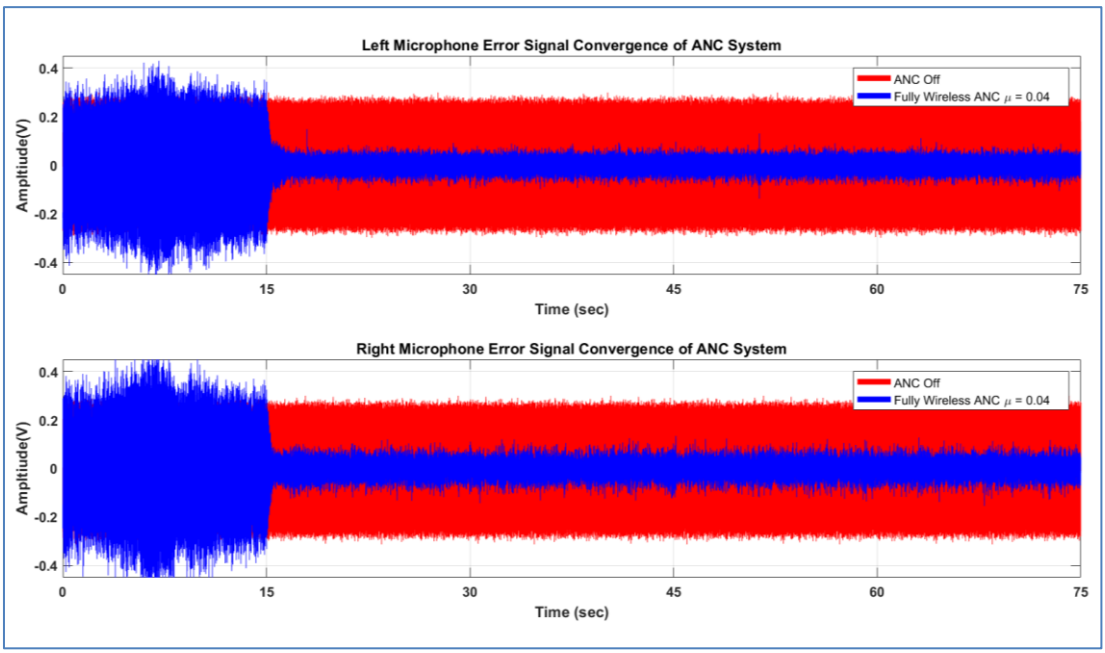

Fig. 5.18. Online Stationary Experimental ANC, μ = 0.04 for wireless error microphones and wireless control signal.

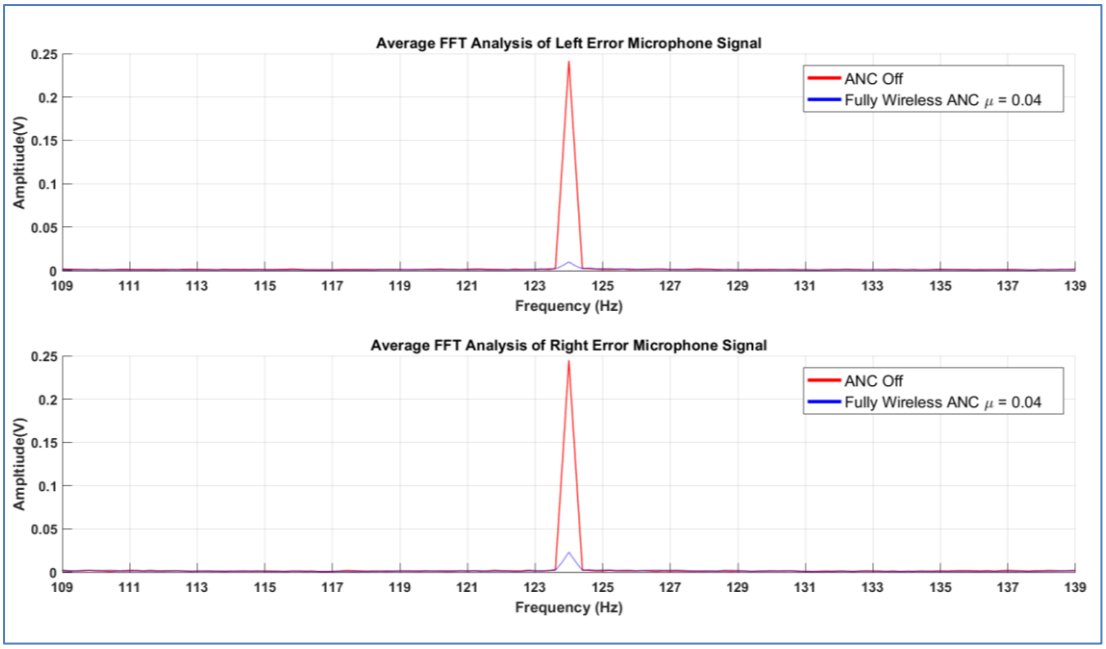

Fig. 5.19. FFT Analysis of Online Stationary Experimental ANC, μ = 0.04 for wireless error microphones and wireless control signal.

As shown in **Fig.** 5.19, the tonal noise attenuations are similar for both ears. Only a slight difference in secondary paths between the secondary source and the error microphones.

5.3 Steady pace head rotation in-ear ANC experiments

In the second part of the experiments, the in-ear microphone is worn by a user sitting on a chair, and the user rotates the head side to side at a uniform/steady pace. Again, the aim is to investigate the wireless ANC as before but with a moving microphone.

5.3.1 Local noise control (separated loudspeakers)

5.3.1.1 Uniform Pace Head Rotations with offline system identification Setup W.1.1 (Wireless error channel)

During control with offline system identification, it is observed that as the head rotates, the controller tries to adapt and minimize the error at the microphone. There is a slight drop in overall performance compared to the stationary cases in section **5.2**, but the system is still able to control the tonal noise effectively. It should be noted that the system identification convergence coefficient also affects the performance when the secondary path changes continuously. If selected carefully, fast update of the secondary path is possible and will lead to improved noise control results. For step-size a controller $\mu = 0.1$, the average tonal attenuation is **36 dB,** and the average total attenuation is around **22 dB**. The results are shown in **Fig.** 5.20. As the head rotates, it is seen that the control signal changes fast to keep the error microphone signal minimized.

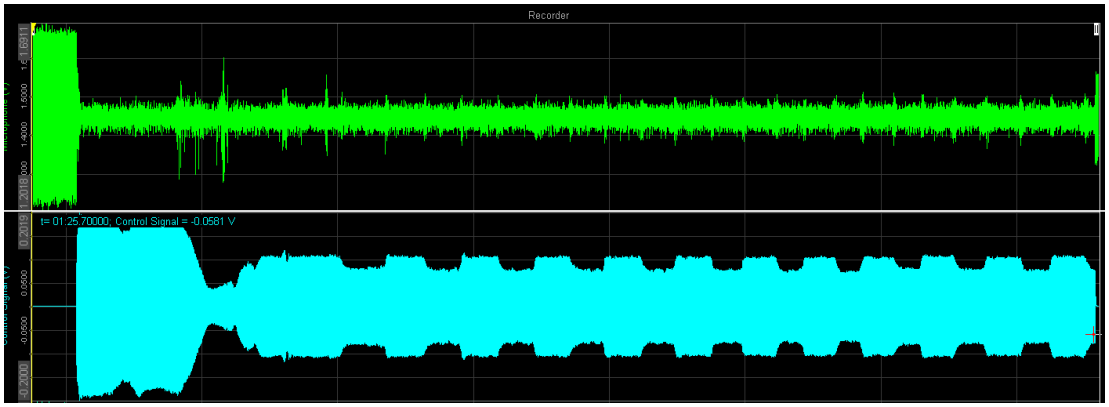

Fig. 5.20: Constant Head Rotations using offline system identification, $\mu = 0.1$ for setup W.1.1

The effect of the controller convergence coefficient μ was studied to see its effect on performance. If **μ** is reduced from **0.1** to **0.025,** the performance is reduced, as shown in **Fig.** 5.21. The error signal is not minimized fast enough during head rotations, and the adaption process is slow.

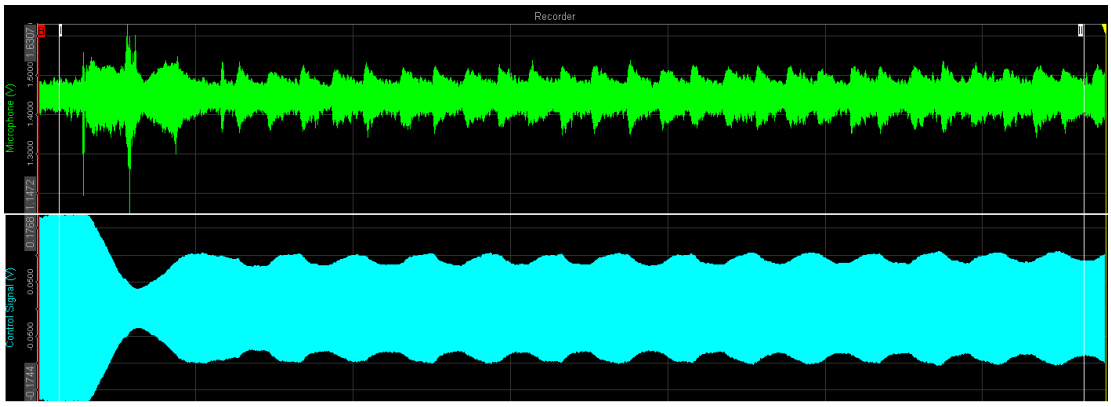

Fig. 5.21: Constant Head Rotations using offline system identification, $\boldsymbol{\mu} = 0.025$

Hence with a lower step-size coefficient $\boldsymbol{\mu}$, the control response becomes slower for the same head rotation pace. Also, there appears to be an averaging effect in the level of noise reduction, which is less than for the optimized value of $\boldsymbol{\mu}$.

5.3.1.2 Uniform Pace Head Rotations with offline system identification Setup W.W.1

When **Setup W.1.1** is changed to **Setup W.W.1**, the same effect is observed for the offline system identification experiment in the previous section **5.3.1.1**. For a step size $\mu = 0.2$, the average tonal attenuation is **33 dB,** and the average total attenuation is around **17 dB**. These were obtained after FFT analysis was performed as before. **Fig.** 5.22 shows the response for this setup. If the value $\boldsymbol{\mu}$ is reduced, the control performance deteriorates slightly as shown in **Fig.** 5.23. The reason is because of the system's slow adaptability, especially with offline system identification.

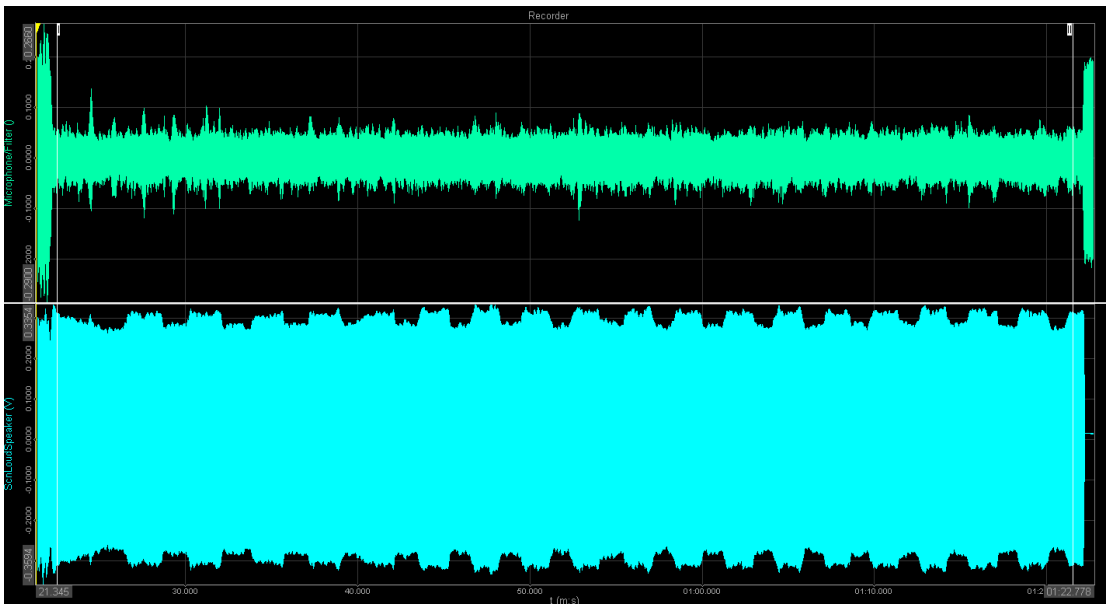

Fig. 5.22: Constant Head Rotations using offline system identification, $\mu = 0.2$

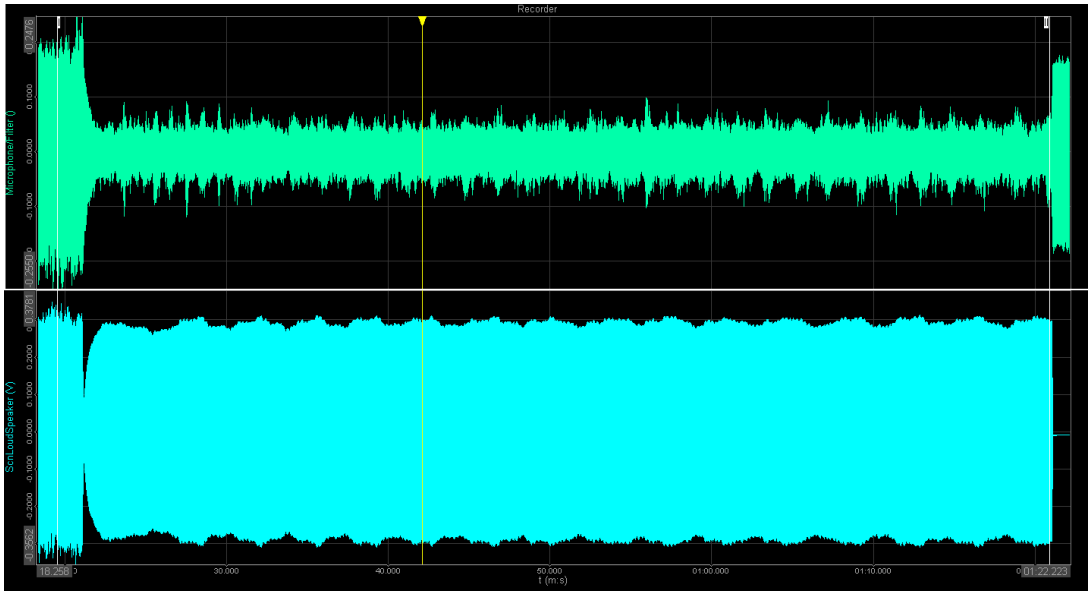

Fig. 5.23: Constant Head Rotations using offline system identification, μ = 0.05 showing decreased performance.

When the step size is reduced, the performance is slightly less, with some variation in the error and control signals, as shown in **Fig.** 5.23. This shows the importance of the proper selection of the convergence factor $\boldsymbol{\mu}$.

5.3.1.3 Uniform Pace Head Rotations with online system identification Setup W.1.1

When online system identification is used, and the head is moved side to side at a relatively fast pace, the system modelling can track minor secondary path changes. It can also provide slightly better noise reduction than with offline system identification experiments with small step-sizes shown in **Fig.** 5.21 and **Fig.** 5.23 for the experiments which had slower control response. **Fig.** 5.24 shows the performance plots when online system identification is used.

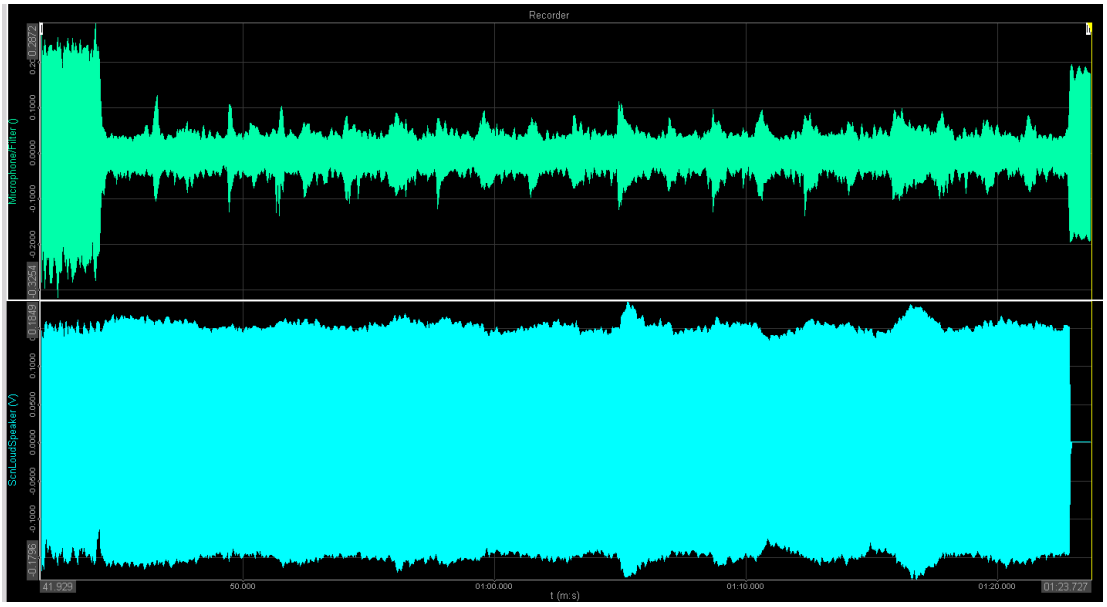

Fig. 5.24: Constant Head Rotations using online system identification, μ = 0.05

It was noted that with online system identification, the attenuation results were more consistent and less variable than in offline system identification cases. A step size of **0.05** was chosen as the optimal step size for **setup W.1.1**. The average tonal attenuation was **23 dB,** and the average total attenuation was around **16 dB**. The experiments show that offline system identification provides better noise reduction for head rotations. This is mainly because of the tracking of the changing secondary path.

5.3.1.4 Uniform Pace Head Rotations with online system identification Setup W.W.1

When **setup W.W.1** is used, the same effect is observed with the online system identification experiment. The noise reduction is slightly better than the previous experiment with online system identification depicted in section **5.3.1.3**. The average tonal attenuation is **27 dB,** and the average total attenuation is around **15 dB**.

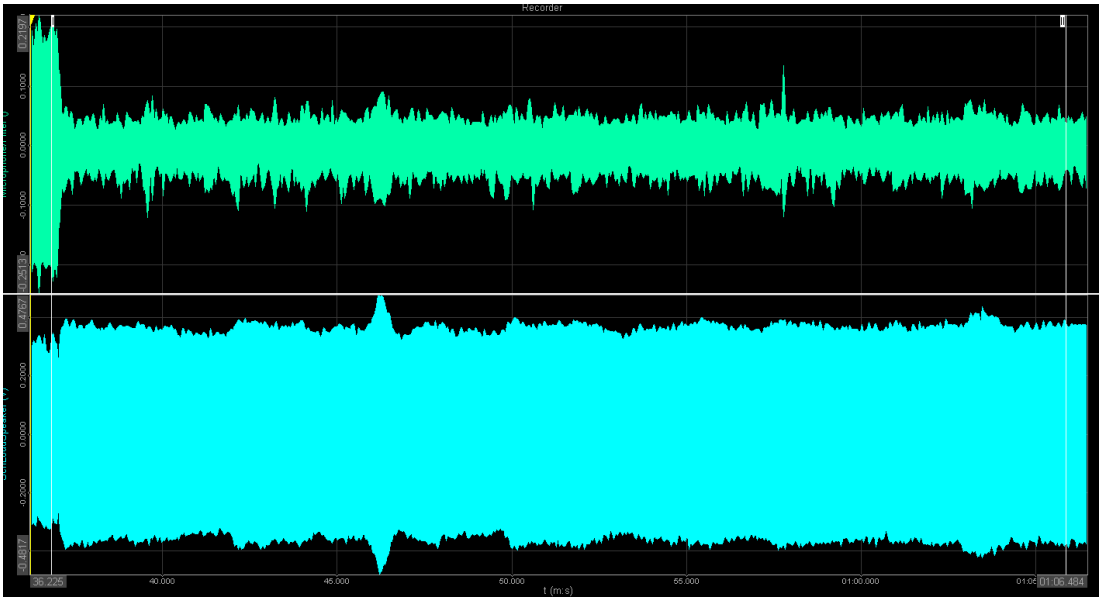

Fig. 5.25: Constant Head Rotations using online system identification, $\boldsymbol{\mu} = 0.4$ for setup W.W.1.

The wireless ANC system is able to reduce the total noise at the ear well when the head rotates.

5.3.1.5 Uniform Pace Head Rotations with online system identification using Setup 2W.1.1 (two wireless error microphones)

Online system identification was used with **setup 2W.1.1** using an additional error microphone. For both ears, the average tonal attenuation is **9 dB,** and the average total attenuation is around **10 dB**. The individual tonal noise reductions are **12 dB** for the left ear and **5 dB** for the right ear. **Fig.** 5.27 shows the FFT plot for this case at both ears. There is only a slight difference between the channels.

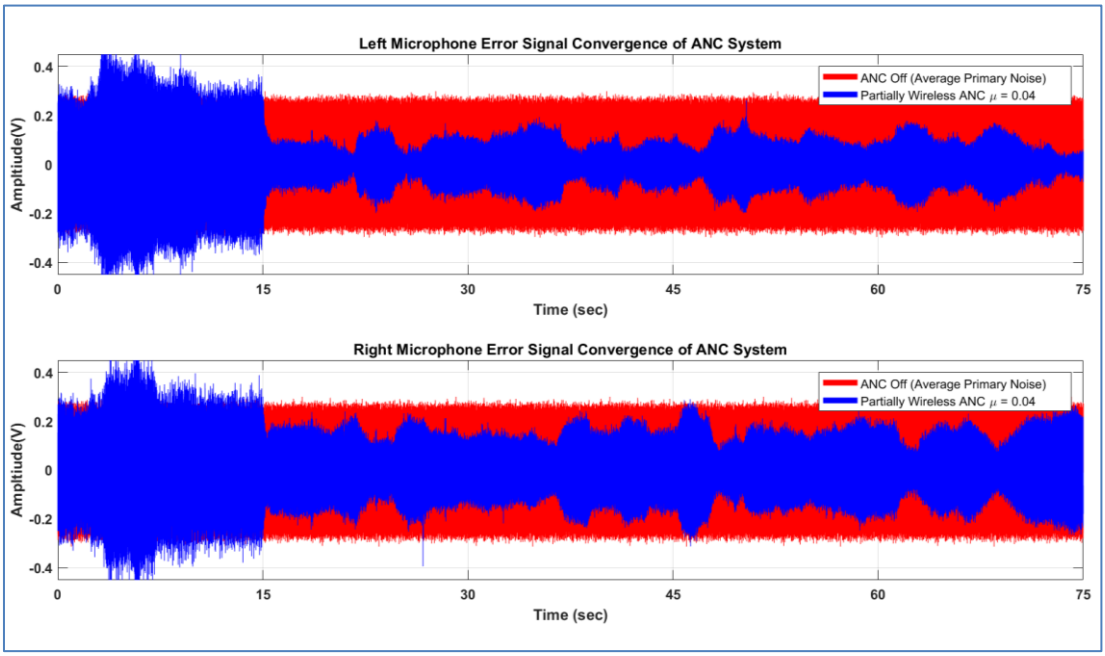

Fig. 5.26: Constant Head Rotations using online system identification, $\mu = 0.04$

Fig. 5.26 shows that the algorithm tries to maintain control for both ears and minimize the error signals. However, looking closely at both channels, it appears that a reduction in one channel leads to a slight increase in tonal noise for the other channel. There seems to be a competing effect between both error microphones. Nevertheless, both ears experience good noise reduction.

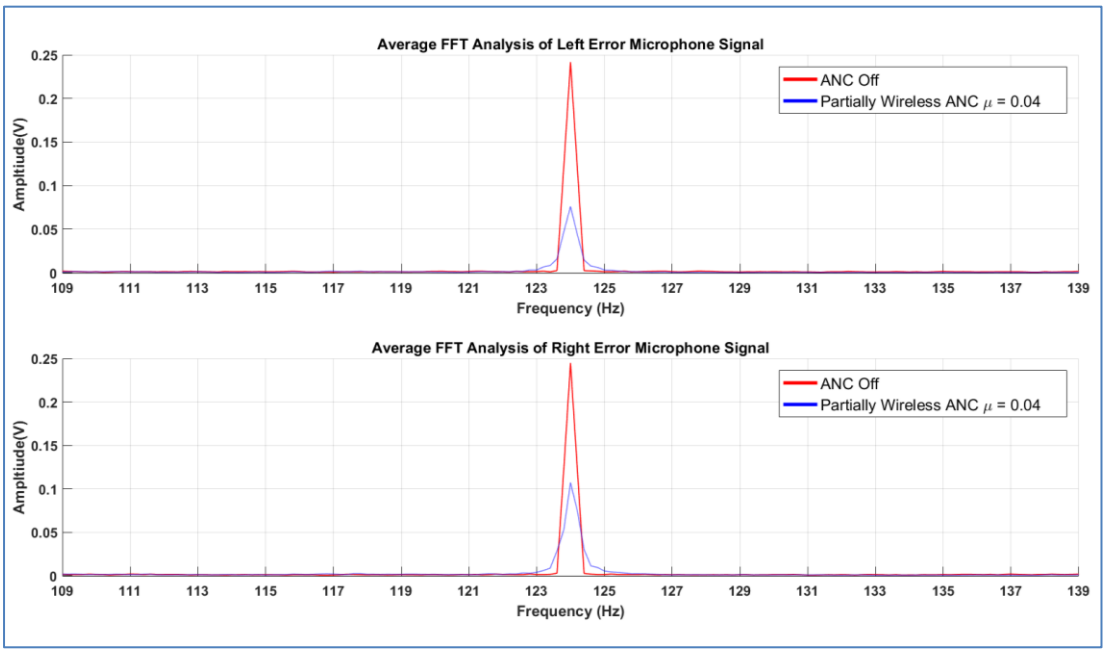

Fig. 5.27. FFT Analysis, Uniform pace head rotation Experimental ANC, $\mu = 0.04$

In the experiments presented previously, the effect of $\boldsymbol{\mu}$ appears to affect mainly the speed of convergence and not the amount of attenuation by any significant amount. Local control around the microphones is possible when the loudspeakers are well separated. Each error microphone tends to be minimized individually. The slight difference is that the change in secondary paths causes a slight difference between left and right ear performance.

5.3.2 Active Noise Control using closely spaced loudspeakers

5.3.2.1 Uniform Pace Head Rotations with offline system identification Setup W.1.1 (wireless error microphone only)

When the two loudspeakers were closely located, setups **W.1.1** single-channel and **2W.W.1** dual-channel were tested. With the offline system identification, it is observed that the error stays consistently minimized and does not change significantly as the head rotates. Rotating the head left and right frequently did not affect control. The time-domain signals are shown in **Fig.** 5.28. The average tonal attenuation is **37 dB,** and the average total attenuation is around **18 dB**.

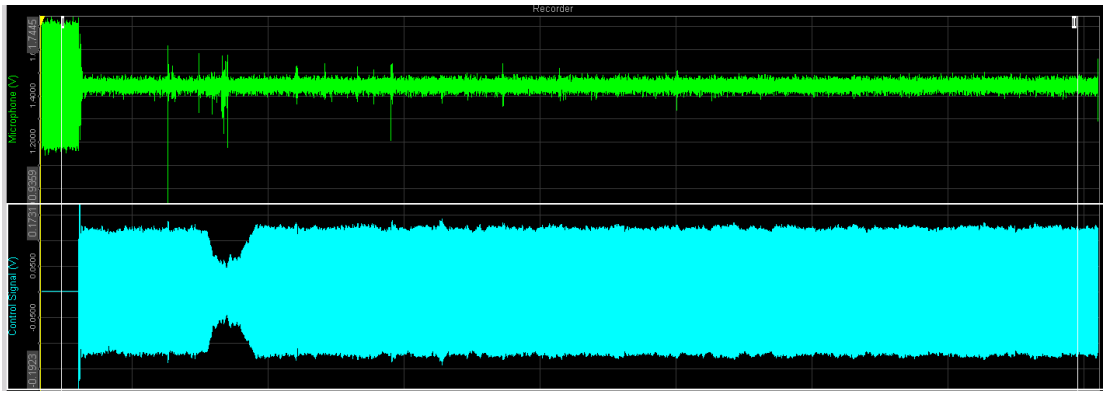

Fig. 5.28. Constant Head Rotations using offline system identification, μ = 0.1 using closely spaced loudspeakers.

The effect of the controller convergence coefficient μ was also studied to see its effect on performance. However, if **μ** is reduced from **0.1** to **0.01**, there is no significant change in the performance as the error stays minimized. The recorded changes are illustrated in **Fig.** 5.28 and **Fig.** 5.29. Since the loudspeakers are closely spaced, it seems that global control is achieved, and the effect of head rotation is not significant,

even though the secondary paths may change slightly.

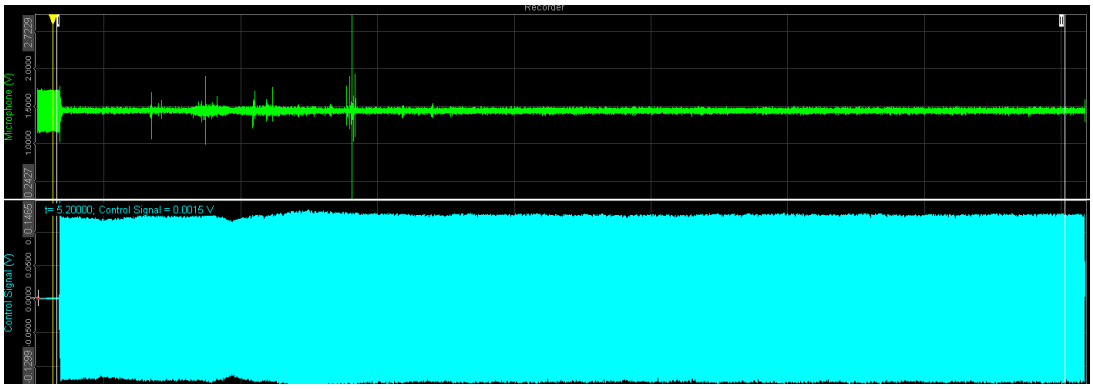

Fig. 5.29: Constant Head Rotations using offline system identification, μ = 0.01

5.3.2.2 Uniform Pace Head Rotations with online system identification Setup 2W.W.1

In **setup 2W.W.1**, the same experiment shows a similar result that was previously carried out in the single-channel experiment. The minor movement of the head does not significantly impact the control system's performance. The average tonal attenuation is **26 dB,** and the average total attenuation is around **19-20 dB**.

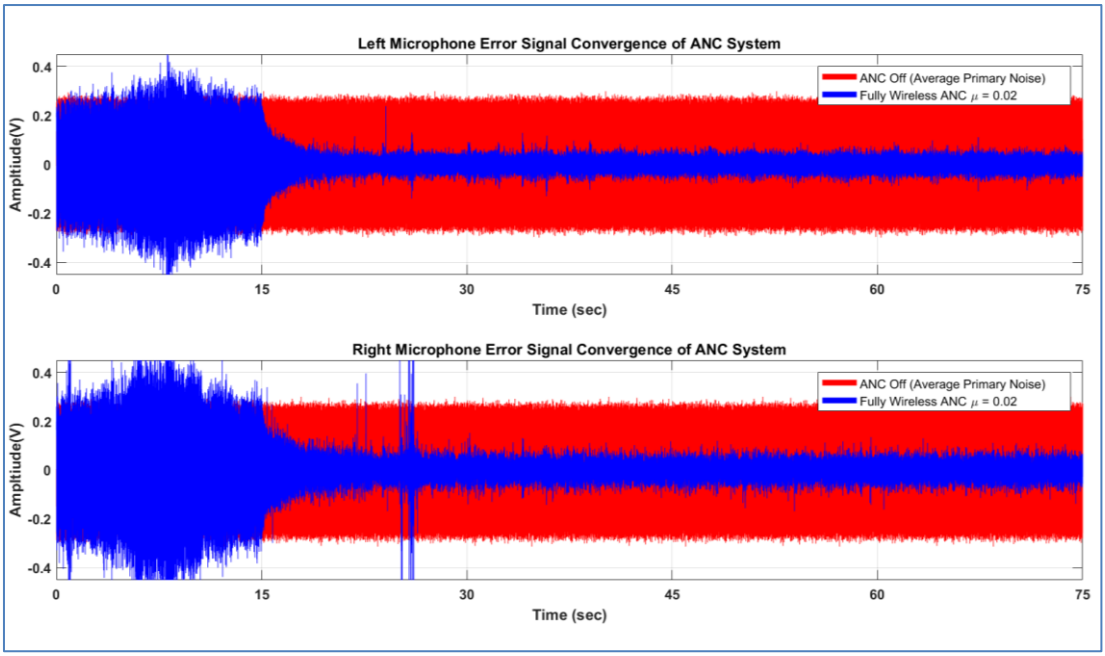

Fig. 5.30. Constant Pace Head Rotations using online system identification, μ = 0.02

Fig. 5.30 shows the attenuation results for both ears. Again, good noise reduction is achieved. Slight radio interference can be spotted at the beginning for the right ear time-domain signal, but the attenuation here is still considered good. Fast-paced rotational movement of the head does not seem to significantly affect the control responsiveness or attenuation level compared to previous stationary experiment results. The FFT analysis in **Fig.** 5.31 shows that the left ear channel is still attenuating better than the right ear channel. However, the difference is insignificant and is possibly due to the system's impulse response error.

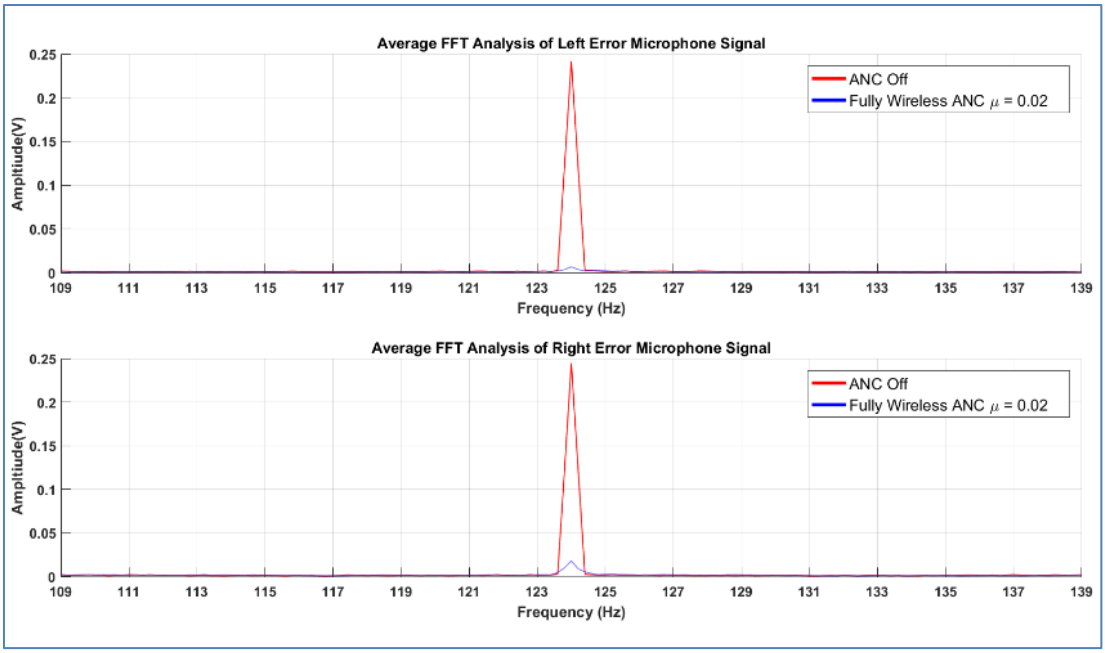

Fig. 5.31. FFT Analysis, Constant Head Rotations using online system identification, $\mu = 0.02$

5.4 Walking experiments for in-ear ANC

The third set of experiments was performed for the case when the user walked back and forth in the laboratory at an average pace. This is a practical example of workers moving from one machine to another in a working environment. In chapter 3, **Fig.** 5.5 shows an example of the performed experiment. The purpose of the experiments is to show the potential application of the developed wireless ANC system for practical use.

The walking pace was estimated with a timer over a distance of 10 meters. The estimated pace is about 30 $\pm$ 5 cm/s, equivalent to about one foot per second. During mobility experiments, the primary noise profile will vary slightly with distance. Each time the primary noise is recorded. However, if the walking pace is kept the same, one profile is enough to represent the primary noise. A typical plot for the primary noise is shown in **Fig.** 5.32.

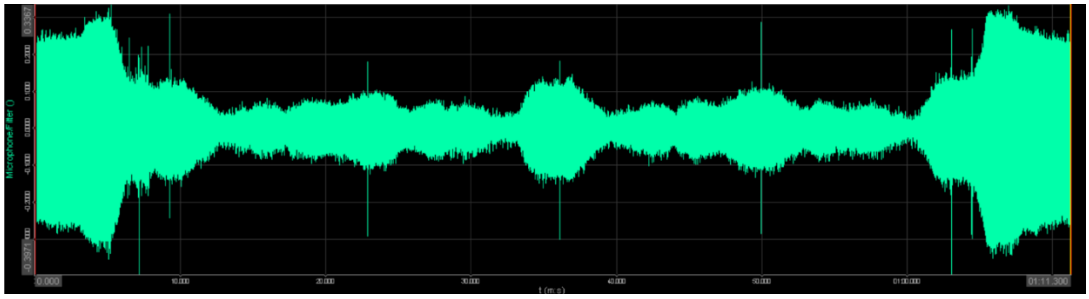

Fig. 5.32. Primary noise profile without ANC control for constant pace walking experiments.

5.4.1 Local noise control (separated loudspeakers)

5.4.1.1 Walking experiment with offline system identification using Setup W.1.1 (wireless error only)

In this experiment, the online system identification was disabled. The secondary path was measured and assumed fixed for the ANC. After the initial 15 seconds of secondary path modelling, the control process is initiated. The user then walks at a regular pace, and the performance is recorded, as shown in **Fig.** 5.33.

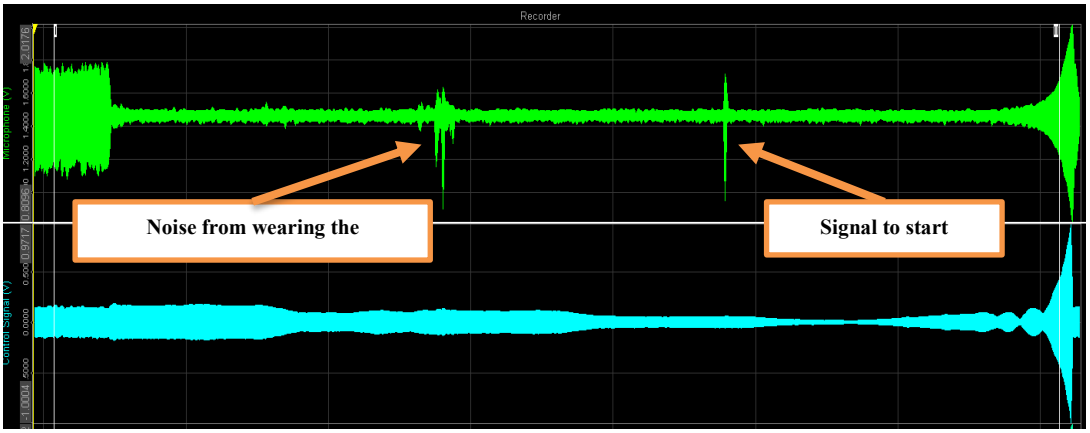

Fig. 5.33. Walking experiment using offline system identification, μ = 0.1

Although the error signal is reduced after control is initiated, the system diverges after walking about 2.5 meters from the original walking point. This is because the secondary path has changed significantly, and the controller cannot maintain stability. It is observed that the control output increases significantly at the divergence region. Reducing the step size does not significantly affect the outcome, except that it controls how fast or slow the divergence will be. The divergence distances of the algorithm were noted, as shown in **Table 5.1**.

Table 5.1. Divergence distance for each step size recorded for setup W.1.1

Step-size coefficient μ	0.2	0.1	0.05	0.025	0.01
Divergence Distance (cm) $\pm$ 20 cm	200	250	370	470	450

5.4.1.2 Walking experiment with offline system identification using Setup W.W.1

Similarly, when using **Setup W.W.1** (wireless error, wireless control), the same effect is observed during the offline system identification experiment as in the previous section. The time-domain signals are depicted in **Fig.** 5.34 and **Fig.** 5.35.

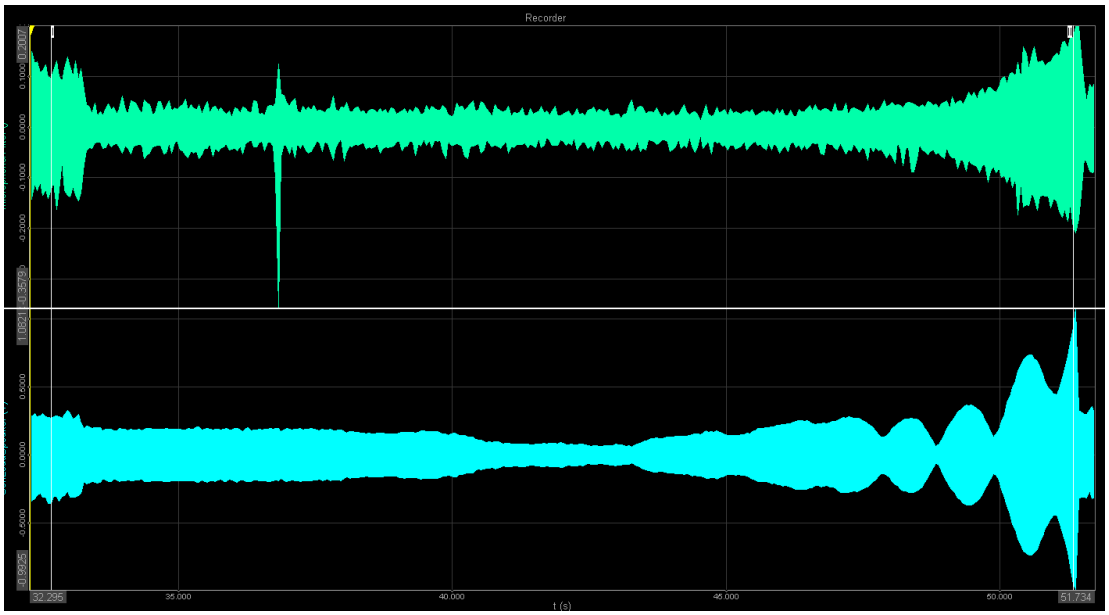

Fig. 5.34. Walking experiment using offline system identification, μ = 0.4

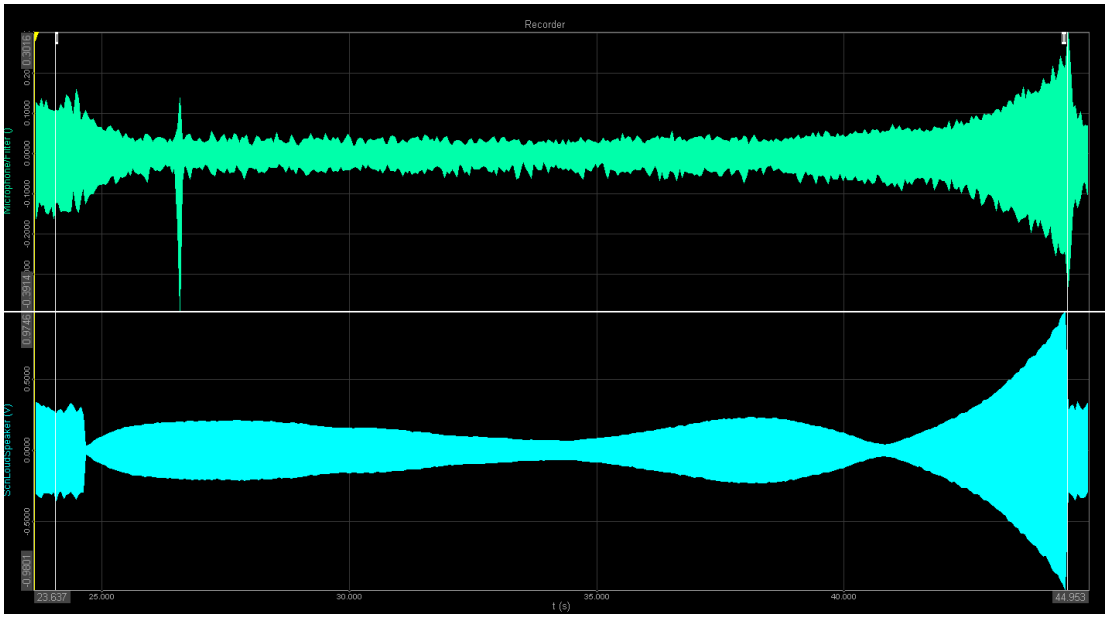

Fig. 5.35. Walking experiment using offline system identification, $\mu = 0.05$

Again, varying the value of $\boldsymbol{\mu}$ does not stop instability but extends the walking distance.

5.4.1.3 Walking experiment with online system identification using Setup W.1.1

The previous sections showed that if offline system identification is used, the performance may be compromised. The effect of adding online system identification is presented in sections **5.4.1.3, 5.4.1.4, 5.4.1.5** and **5.4.1.6**. When online system identification is enabled, the system remains stable and can track any changes in the secondary path. The controller can then adapt in real time to slow changes, ensuring that the system's performance is maintained and remains stable. **Fig.** 5.36 shows the control result with online system identification. There are no divergent behaviours during walking at a normal pace.

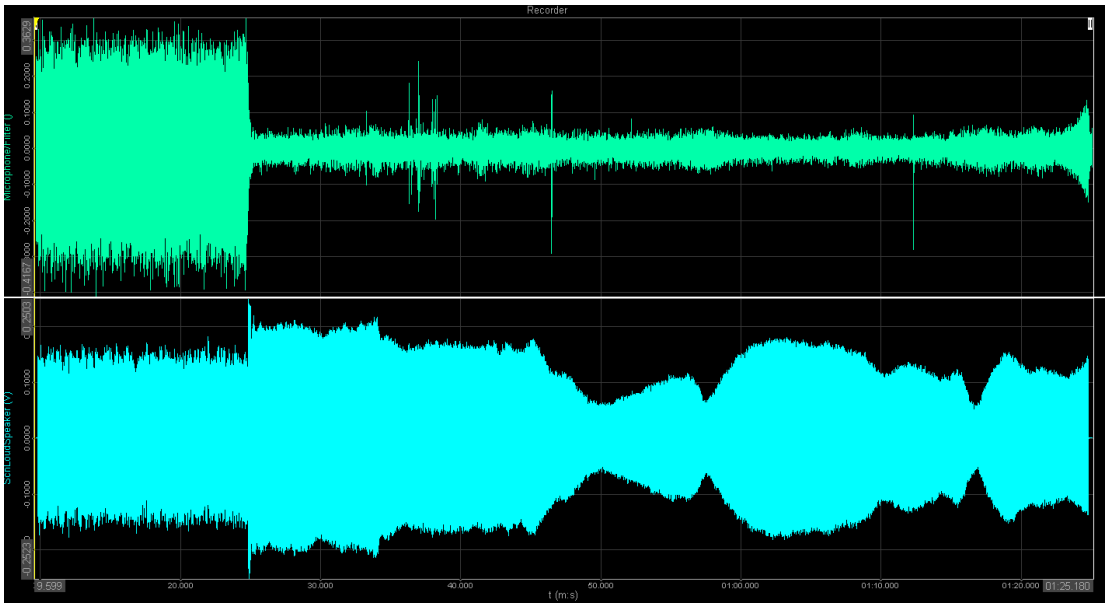

Fig. 5.36. Walking experiment using online system identification, μ = 0.1

The optimal step size here is 0.1 for **setup W.1.1**. When using online system identification, the system adapts and tries not to diverge over longer distances. When the user walks far away from the noise source, the convergence rate becomes slower, but the ANC is still able to adapt to the changes without any issues. When the user

approaches the noise source from a further distance, the convergence becomes quite fast and converges when approached at an average walking pace. This is because the background system identification excitation noise can still be carried out over a range of distances from the primary loudspeaker. The control covered up to **7.5m**, which is more than half of the enclosure. Some minor interference noises can be noticed and are mainly due to transmission loss in the wireless system at certain distances. The experimental results show that the wireless ANC system can significantly reduce noise during mobility. The average tonal attenuation is about **26 dB,** and the average total attenuation is around **21 dB**.

5.4.1.4 Walking experiment with online system identification Setup W.W.1

When the in-ear error microphone and the control loudspeaker signals are wireless, this corresponds to setup **W.W.1**. The same effect is observed with online system identification as in the previous section. The time-domain signals are shown in **Fig.** 5.37. Similarly, the average tonal attenuation is **23-24 dB,** and the average total attenuation is around **20-21 dB**.

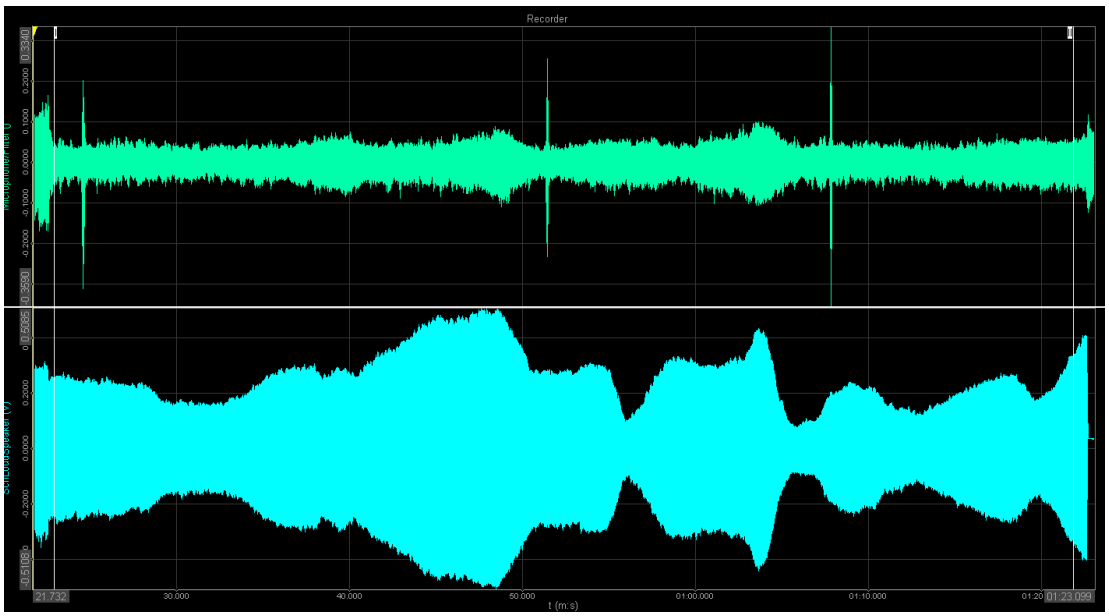

Fig. 5.37. Walking experiment using online system identification, $\mu = 0.4$ for setup W.W.1

The results show good tracking of the changes in the secondary path as the user moves from one position to another.

5.4.1.5 Walking experiment with online system identification using Setup 2W.1.1

Online system identification was also used with **setups 2W.1.1** and **2W.W.1**. This is done by adding an additional error microphone in the right ear. The effect of having online system identification on the noise reduction performance is shown in **Fig.** 5.38 for **setup 2W.1.1**. After experimenting several times using trial and error to obtain the optimal step-size $\boldsymbol{\mu}$, the system performed well with noise control achieved at both ears.

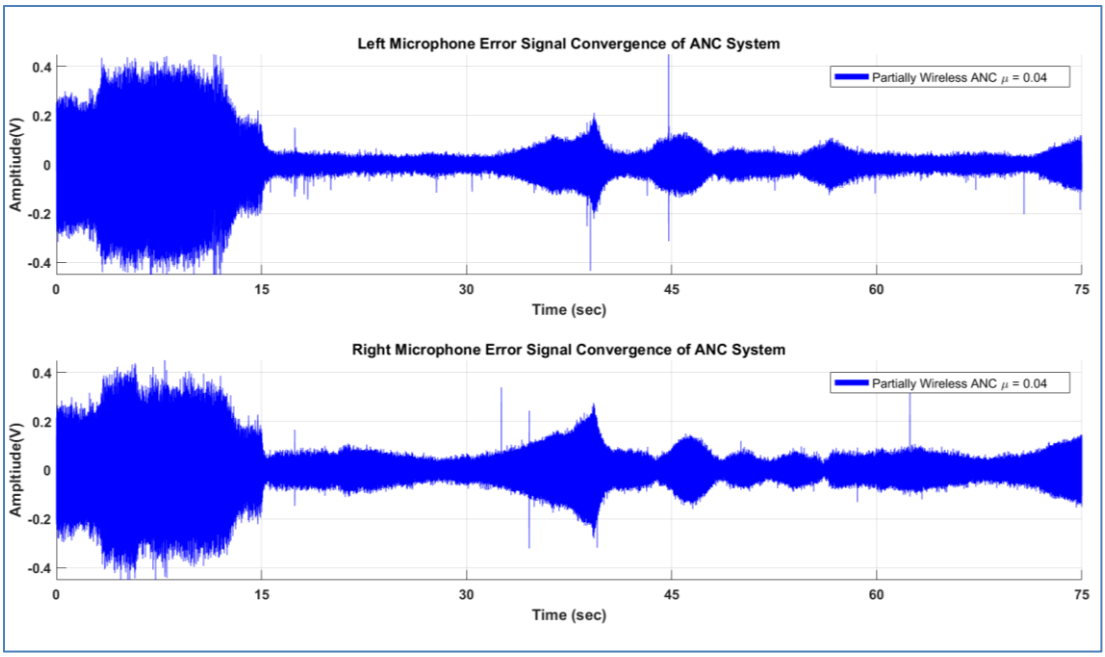

Fig. 5.38. Walking experiment using online system identification, μ = 0.04 using setup 2W.1.1

The system is able to handle the control with changes in the secondary paths for both in-ear microphones. When the user walks away from the source, the noise reduction in both ears appears similar. When the user walks away, the primary and secondary paths for the in-ear microphones become more similar, and the online system

identification ensures noise reduction further away from the noise source. The average tonal reduction is **18 dB,** and the average total attenuation is around **17 dB**.

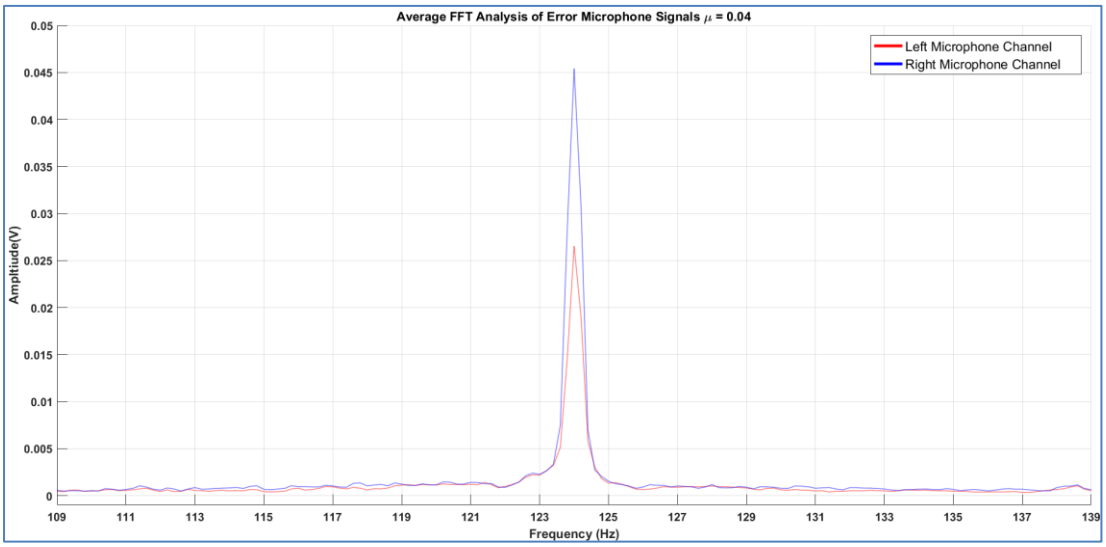

Fig. 5.39. FFT Analysis using online system identification, $\mu = 0.04$

Fig. 5.39 shows the FFT Analysis after the first 5 seconds of control. There is no primary noise plotted here since the noise profile differs for each trial. Both error channels are plotted instead. The left ear microphone has almost double attenuation compared to the right ear microphone. This difference is due to one error microphone competing with the other. And the control system favours the channel with faster convergence. The control system is effective up to **7 meters**. The same analysis was applied to setup **2W.W.1**, and the observations remained the same.

5.4.1.6 Walking experiment with online system identification using Setup 2W.W.1

When setup **2W.W.1** is used, it behaves similarly to the partially wireless experiment setup **2W.1.1** and has similar attenuation behaviour. The time-domain signals are shown in **Fig.** 5.40**.**

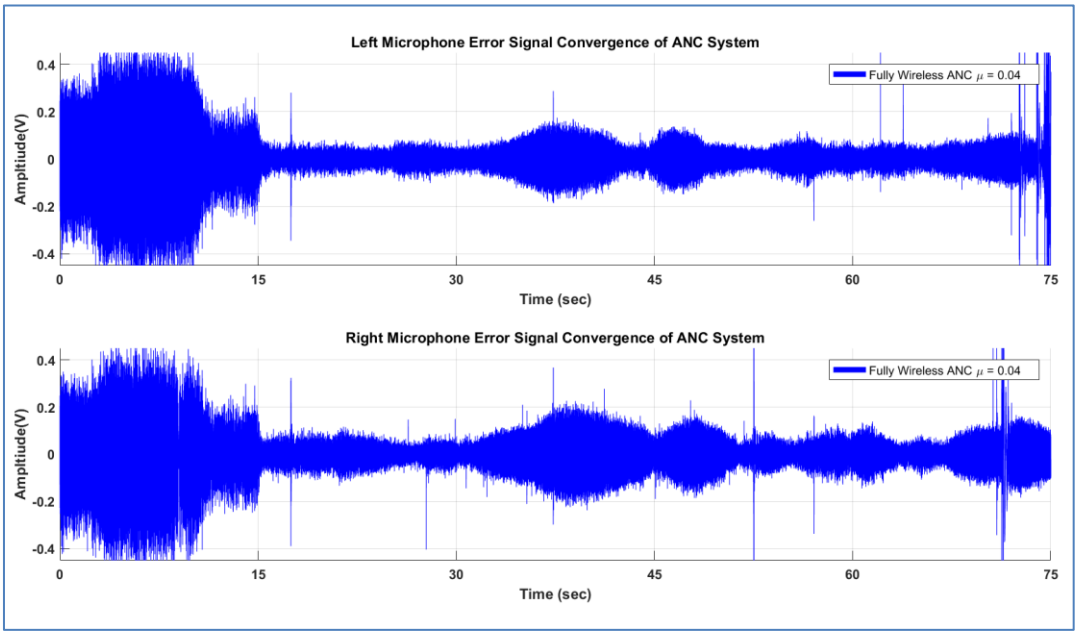

Fig. 5.40. Walking experiment using online system identification, μ = 0.04

Some temporary crackling noises can be spotted at the end of the time domain signals and are mainly due to transmission loss in the wireless system at certain distances. The average tonal reduction is around **17 dB,** and the average total attenuation is around **15 dB**.

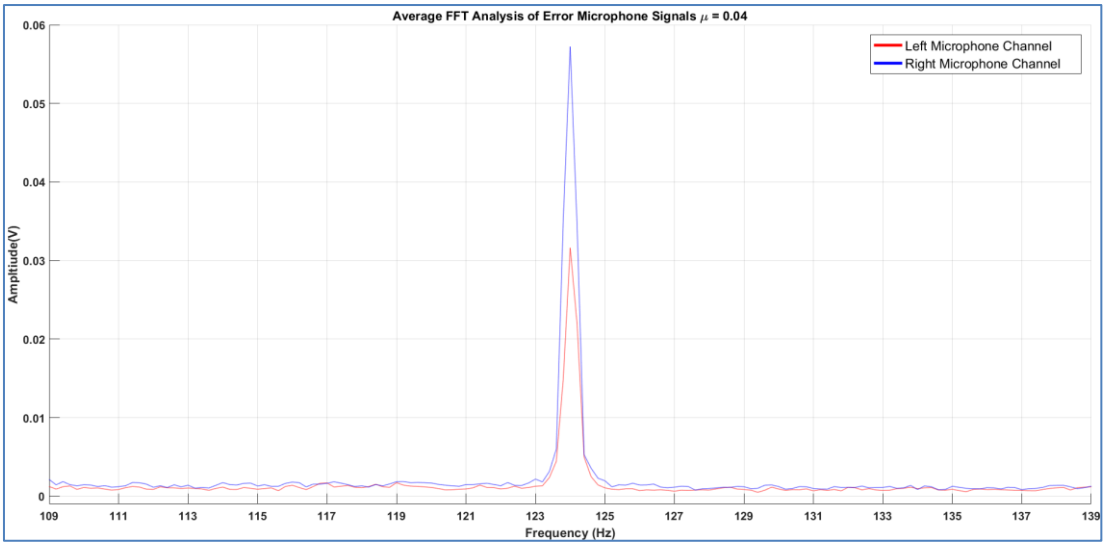

Fig. 5.41. FFT Analysis using online system identification, μ = 0.04

Fig. 5.41 shows the FFT plots for both ears. The left microphone has better noise reduction than the right one.

5.4.2 Active Noise Control using closely spaced

5.4.2.1 Walking experiment with online system identification using Setup W.W.1

In **setup W.W.1**, with online system identification enabled, an experiment was performed with the loudspeakers placed close. The system handles noise control well at a normal walking pace. The performance recorded is shown in **Fig.** 5.42. In this case, it appears that online system identification is able to keep the control stable and maintain good noise reduction. Both wireless error and control worked well.

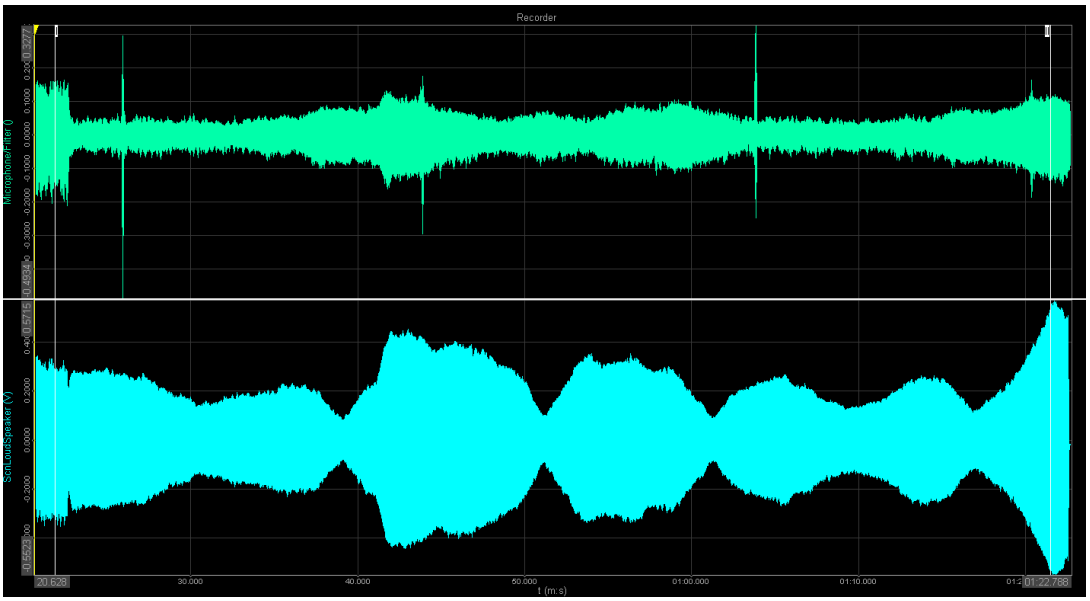

Fig. 5.42: Walking experiment using online system identification, μ = 0.2

When reducing the step-size $\boldsymbol{\mu}$ of the ANC system, the system eventually diverges after walking for a few seconds, as shown in **Fig.** 5.43. That is because the adaptive algorithm could not track changes with a slower online path identification. For a step size of 0.2, the average tonal reduction is around **8 dB,** and the average total

attenuation remains about the same at **8 dB**.

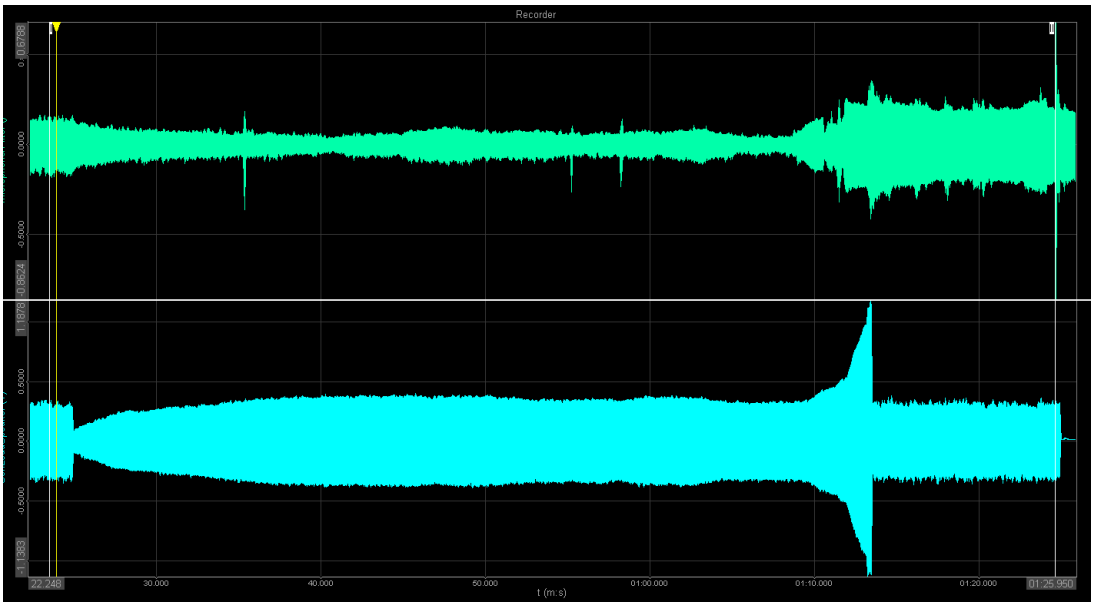

Fig. 5.43: Walking experiment using online system identification, μ = 0.05

5.4.2.2 Walking experiment with online system identification using Setup 2W.1.1

The dual-channel **setup 2W.1.1** was also tested in this section. After obtaining the optimal step size for the normal walking pace by trial and error, the time-domain signals are shown in **Fig.** 5.44. With the same walking pace in this experiment, the control adapts to provide noise control at both ears. There is a slight disconnection spotted at the right ear channel due to a loss of signal from the wireless microphone. However, this was for a small duration and did not affect the control. For both ears, the average tonal reduction is around **13-14 dB,** and the average total attenuation is around **15 dB** for both ears. It can be noted that the system's performance, although stable, is variable as the adaptive controller tries to compensate for the changes in real time.

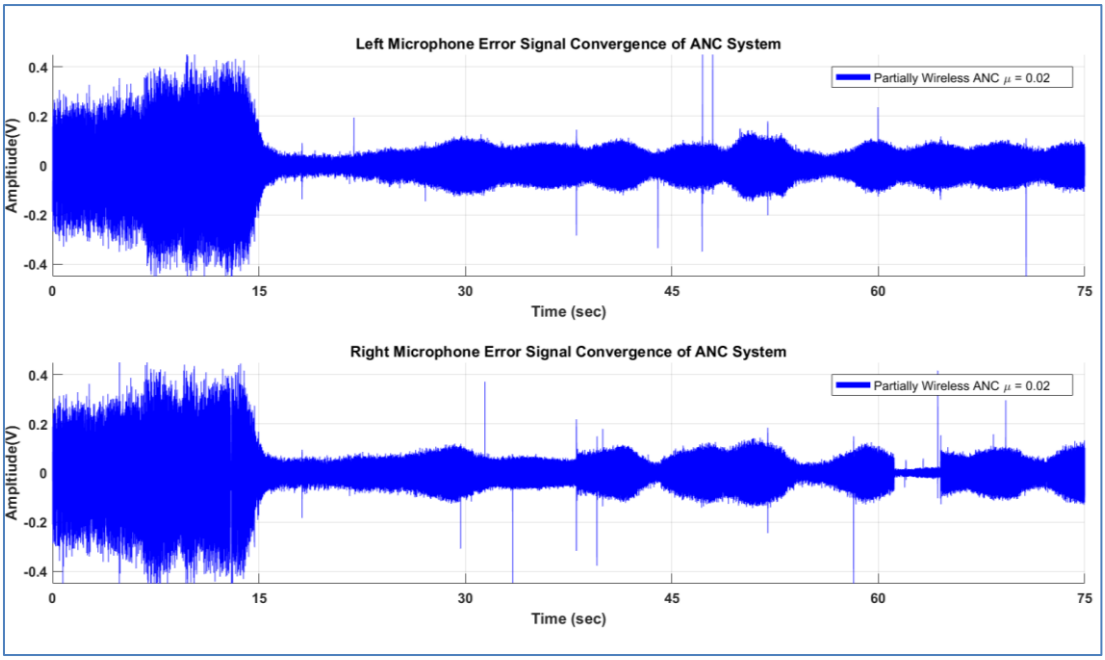

Fig. 5.44. Walking experiment using online system identification, $\mu = 0.02$

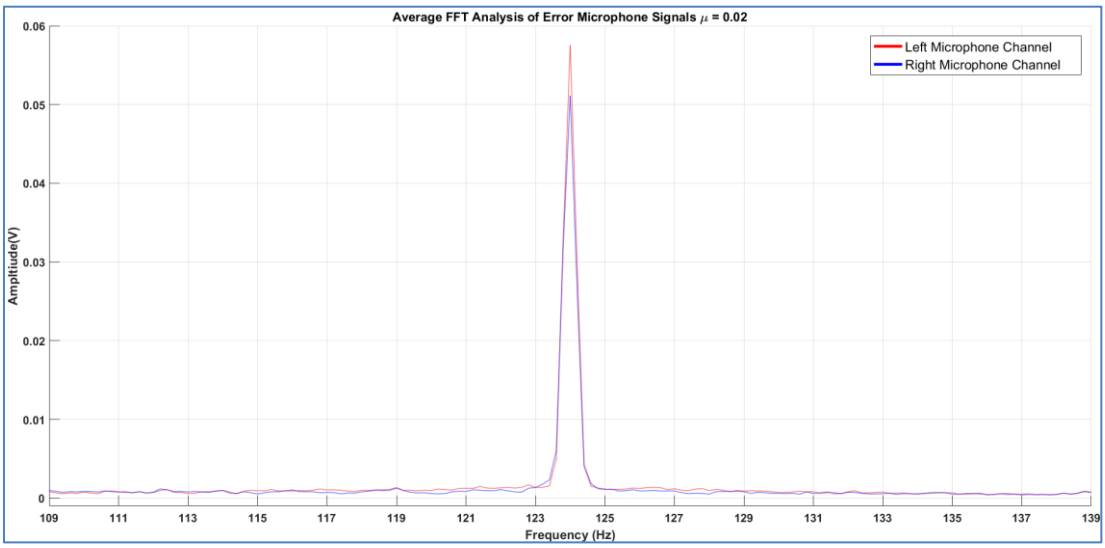

Fig. 5.45. FFT Analysis using online system identification, $\mu = 0.02$

5.4.2.3 Walking experiment with online system identification using Setup 2W.W.1

With **setup 2W.W.1**, where the control channel is through wireless transmission, a similar performance is obtained, as shown in the time-domain signals plotted in **Fig.** 5.46. The control system adapts to changes. The right ear channel time-domain signal experienced a disconnection due to a loss of connectivity. This is temporary and the control system operated continuously in the experiment. For both ears, the average tonal reduction is around **7 dB,** and the average total attenuation is around **9 dB**. The FFT analysis shown in **Fig.** 5.47 confirms that good noise reduction is possible in both ears. However, the reduction is less than in previous cases.

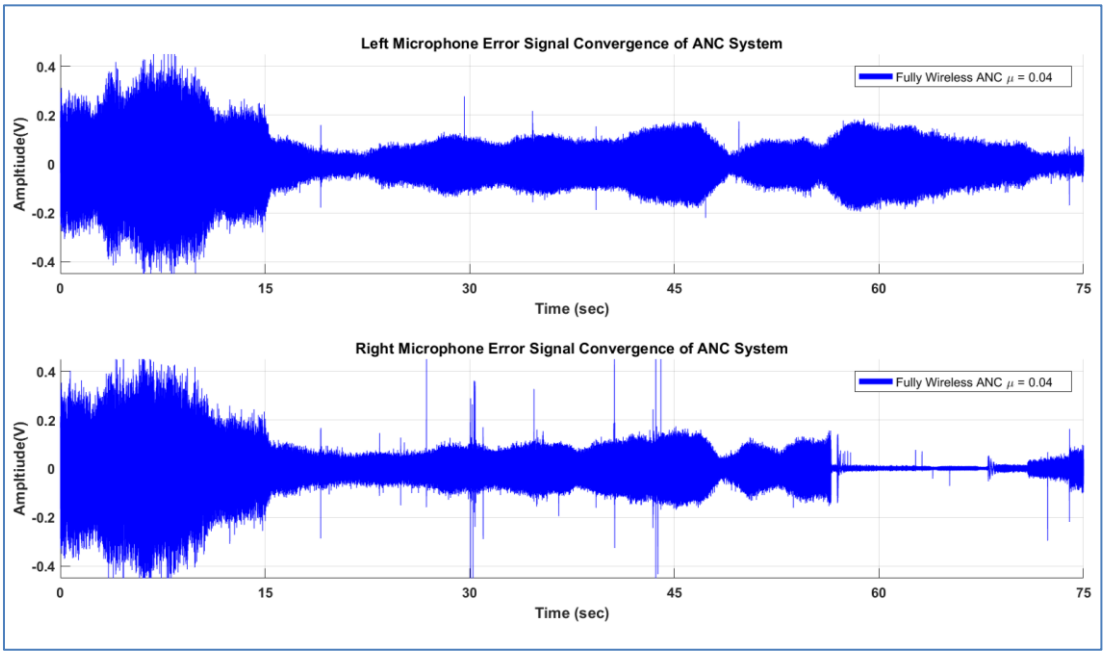

Fig. 5.46: Walking experiment using online system identification, μ = 0.04

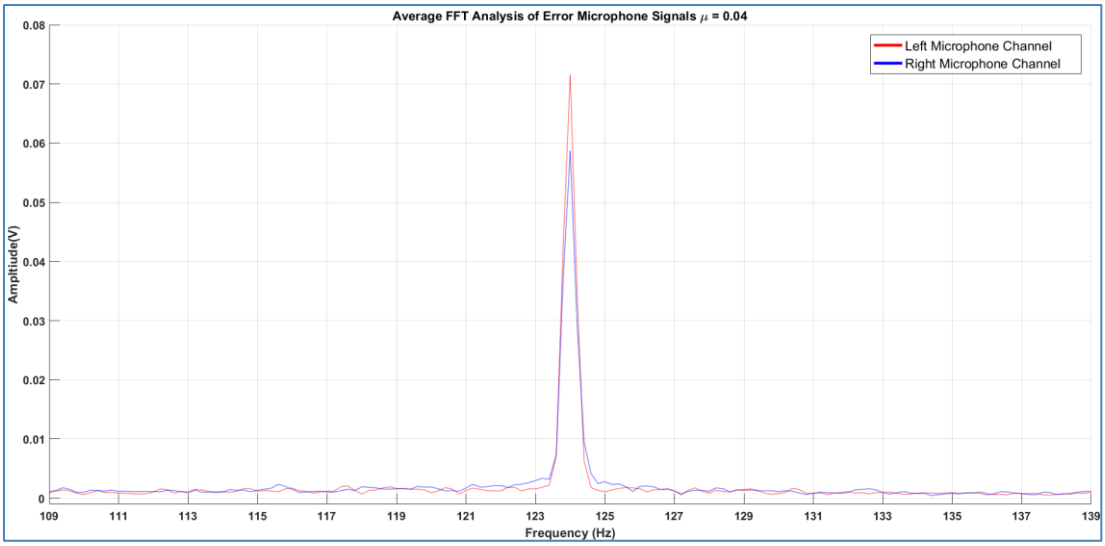

Fig. 5.47: FFT Analysis using online system identification, μ = 0.04

The FFT analysis was applied for the time period 5 seconds after convergence up till just before the disconnection at the right ear.

5.5 Stationary In-Ear ANC experiments with speech

Often workers need to communicate with each other while working in a noisy environment. The use of ANC can improve this communication. This section's main purpose is to investigate the impact of speech on the ANC performance using the in-ear microphones. In particular, the effect of bone conduction can carry low-frequency noise from the vocal cords to the microphone and may affect the performance of the system. A partially wireless single-channel **(W.W.1)** and a dual-channel **(2W.W.1)** system were studied for stationary and mobile cases. The results show that speaking while ANC is enabled does not affect the performance. A subjective evaluation by the wearer also confirms this. The user was reading a sample text from a document while using the wireless ANC system developed.

5.5.1 Local Noise Control (separated primary and control sources)

5.5.1.1 Setup W.W.1 using offline system identification.

The experiment was done with offline and online system identification for **setup W.W.1**, and the result is shown in **Fig.** 5.48. This was done mainly to investigate the impact of offline system identification on speech interference. The tonal noise attenuation is about **55 dB** without speech and **45 dB** with speech. The time domain signals are shown in **Fig.** 5.48 with and without speech. The primary noise was plotted without speech for reference (this applies to all time-domain signals). An average FFT analysis is carried out after convergence, as shown in **Fig.** 5.49.

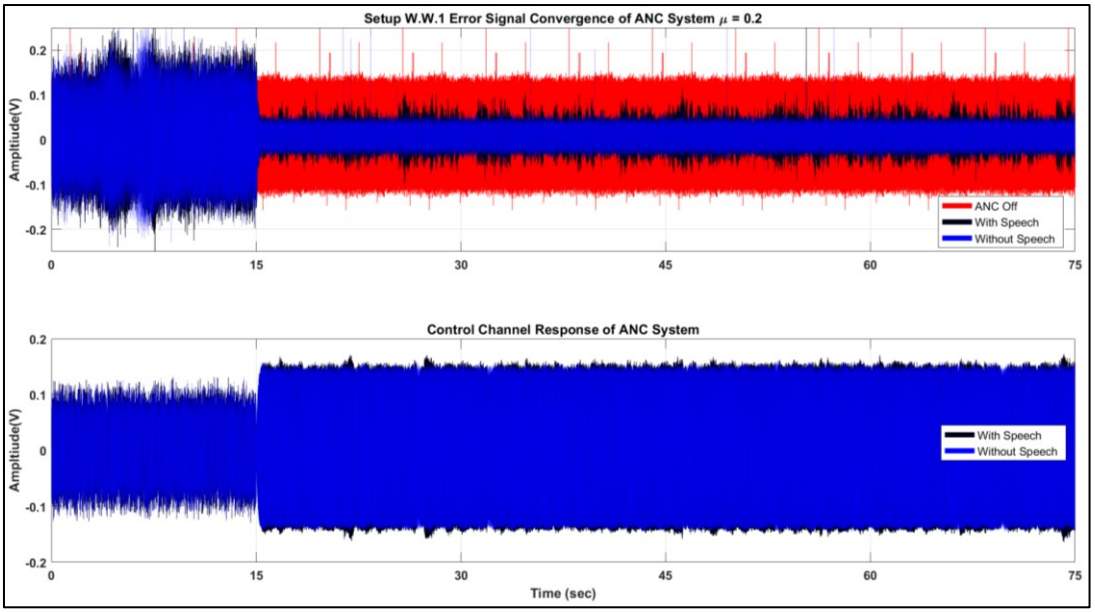

Fig. 5.48. Time-domain signals for speech interference using offline system identification.

The results show that the control system converges and maintains control despite the speech. This is also confirmed by the control signal being bounded and stable.

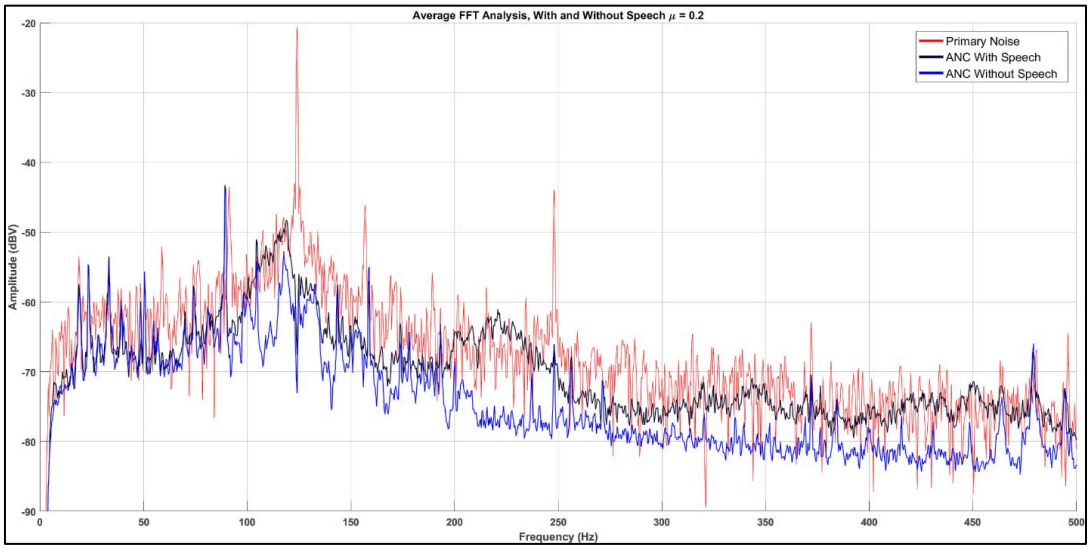

Fig. 5.49. Frequency-domain signals for speech interference using offline system identification.

Fig. 5.49 shows the noise spectrum before and after the control, with and without speech. Some harmonics of 124 Hz are visible in the primary noise due to the nonlinearity of the loudspeaker. However, there is a significant noise reduction in both cases. With speech, a slightly less noise reduction is apparent due to the speech affecting the coherence between the error signal and reference signal.

5.5.1.2 Setup W.W.1 using online system identification.

When online system identification is used, the performance is similar to the offline case, as shown in **Fig.** 5.50. However, in this case, the tonal noise reduction is dropped to about **30 dB** (with and without speech interference), as shown in **Fig.** 5.51.

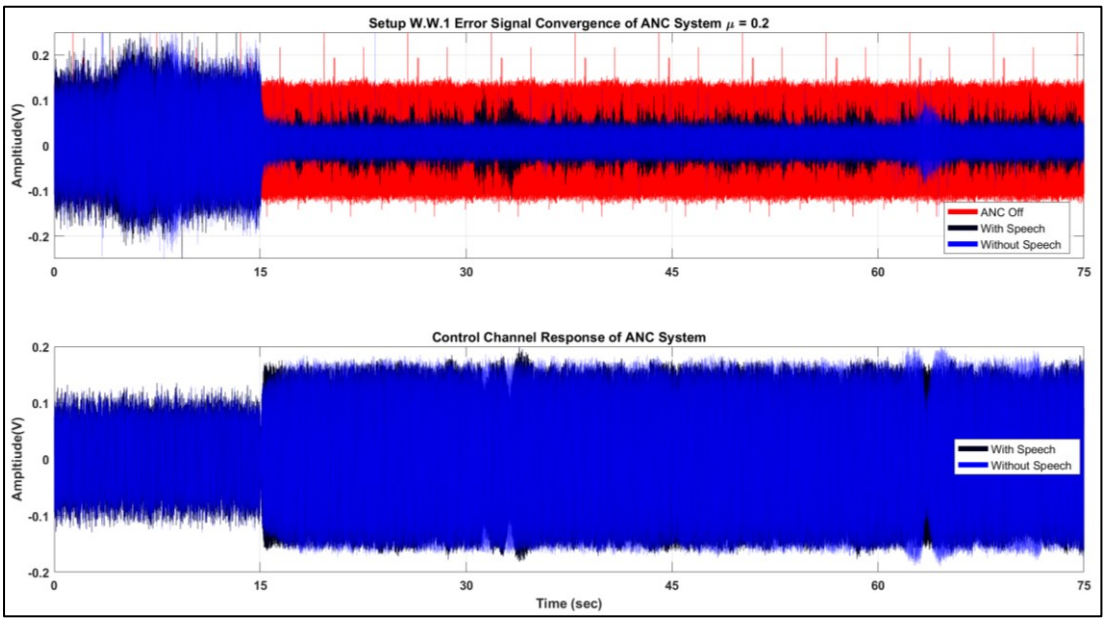

Fig. 5.50. Time-domain signals for speech interference using online system identification.

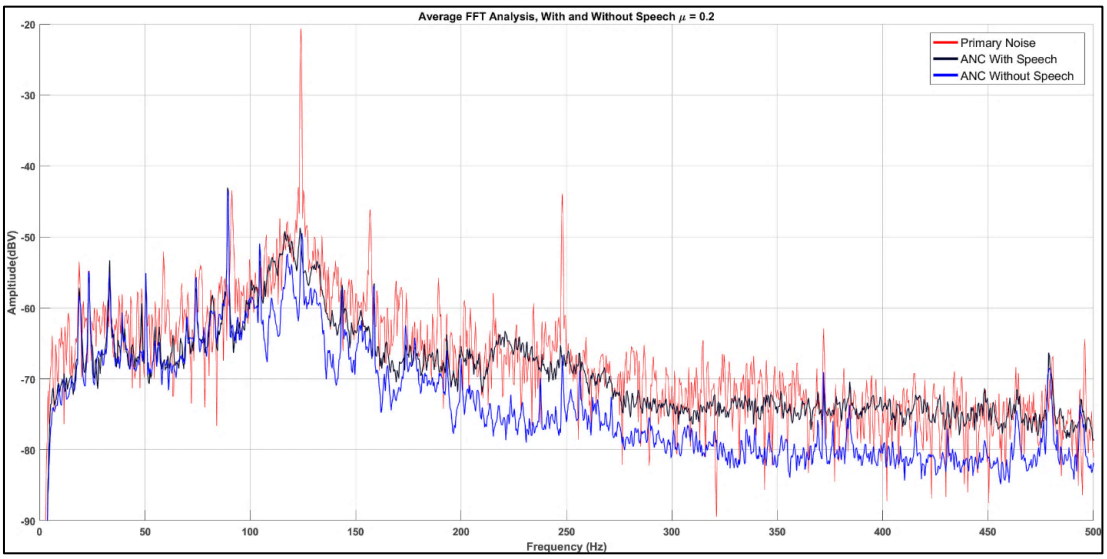

Fig. 5.51. Frequency-domain signals for speech interference using online system identification.

The result is still significant. This is because online system identification generates a binomial pseudo-random noise generated by the control loudspeaker all the time. Hence, this alters the noise reduction slightly.

5.5.1.3 Setup 2W.W.1 using online system identification.

When the dual-channel error microphone is used **(2W.W.1)**, the control performance at both ears (with and without speech) is shown in **Fig.** 5.52. The average tonal attenuation is about **7 dB** for the left ear and **3 dB** for the right ear. The average FFT analysis is shown in **Fig.** 5.53.

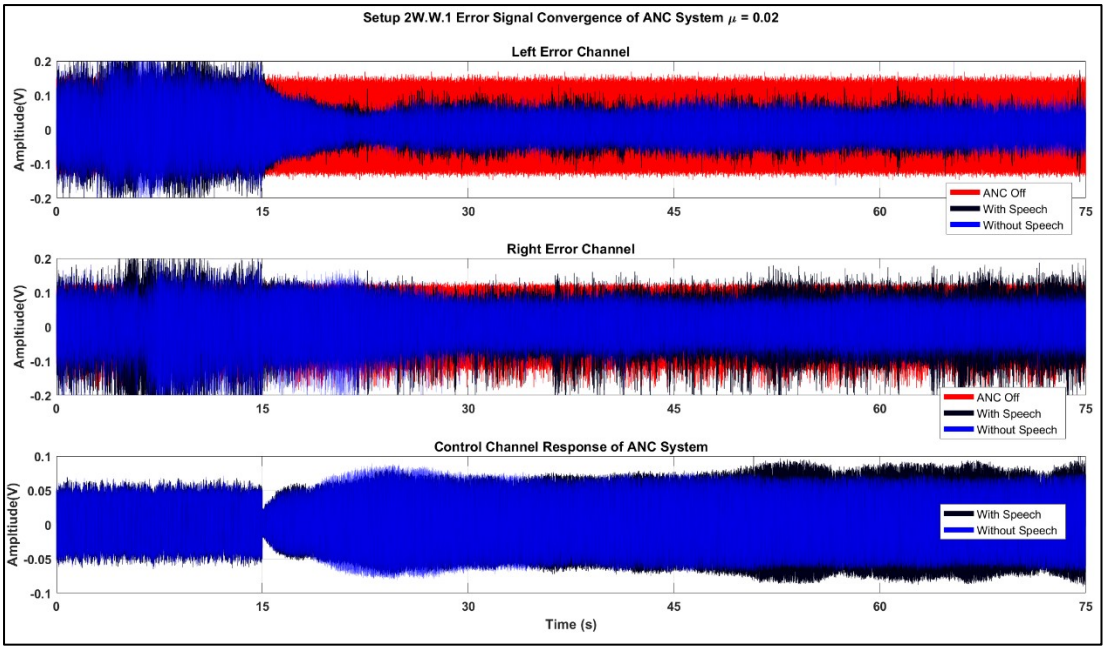

Fig. 5.52. Time-domain signals for speech interference using online system identification.

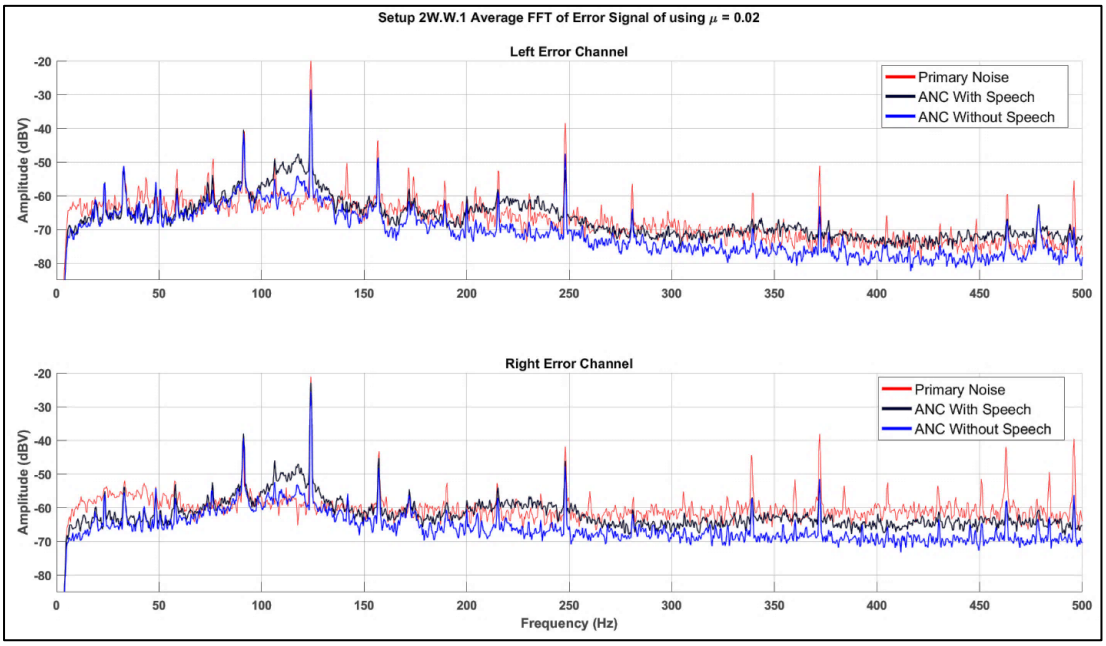

Fig. 5.53. Frequency-domain signals for speech interference using online system identification.

As discussed in previous experiments without speech, the dual-channel case appears

less performant due to the competing convergence between the left and right channels. However, there is still some noise reduction, and the system remains stable. Speech does not appear to affect the control performance significantly from a measurement and subjective point of view.

5.5.2 ANC using closely spaced loudspeakers.

5.5.2.1 Setup W.W.1 using offline system identification.

The control loudspeaker is placed close to the primary noise. The impact on performance is expected to be minimal for the single-channel ANC system. Similar to local noise control, the tonal noise attenuation is **55 dB** without speech and **45 dB** with speech. Minor radio disconnections can be spotted at the beginning of the time-domain signal without speech, but these do not affect the performance of the ANC, as shown in **Fig.** 5.54. The average FFT analysis is shown in **Fig.** 5.55.

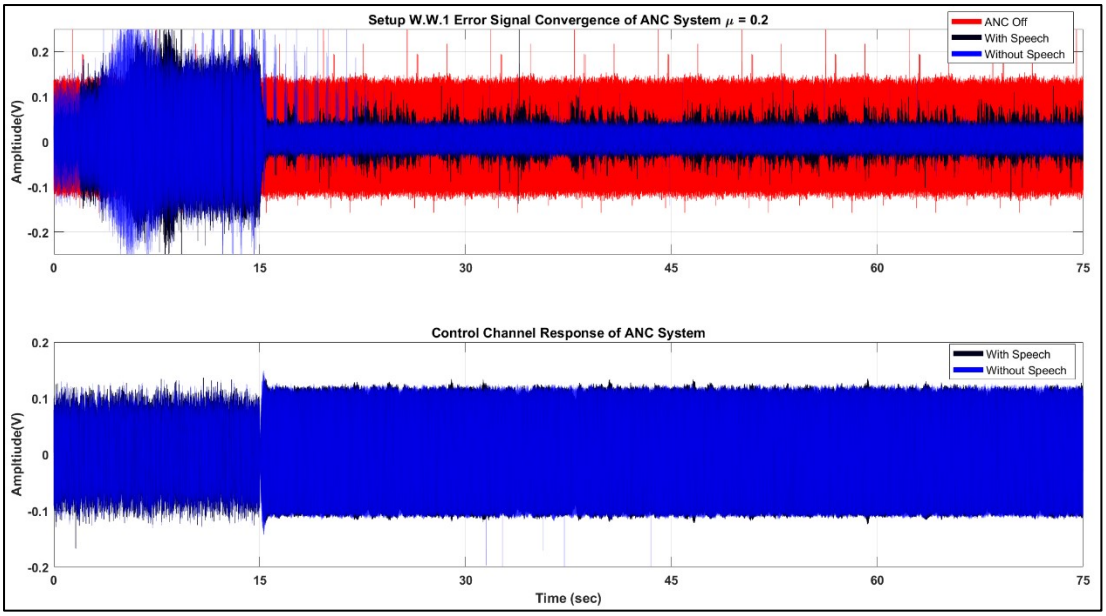

Fig. 5.54. Time-domain signals for speech interference using offline system identification.

It is clear from the results that the control system works very well, and good performance is achieved even when speech is present.

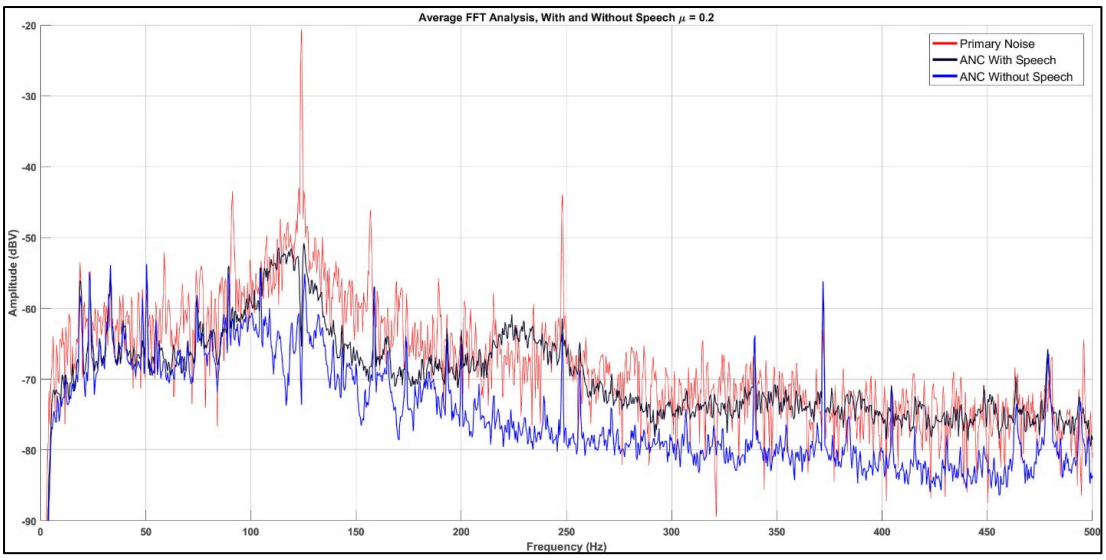

Fig. 5.55. Frequency-domain signals for speech interference using offline system identification.

5.5.2.2 Setup W.W.1 using online system identification.

Similarly, online system identification with closely spaced loudspeakers has the same effect as local noise control. However, in this case, the tonal noise reduction is dropped to an average of **30 dB** with speech and **35 dB** without speech, as shown in time-domain signals in **Fig.** 5.56 and the average FFT analysis depicted in **Fig.** 5.57.

Again, there is good performance for the system with online system identification. The drop in noise reduction is only because of the pseudo-random noise due to system identification in the background.

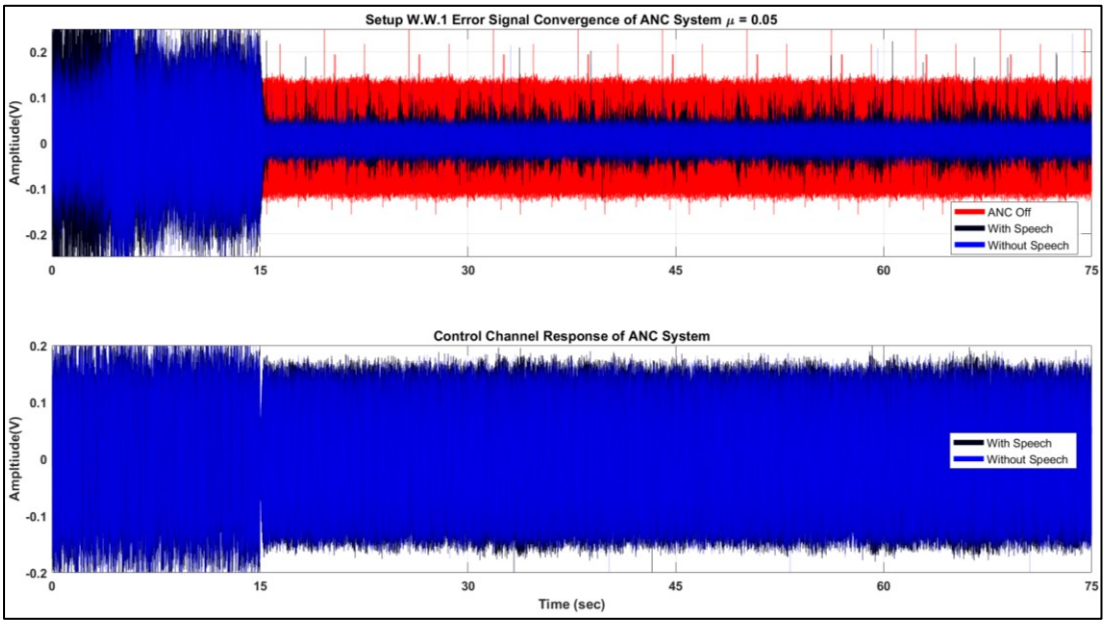

Fig. 5.56. Time-domain signals for speech interference using online system identification.

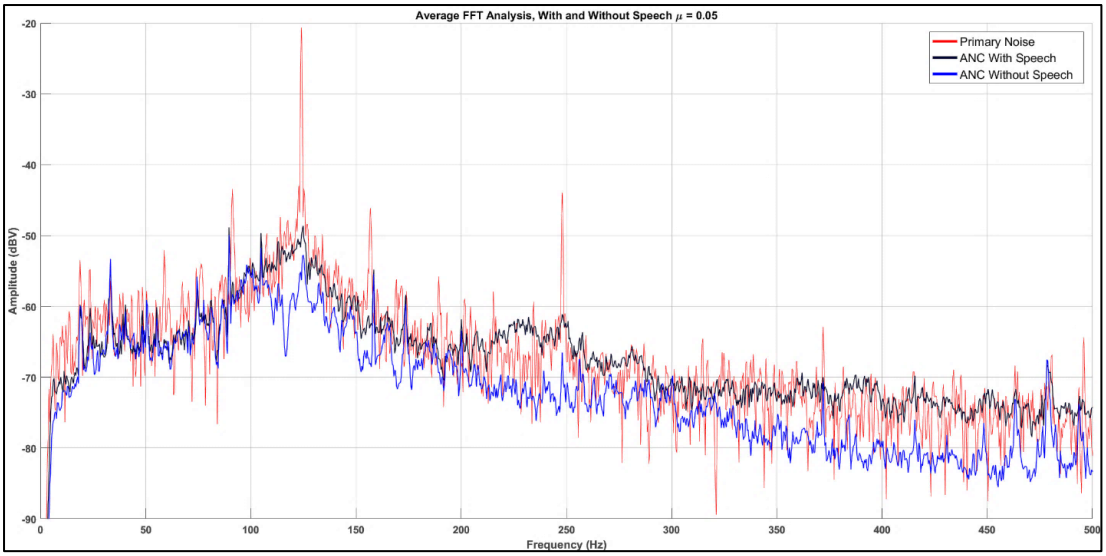

Fig. 5.57. Frequency-domain signals for speech interference using online system identification.

5.5.2.3 Setup 2W.W.1 using online system identification.

When online system identification is enabled for closely spaced loudspeakers, the ANC performance for the dual-error channel is still significant. The average tonal attenuation is about **20 dB** for both ears (with and without speech), as shown in time-domain signals in **Fig.** 5.58 and the average FFT analysis in **Fig.** 5.59.

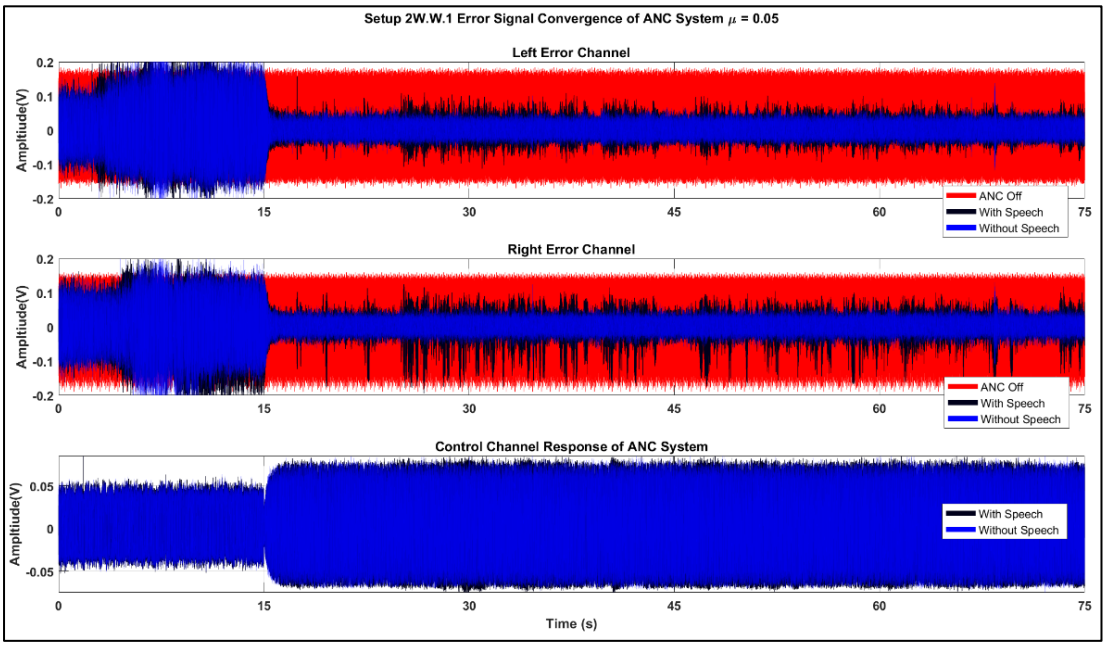

Fig. 5.58. Time-domain signals for speech interference using online system identification.

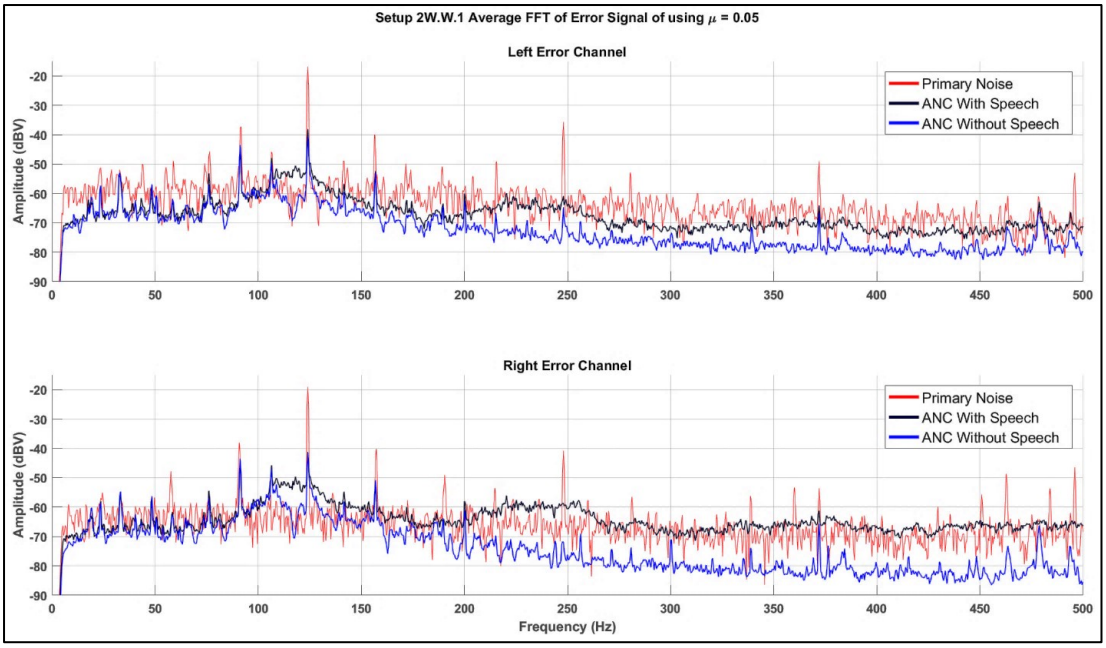

Fig. 5.59. Frequency-domain signals for speech interference using online system identification.

Again, the speech did not affect the performance of the ANC much. The online system identification does not improve noise reduction ability in the stationary case. In the following sections, the case of moving error microphones is investigated. The case of online system identification will only be considered for speech experiments since it has shown good stability and performance with moving error microphones. It is necessary for convergence and stable operation.

5.6 Steady pace head rotation in-ear ANC experiments with speech

In this section, head rotation movements are studied with the addition of speech interference to see the impact on the wireless ANC system.

5.6.1 Local noise control (separated primary and control sources)

5.6.1.1 Setup 2W.W.1 using online system identification.

With two error microphones and well-separated loudspeakers, i.e., for the case of local noise control, noise reduction remains the same where the average tonal attenuation is about **7 dB** for the left ear and **3 dB** for the right ear (with and without speech). The frequency-domain signal of the control channel was added to observe the impact of speech interference, as shown in the average FFT analysis in **Fig.** 5.61, and time-domain signals shown in **Fig.** 5.60.

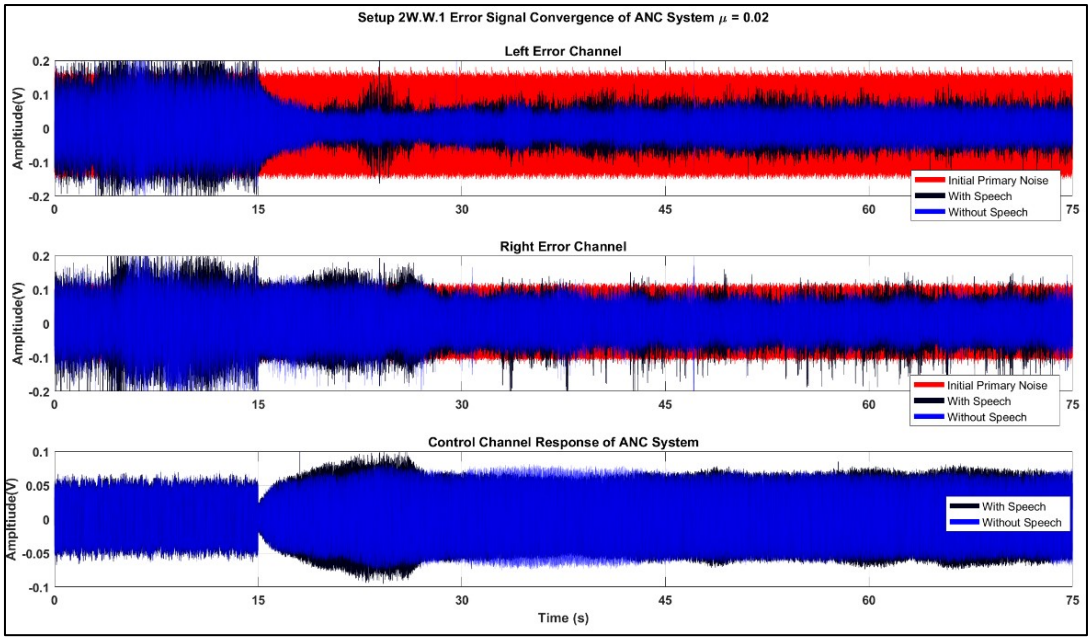

Fig. 5.60. Time-domain signals for speech interference using online system identification.

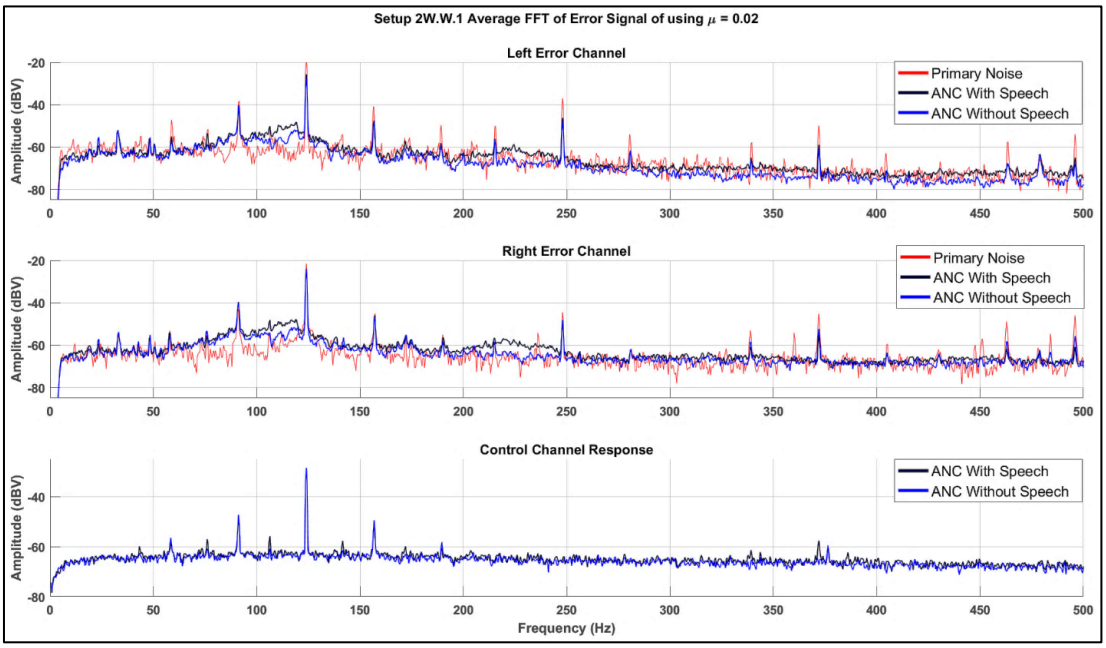

Fig. 5.61. Frequency-domain signals for speech interference using online system identification.

The results show that for this case, the performance is less than for the stationary case. It appears that the two error microphones compete to converge fast, as explained before.

5.6.2 ANC using closely spaced loudspeakers.

5.6.2.1 Setup 2W.W.1 using online system identification.

With the closely placed loudspeakers, the average noise reduction for the dual-error channel ANC is approximately **10 dB** reduction for both ears (with and without speech interference), as shown in time-domain signals in **Fig.** 5.62 and average FFT analysis depicted in **Fig.** 5.63.

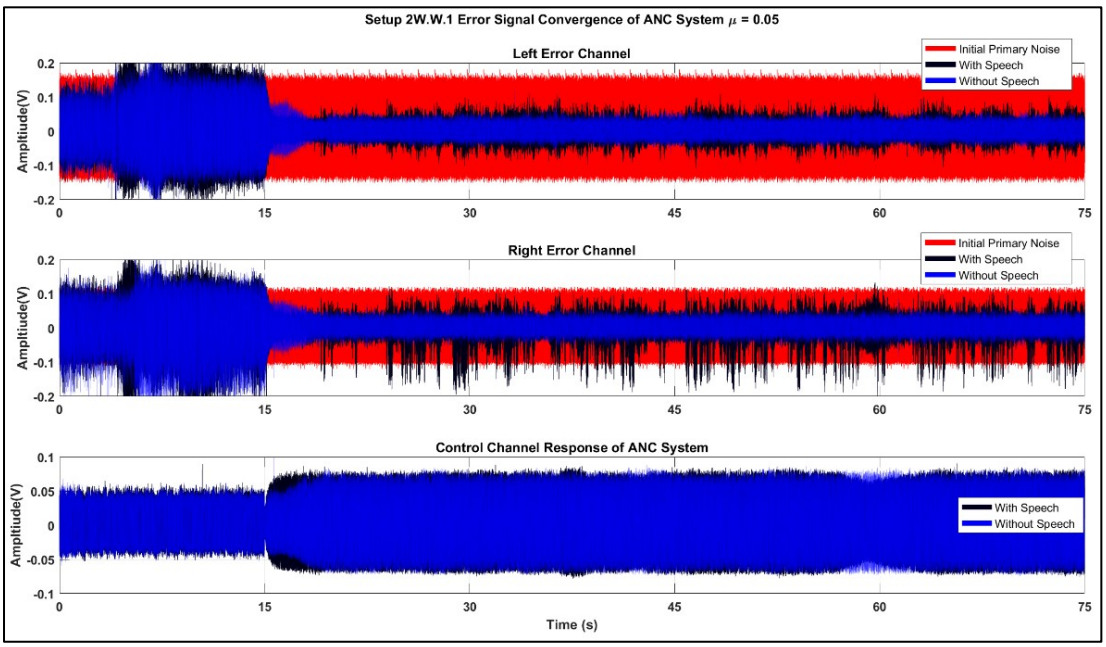

Fig. 5.62. Time-domain signals for speech interference using online system identification.

It is noted that the because the two loudspeakers are closely located, a global noise

reduction effect occurs and makes the reduction of noise at both ears similar.

The speech signal did not affect the noise control capability of the ANC system much. Instead, the background system identification caused a slight deterioration of the performance. But this is necessary to keep the system stable in the moving error microphone/s case.

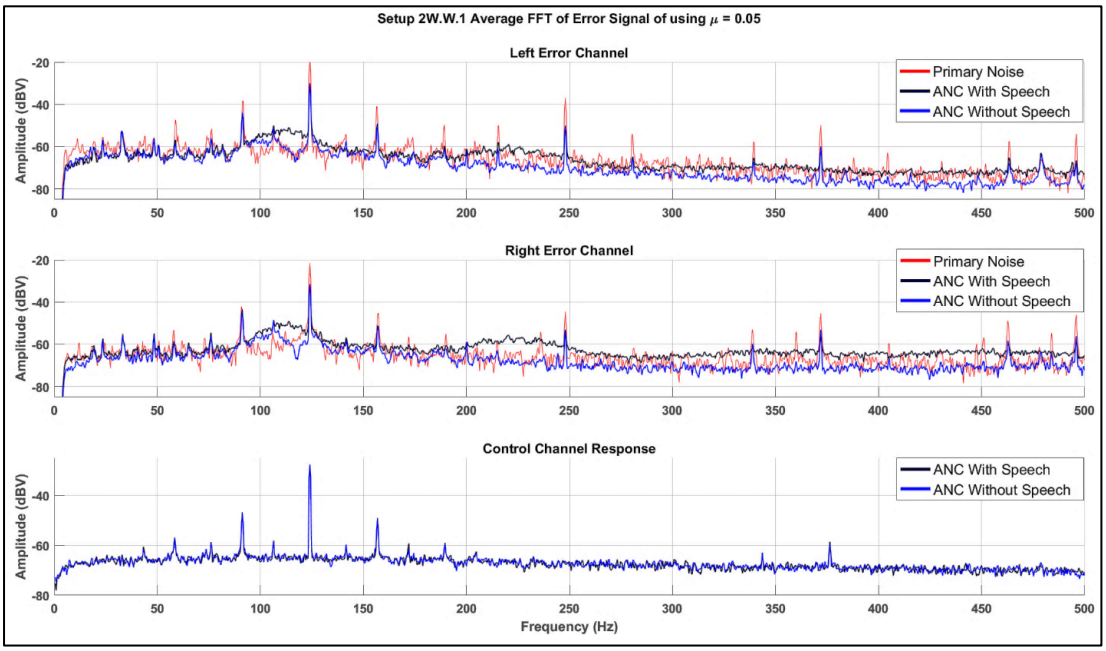

Fig. 5.63. Frequency-domain signals for speech interference using online system identification.

5.7 Walking experiments for in-ear ANC with speech

5.7.1 Local noise control (separated primary and control sources)

5.7.1.1 Setup 2W.W.1 using online system identification.

The final experiment that was carried out was the case when the user was walking and speaking at the same. The obtained time-domain signals are shown in **Fig.** 5.64**,** and the average FFT analysis is plotted in **Fig.** 5.65.

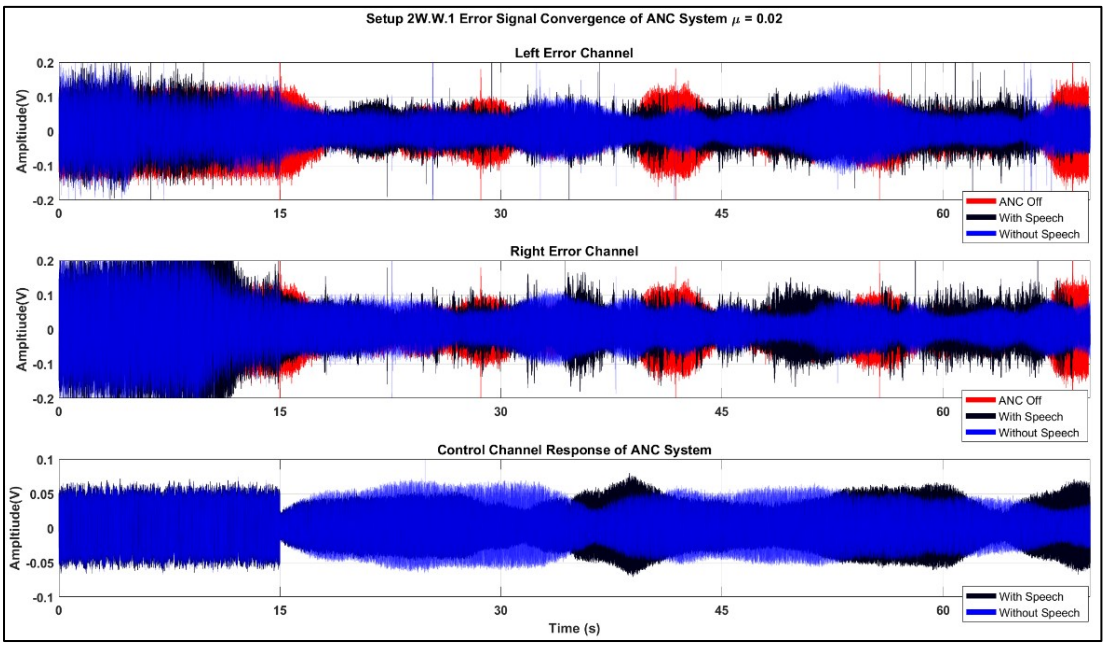

Fig. 5.64. Time-domain signals for speech interference using online system identification.

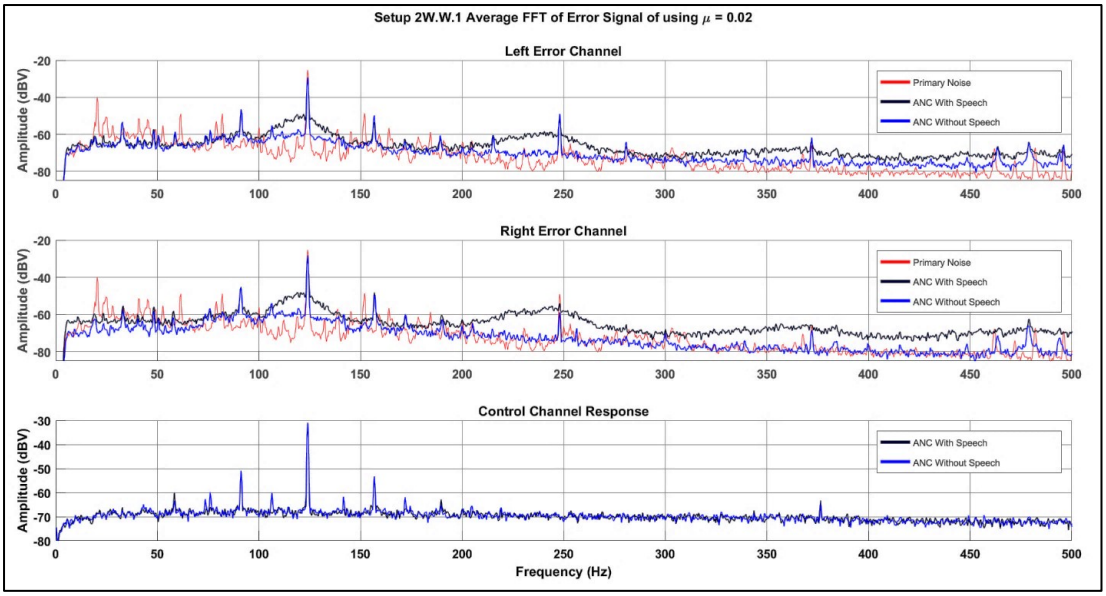

Fig. 5.65. Frequency-domain signals for speech interference using online system identification

The frequency-domain plots show that the average tonal noise reduction is not reduced significantly in the walking experiment. However, the initial system identification was carried out with a slightly smaller convergence factor to avoid system divergence. After initial system identification, the system attenuates the noise that is initially loud and resumes to adapt and control the noise. The control response shows that speech does not appear to affect the control system. Results for in-ear ANC speech experiments have been tabulated in **Appendix D.2**. It shows the tonal noise reduction with and without speech presented in sections **5.5**, **5.6** and **5.7**.

5.8 Summary and discussion of the results.

The experimental work was divided into several parts. First, noise control was performed for the following cases:

1. Noise control with the two loudspeakers well separated and apart from each other.
2. Noise control with the two loudspeakers closely spaced together.
    a. For both cases #**1** and #**2,** experiments were conducted for:
        i. ANC using offline system identification.
        ii. ANC using online system identification.
3. The cases described in points #**1** and #**2** were then performed for three scenarios:
    a. A user is sitting on a chair.
    b. A user is sitting on a chair with head rotation.
    c. A user is walking inside the lab at a normal walking pace.
4. An additional scenario was investigated for when a user is speaking while doing one of the scenarios described in case #**3**.

Tables are also provided in **Appendix D** for the purpose of comparing different experimental results.

5.8.1 Impact of Online System Identification on experiments

The effect of using online system identification in the stationary and head rotation experiments can be observed using tables in **Table. D.1-1** and **Table. D.1-2** located in **Appendix D.1**. The results show that enabling online system identification has a slightly negative effect on noise reduction, where the average noise reduction for stationary experiments of single-channel setups is about **40 dB**. With online system identification enabled, the reduction drops slightly to **37 dB**. Similarly, with the head rotation experiment, the offline system identification experiment had an average reduction of **34 dB**, and enabling background system identification lowers the average reduction to **25 dB**. The possible reason for this slight drop is that the continuous background pseudo-random noise used for the system identification slightly affects the coherence. However, this is not considerable and thus acceptable. The walking experiments are shown in table **Table. D.1-3**, these were carried out mainly with online system identification enabled since the ANC did not converge or stabilize without background system identification.

The average noise signal without ANC was obtained and compared to each experiment to obtain the average noise reduction. Here, the primary noise profile is assumed to be the same for each run. In general, it is observed that the noise reduction for walking experiments is effective for the locally controlled noise (well-separated loudspeakers) and is most effective for single-channel experiments. Moreover, the effectiveness of the ANC is best when the user is nearby the secondary control source. This is because the control filter coefficients converge faster, increasing control responsiveness. For such cases, the secondary path impulse response is simpler and more accurate. This leads to good noise reduction performance.

5.8.2 Effect of control loudspeaker placement on the experiments

When the dual-channel experiment was conducted with loudspeakers placed well separated, the ANC system struggled to control both in-ear microphones simultaneously. Closely spaced loudspeakers were then investigated, and it was found to be effective, with a better average tonal noise reduction of about **15 dB**. The results are shown in **Table. D.1-1**. The head rotation experiments are shown in **Table. D.1-2** show the same effect with single and dual-channel experiments with online system identification. The tonal and overall noise reduction increased by about **10 dB** with adjacent loudspeaker placement. However, when it comes to walking in a room, **Table. D.1-3** indicates that local noise reduction performed better than the closely placed loudspeakers. A possible explanation for this effect is the similarity in primary and secondary paths for closely spaced loudspeakers. For example, in local noise control where the loudspeakers are well separated, if the user was walking further, the secondary path changes can be modelled better if the secondary source is close to the primary source. Hence better control can be achieved.

5.8.3 Effect of ANC structural setup on experiments

Tables in **Appendix D.1** show that setup W.1.1 has better overall results than the remaining setups. Stationary experiments are considered good compared to the other experiments for each setup. In general, the single-channel experiments are not comparable to dual-channel experiments since one control loudspeaker tries to control both microphone noise levels for the dual-error channel setup.

5.8.4 Impact of speech interference on ANC performance and subjective evaluation.

Speech interference was studied for stationary and mobile cases. The effect of using online system identification is also studied during speech. Additionally, the placement of the loudspeakers is considered in these cases. It was found that the ANC performance behaved similarly without speech for all previous cases. Referring to the tables in **Appendix D.2.** It is clear that speech does not heavily impact the performance of the ANC system. The subjective evaluation of the user indicates that speech does not affect the control performance significantly. At lower vocal tones, the user senses insignificant noise generated by the secondary loudspeaker. This is not considered a generated noise but is a slightly reduced reduction of the ANC that happens for a very short time. This is possibly due to the coherence between the error signal and the reference signal being affected by speech. However, the effect is insignificant and did not bother the user.

Chapter 6: Conclusion and Future Work

6.1 Conclusion

This thesis presented the development and investigation of wireless in-ear ANC in an enclosed space such as an industrial workshop or machine room. After an introduction, broad literature, and background work review, a model was presented in Chapter 3 to allow numerical simulation of an ANC system, including wireless transceivers. Chapter 4 addressed the validity of the wireless system developed through experiments in an air handling duct in a laboratory. This was done by comparing a fully wired ANC system to one with wireless transceivers. After validation, an extensive array of in-ear experiments was carried out, and the results presented in Chapter 5 are discussed to show the potential of wireless ANC in future applications. Finally, this chapter presents the main conclusions and recommendations for future work.

In the wireless ANC numerical analysis chapter, it was found that sampling rate can have a significant effect on the ANC performance. Nonetheless, changing the bitrate or operating frequency channel does not significantly change the ANC performance. Chapter 4 validated the wireless ANC system in an air duct test rig. It was shown that transceivers were relatively effective and did not heavily impact or deteriorate the ANC performance. Following that, in-ear ANC experiments were carried out and presented in Chapter 5. The results show that the system performs well in both stationary and mobile cases. In mobile cases, in the walking experiment, the control performance is at its peak when a user is close to the secondary source. The head rotation experiments show that good control can be achieved by placing the

loudspeakers together. A summary is put at the end of the chapter to comprehensively discuss the in-ear ANC results.

6.2 Future work and Recommendation

Future research recommendations can be made based on the material presented in this thesis. As this thesis's work is finalized, an overview of the previous investigations raises further research questions. For example, most experiments are carried out with one control loudspeaker to reduce the cost due to the limited time and resources as well. The impact of adding another secondary loudspeaker to the ANC system can additionally be investigated. It is expected that the ANC system will behave better with regard to the attenuation of noise at both ears compared to the single control source. Developing a fully wireless dual-channel ANC is worth investigating in this case. The single-channel system can still be applied under some conditions for some practical cases.

In addition, the step size of the algorithm has to be tuned for each experiment currently. Therefore, the interest in developing an FxLMS algorithm with variable step sizes is worth a different investigation since changing the step sizes for each experiment is slightly inconvenient and impractical.

For the final thought, the background system identification is based on acoustic measures of the secondary path signal. The tuning of the convergence factor and background noise level affects the accuracy of the secondary path model. Further research can therefore be carried out to optimize these two parameters for practical applications.

References

[1] P. Lueg, "1936,'Process of silencing sound oscillations', US Patent 2043416."

[2] H. F. Olson and E. G. May, "Electronic sound absorber," *The Journal of the Acoustical Society of America,* vol. 25, no. 6, pp. 1130-1136, 1953.

[3] E. Öhrström, L. Barregärd, E. Andersson, A. Skänberg, H. Svensson, and P. Ängerheim, "Annoyance Due to Single and Combined Sound Exposure from Railway and Road Traffic," *Noise & Vibration Worldwide,* vol. 39, no. 6, pp. 11-24, 2008, doi: 10.1260/095745608785082457.

[4] T. Pàmies, J. Romeu, M. Genescà, and R. Arcos, "Active control of aircraft fly-over sound transmission through an open window," *Applied Acoustics,* Article vol. 84, pp. 116-121, 2014, doi: 10.1016/j.apacoust.2014.02.018.

[5] "Noise Control Mechanisms." https://en.wikibooks.org/wiki/Engineering_Acoustics/Sound_Absorbing_Structures_and_Materials (accessed May 28, 2022.

[6] C. M. Harris, "Handbook of acoustical measurements and noise control," 1991.

[7] H. Chen, "Theory and design of spatial active noise control systems," 2017.

[8] L. Håkansson, S. Johansson, M. Dahl, P. Sjösten, and I. Claesson, "Noise Canceling Headsets for Speech Communication," in *Noise Reduction in Speech Applications*: CRC Press, 2018, pp. 305-327.

[9] J. Duan, "Active control of vehicle powertrain and road noise," University of Cincinnati, 2011.

[10] M. Alves-Pereira and N. A. A. Castelo Branco, "Vibroacoustic disease: Biological effects of infrasound and low-frequency noise explained by mechanotransduction cellular signalling," *Progress in Biophysics and Molecular Biology,* Review vol. 93, no. 1-3, pp. 256-279, 2007, doi: 10.1016/j.pbiomolbio.2006.07.011.

[11] A. Fields. "Soundproof Acoustic Foam Panels." https://www.acousticfields.com/product/acoustic-panels/ (accessed May 22, 2022.

[12] W. Zhu, S. Shi, L. Luo, and J. Sun, "A Novel Adaptive State Detector-Based Post-Filtering Active Control Algorithm for Gaussian Noise Environment with Impulsive Interference," *Applied Sciences,* vol. 9, no. 6, p. 1176, 2019.

[13] C. C. Fuller, S. J. Elliott, and P. A. Nelson, *Active control of vibration*. Academic Press, 1996.

[14] M. Bergamasco, F. Della Rossa, and L. Piroddi, "Active noise control with on-line estimation of non-Gaussian noise characteristics," *Journal of Sound and Vibration,* Article vol. 331, no. 1, pp. 27-40, 2012, doi: 10.1016/j.jsv.2011.08.025.

[15] S. M. Kuo and D. R. Morgan, *Active noise control systems*. New York: Wiley, 1996.

[16] J. D. McIntosh, "Active noise cancellation aircraft headset system," ed: Google Patents, 2001.

[17] S. M. Kuo, S. Mitra, and W. S. Gan, "Active noise control system for headphone applications," *IEEE Transactions on Control Systems Technology,* Article vol. 14, no. 2, pp. 331-335, 2006, doi: 10.1109/TCST.2005.863667.

[18] R. M. Reddy, I. M. S. Panahi, and R. Briggs, "Hybrid FxRLS-FxNLMS adaptive algorithm for active noise control in fMRI application," *IEEE Transactions on Control Systems Technology,* Article vol. 19, no. 2, pp. 474-480, 2011, Art no. 5428777, doi: 10.1109/TCST.2010.2042599.

[19] D. Li and M. Hodgson, "Active control of low-frequency noise in industrial workrooms," in *Proceedings of the Tenth International Congress on Sound and Vibration*, 2003, pp. 3705-3712. [Online]. Available: https://www.scopus.com/inward/record.uri?eid=2-s2.0-2342435675&partnerID=40&md5=c8144287af11ec1a0249a592fce2e1b2

[20] T. J. Sutton, S. J. Elliott, A. M. McDonald, and T. J. Saunders, "Active control of road noise inside vehicles," *Noise Control Engineering Journal,* Article vol. 42, no. 4, pp. 137-147, 1994, doi: 10.3397/1.2828351.

[21] H. Sano, T. Inoue, A. Takahashi, K. Terai, and Y. Nakamura, "Active control system for low-frequency road noise combined with an audio system," *IEEE Transactions on Speech and Audio Processing,* Article vol. 9, no. 7, pp. 755-763, 2001, doi: 10.1109/89.952494.

[22] J. Cheer and S. J. Elliott, "The design and performance of feedback controllers for the attenuation of road noise in vehicles," *International Journal of Acoustics and Vibrations,* Article vol. 19, no. 3, pp. 155-164, 2014, doi: 10.20855/ijav.2014.19.3349.

[23] P. N. Samarasinghe, W. Zhang, and T. D. Abhayapala, "Recent Advances in Active Noise Control Inside Automobile Cabins: Toward quieter cars," *IEEE Signal Processing Magazine,* Article vol. 33, no. 6, pp. 61-73, 2016, Art no. 7736174, doi: 10.1109/MSP.2016.2601942.

[24] M. D. P. Emilio. "Reducing Unwanted Noise in Automobiles." https://www.electronicdesign.com/markets/automotive/article/21805161/reducing-unwanted-noise-in-automobiles (accessed May 22, 2022).

[25] S. J. Elliott and P. A. Nelson, "Active Noise Control," *IEEE Signal Processing*

Magazine, Article vol. 10, no. 4, pp. 12-35, 1993, doi: 10.1109/79.248551.

[26] H. Chen, P. Samarasinghe, T. D. Abhayapala, and W. Zhang, "Spatial noise cancellation inside cars: Performance analysis and experimental results," in *2015 IEEE Workshop on Applications of Signal Processing to Audio and Acoustics, WASPAA 2015*, 2015, doi: 10.1109/WASPAA.2015.7336947. [Online]. Available: https://www.scopus.com/inward/record.uri?eid=2-s2.0-84960914443&doi=10.1109%2fWASPAA.2015.7336947&partnerID=40&md5=5483260d8795ba4cabc688da18bc8b66

[27] T. Habib and M. Kepesi, "Open IEN issues of active noise control applications," in *2007 17th International Conference Radioelektronika*, 2007: IEEE, pp. 1-4.

[28] J. Lipper, "Active Nosie Control," ed. Dallas, TX, USA: Occupational Health and Safety, 2007.

[29] WolfeAviation. "Quiet Flight Active Noise & Vibration Control System: Overview." http://www.wolfeaviation.com/aircraft_quiet_flight.html (accessed 2020).

[30] S. M. Kuo and D. R. Morgan, "Active noise control: a tutorial review," *Proceedings of the IEEE,* Article vol. 87, no. 6, pp. 943-973, 1999, doi: 10.1109/5.763310.

[31] J. Sanjuán Juaristi and M. Sanjuán Martínez-Conde, "Auditory fatigue," *Acta Otorrinolaringologica Espanola,* Article vol. 66, no. 1, pp. 36-42, 2015, doi: 10.1016/j.otorri.2014.05.004.

[32] R. F. Barron, *Industrial noise control and acoustics*. CRC Press, 2002.

[33] C. Clark and K. Paunovic, "WHO environmental noise guidelines for the european region: A systematic review on environmental noise and cognition," *International Journal of Environmental Research and Public Health,* Review vol. 15, no. 2, 2018, Art no. 285, doi: 10.3390/ijerph15020285.

[34] J. M. Ellenbogen *et al.*, "Sleep disruption due to hospital noises," in *Proceedings of the Institute of Acoustics*, 2011, vol. 33 2, PART 3 ed., pp. 618-626. [Online]. Available: https://www.scopus.com/inward/record.uri?eid=2-s2.0-84871507627&partnerID=40&md5=6e3c66811fe8cf48dc3ecfab7c8adc76

[35] D. Connolly, J. Dockrell, B. Shield, R. Conetta, C. Mydlarz, and T. Cox, "The effects of classroom noise on the reading comprehension of adolescents," *Journal of the Acoustical Society of America,* Article vol. 145, no. 1, pp. 372-381, 2019, doi: 10.1121/1.5087126.

[36] C. Stanger, *Report: Low Frequency Noise: Technical Research Support for DEFRA Noise Programme*. Department for the Environment, Food and Rural Affairs, 2002.

[37] J. N. Peter Lercher, "Combined Transportation Noise Exposure in Residential Areas," *Encyclopedia of Environmental Health (Second Edition),* pp. 695-712, 2019.

[38] T. A. Leader, "High Blood Pressure and High Cholesterol

Associated with Noisy Jobs," ed: American Speech-Language-Hearing Association, 2018, p. 14.

[39] J. Cheer and S. J. Elliott, "Multichannel control systems for the attenuation of interior road noise in vehicles," *Mechanical Systems and Signal Processing,* Article vol. 60, pp. 753-769, 2015, doi: 10.1016/j.ymssp.2015.01.008.

[40] J. I. Mohammad, S. J. Elliott, and A. Mackay, "The performance of active control of random noise in cars," *Journal of the Acoustical Society of America,* Article vol. 123, no. 4, pp. 1838-1841, 2008, doi: 10.1121/1.2836745.

[41] S. J. Elliot, P. A. Nelson, I. M. Stothers, and C. C. Boucher, "In-flight experiments on the active control of propeller-induced cabin noise," *Journal of Sound and Vibration,* Article vol. 140, no. 2, pp. 219-238, 1990, doi: 10.1016/0022-460X(90)90525-5.

[42] T. Betlehem, W. Zhang, M. A. Poletti, and T. D. Abhayapala, "Personal Sound Zones: Delivering interface-free audio to multiple listeners," *IEEE Signal Processing Magazine,* vol. 32, no. 2, pp. 81-91, 2015, doi: 10.1109/MSP.2014.2360707.

[43] Fisitech. "Active Noise Control: Wiping Up Unwanted Sound." https://fisitech.wordpress.com/2010/07/06/active-noise-control-wiping-up-unwanted-sound/ (accessed May 22, 2022).

[44] A. Zaknich, *Principles of adaptive filters and self-learning systems*. Springer Science & Business Media, 2005.

[45] S. D. Snyder and S. Snyder, *Active noise control primer*. Springer, 2000.

[46] R. W. Hamming, *Digital filters*. Courier Corporation, 1998.

[47] M. J. Grimble and M. A. Johnson, *Optimal control and stochastic estimation: theory and applications*. John Wiley & Sons, Inc., 1986.

[48] S. S. Haykin, *Adaptive filter theory*. Pearson Education India, 2008.

[49] S. V. Vaseghi, *Advanced digital signal processing and noise reduction*. John Wiley & Sons, 2008.

[50] R. M. Gray, "Toeplitz and circulant matrices: A review," *Foundations and Trends® in Communications and Information Theory,* vol. 2, no. 3, pp. 155-239, 2006.

[51] S. J. Elliott and P. A. Nelson, "The application of adaptive filtering to the

active control of sound and vibration," *NASA STI/Recon Technical Report N,* vol. 86, p. 32628, 1985.

[52] L. J. Eriksson and M. C. Allie, "Use Of Random Noise For On-Line Transducer Modeling In An Adaptive Active Attenuation System," *Journal of the Acoustical Society of America,* Article vol. 85, no. 2, pp. 797-802, 1989, doi: 10.1121/1.397552.

[53] W. Zhang, C. Hofmann, M. Buerger, T. D. Abhayapala, and W. Kellermann, "Spatial noise-field control with online secondary path modeling: A wave-domain approach," *IEEE/ACM Transactions on Audio Speech and Language Processing,* Article vol. 26, no. 12, pp. 2355-2370, 2018, Art no. 8432092, doi: 10.1109/TASLP.2018.2864577.

[54] T. Schumacher, H. Krüger, M. Jeub, P. Vary, and C. Beaugeant, "Active noise control in headsets: A new approach for broadband feedback ANC," in *ICASSP, IEEE International Conference on Acoustics, Speech and Signal Processing - Proceedings*, 2011, pp. 417-420, doi: 10.1109/ICASSP.2011.5946429. [Online]. Available: https://www.scopus.com/inward/record.uri?eid=2-s2.0-80051646617&doi=10.1109%2fICASSP.2011.5946429&partnerID=40&md5=2d65f716c98fdb7f6630085097f9c704

[55] T. Kosaka, S. J. Elliott, and C. C. Boucher, "Novel frequency domain filtered-X LMS algorithm for active noise reduction," in *ICASSP, IEEE International Conference on Acoustics, Speech and Signal Processing - Proceedings*, 1997, vol. 1, pp. 403-406. [Online]. Available: https://www.scopus.com/inward/record.uri?eid=2-s2.0-0030710653&partnerID=40&md5=b55b924c4c7f421b9c4c1cbc350cd9ca

[56] O. J. Tobias and R. Seara, "Leaky-FXLMS algorithm: Stochastic analysis for Gaussian data and secondary path modeling error," *IEEE Transactions on Speech and Audio Processing,* Article vol. 13, no. 6, pp. 1217-1230, 2005, doi: 10.1109/TSA.2005.852018.

[57] L. Wu, X. Qiu, and Y. Guo, "A generalized leaky FxLMS algorithm for tuning the waterbed effect of feedback active noise control systems," *Mechanical Systems and Signal Processing,* Article vol. 106, pp. 13-23, 2018, doi: 10.1016/j.ymssp.2017.12.021.

[58] I. T. Ardekani, "Stability analysis of adaptation process in FxLMS-based active noise control," University of Auckland, 2011.

[59] L. Sujbert, K. Molnar, G. Orosz, and L. Lajko, *Wireless Sensing for Active Noise Control*. 2006, pp. 123-128.

[60] M. I. Michalczyk, "Active noise control systems with time varying sound sensor position," *IFAC Proceedings Volumes,* vol. 43, no. 24, pp. 44-47, 2010/01/01/ 2010, doi: https://doi.org/10.3182/20101006-2-PL-4019.00010.

[61] Y. Kajikawa and Y. Nomura, "Multi-channel active noise control with freely movable quiet zone," in *Proceedings - 8th International Symposium on Signal Processing and its Applications, ISSPA 2005*, 2005, vol. 2, pp. 767-770, doi: 10.1109/ISSPA.2005.1581051. [Online]. Available: https://www.scopus.com/inward/record.uri?eid=2-s2.0-33847153918&doi=10.1109%2fISSPA.2005.1581051&partnerID=40&md5=1931302d6edf4000fc54277d7248af53

[62] M. R. Paurobally, S. Sassi, K. Moses, and D. Khadembashi, "Wireless active noise control results," in *ICSV 2016 - 23rd International Congress on Sound and Vibration: From Ancient to Modern Acoustics*, 2016. [Online]. Available: https://www.scopus.com/inward/record.uri?eid=2-s2.0-84987896625&partnerID=40&md5=5ac03ec14310862846dcc01d293d3e3c

[63] S. Shen, N. Roy, J. Guan, H. Hassanieh, and R. R. Choudhury, "MUTE: Bringing IoT to noise cancellation," in *Proceedings of the 2018 Conference of the ACM Special Interest Group on Data Communication*, 2018, pp. 282-296.

[64] F. Mieyeville, W. Du, I. Daikh, and D. Navarro, "Wireless sensor networks for active control noise reduction in automotive domain," in *2011 the 14th International Symposium on Wireless Personal Multimedia Communications: Communications, Networking and Applications for the Internet of Things, WPMC'11*, 2011. [Online]. Available: https://www.scopus.com/inward/record.uri?eid=2-s2.0-83655211893&partnerID=40&md5=ce58f3e43b0a94b894c7aa4fb25e01a0

[65] L. Liu, L. Du, A. Kolla, and S. M. Kuo, "Wireless-communication integrated hybrid active noise control system for infant incubators: Improve health outcomes and bonding," *Noise Control Engineering Journal,* Article vol. 67, no. 3, pp. 168-179, 2019, doi: 10.3397/1/376715.

[66] L. Liu, Y. Li, and S. M. Kuo, "Feed-forward active noise control system using microphone array," *IEEE/CAA Journal of Automatica Sinica,* Article vol. 5, no. 5, pp. 946-952, 2018, doi: 10.1109/JAS.2018.7511171.

[67] P. Thanigai, S. M. Kuo, and R. Yenduri, "Nonlinear active noise control for infant incubators in neo-natal intensive care units," in *ICASSP, IEEE International Conference on Acoustics, Speech and Signal Processing - Proceedings*, 2007, vol. 1, pp. I109-I112, doi: 10.1109/ICASSP.2007.366628. [Online]. Available: https://www.scopus.com/inward/record.uri?eid=2-s2.0-34547494656&doi=10.1109%2fICASSP.2007.366628&partnerID=40&md5=b33cdf2958d64abb290d71a3a1cb57e4

[68] Y. Kajikawa, W. S. Gan, and S. M. Kuo, "Recent advances on Active noise control: Open issues and innovative applications," *APSIPA Transactions on Signal and Information Processing,* Review vol. 1, 2012, Art no. e3, doi: 10.1017/ATSIP.2012.4.

[69] A. Barkefors, S. Berthilsson, and M. Sternad, "Extending the area silenced by active noise control using multiple loudspeakers," in *ICASSP, IEEE*

International Conference on Acoustics, Speech and Signal Processing - Proceedings, 2012, pp. 325-328, doi: 10.1109/ICASSP.2012.6287882. [Online]. Available: https://www.scopus.com/inward/record.uri?eid=2-s2.0-84867601086&doi=10.1109%2fICASSP.2012.6287882&partnerID=40&md5=f2cb5f81caf14c49fd9f405891214228

[70] M. Bouchard and S. Quednau, "Multichannel recursive-least-squares algorithms and fast-transversal-filter algorithms for active noise control and sound reproduction systems," *IEEE Transactions on Speech and Audio Processing,* Article vol. 8, no. 5, pp. 606-618, 2000, doi: 10.1109/89.861382.

[71] J. Benesty and D. R. Morgan, "Frequency-domain adaptive filtering revisited, generalization to the multi-channel case, and application to acoustic echo cancellation," in *ICASSP, IEEE International Conference on Acoustics, Speech and Signal Processing - Proceedings*, 2000, vol. 2, pp. 789-792, doi: 10.1109/ICASSP.2000.859078. [Online]. Available: https://www.scopus.com/inward/record.uri?eid=2-s2.0-0033721613&doi=10.1109%2fICASSP.2000.859078&partnerID=40&md5=0b65d6781f823e18ac456cd3d64a1727

[72] J. Lorente, M. Ferrer, M. De Diego, and A. González, "GPU implementation of multichannel adaptive algorithms for local active noise control," *IEEE Transactions on Audio, Speech and Language Processing,* Article vol. 22, no. 11, pp. 1624-1635, 2014, Art no. 2344852, doi: 10.1109/TASLP.2014.2344852.

[73] S. J. Elliott, I. M. Stothers, and P. A. Nelson, "A multiple error lms algorithm and its application to the active control of sound and vibration," *IEEE Transactions on Acoustics, Speech, and Signal Processing,* Article vol. 35, no. 10, pp. 1423-1434, 1987, doi: 10.1109/TASSP.1987.1165044.

Appendicies

Appendix A. Literature content

A.1. Gradient-based algorithms

Equation (2.15) is used to provide the optimal weight vector. Minimizing the error requires continuous estimation of the auto-correlation matrix $\boldsymbol{R}$ and cross-correlation vector $\boldsymbol{p}$. Practically, the estimation of the matrix and the vector can be computationally expensive if the input signal is a non-stationary signal. Alternatively, some algorithms depend on gradient methods to find the optimal weights to minimize or reduce the performance function. The two conventional gradient methods are Newton's and the steepest descent methods. Both algorithms use the gradient of the performance surface to find the minimum error for the weights of the FIR filter. Newton's method is considered the fastest converging method as it only takes one step to converge but requires the inverse auto-correlation matrix $\boldsymbol{R}^{-1}$ which is computationally heavy and can be hard to compute or inaccurate for non-stationary scenarios. The steepest descent finds the minimum error by following the negative gradient of MSE performance surface, which has the largest rate of decrease. The gradient of the MSE can be obtained from equation (2.10) as

$$\boldsymbol{\nabla\xi} = \frac{\boldsymbol{\partial\xi}}{\boldsymbol{\partial w}} = \left[\frac{\partial\xi}{\partial w_o} \;\; \frac{\partial\xi}{\partial w_o} \cdots \frac{\partial\xi}{\partial w_{L-1}}\right]^T$$

$$\boldsymbol{\nabla\xi} = \boldsymbol{2Rw} - 2\boldsymbol{p} \tag{2.18}$$

A.1.1. Newton's method

Using the gradient of the mean-square error and the equation for the optimal weight vector gives Newton's generalized equation.

$$\boldsymbol{w}(k+1) = \boldsymbol{w}(k) - \boldsymbol{\mu}\boldsymbol{R}^{-1}\,\nabla\xi(k) \qquad (2.19)$$

where $\boldsymbol{\mu}$ is the step size or converging factor, $\boldsymbol{R^{-1}}$ is the inverse auto-correlation matrix and $\boldsymbol{\nabla\xi}(k)$ is the gradient of the MSE [47-49].At certain conditions, if the inverse of the auto-correlation matrix is known exactly and the actual averaged value of the gradient of the mean-square error is used in setting the convergence factor $\boldsymbol{\mu}$ to $\boldsymbol{\frac{1}{2}}$, this will ideally make the coefficients converge with a single step. However, practically the correlation matrix and the gradient are not ideal in practical active control applications and the method cannot be applied widely and successfully.

A.1.2. Method of steepest descent

This method allows the minimum to be reached on the error surface in the negative direction of the gradient in small steps. The coefficients are updated until the gradient of the MSE surface approaches to zero. The algorithm can be written as

$$\boldsymbol{w}(k+1) = \boldsymbol{w}(k) - \boldsymbol{\mu}\nabla\xi(k) \qquad (2.20)$$

Using the gradient equation (2.18), the steepest descent algorithm is written as

$$\boldsymbol{w}(k+1) = \boldsymbol{w}(k) - 2\boldsymbol{\mu}[\boldsymbol{p} - \boldsymbol{R}\boldsymbol{w}(k)] \qquad (2.21)$$

This method assumes the exact values of the gradient vector for each iteration.

However, practically the gradient is estimated and is not considered an exact solution. The algorithm takes some time to process the algorithm over the average past data to enhance the accuracy, which makes the filter coefficients update slowly. This can be impractical and hence a more practical algorithm such as the LMS algorithm is then used in adaptive filtering.

A.2. Multi-channel spatial ANC implementation

There are demands on extending single-channel ANC system to multi-channel ANC system. Multiple sensors and control loudspeakers are adopted in the experiments [68]. The extra components are utilized to reduce the residual errors and generate the anti-noise signals, as well it may include an extra reference sensor based on the number of primary noise sources. Frequency-domain algorithms and time-domain algorithms have been proposed and tested for Multi-channel ANC systems [55, 69-72]. Frequency-domain based algorithms have been widely deployed for Multichannel ANC systems (Leaky LMS-based ANC [73]).

The application of single-channel control configurations works with broadband and narrowband noise suppression, such as controlling noise in an air duct or small areas. The error sensors can have a spatial limit of noise reduction which is approximately $\frac{\lambda_{max}}{10}$ [72], λ_{max} is the wavelength of the maximum undesired frequency. After all, single-channel configuration is not sufficient for large environments or complex enclosure, and it mostly works best with one dimensional noise control such as air ducts. Single-channel ANC configuration can be extended to multi-channel ANC

configuration by adding additional sensors and secondary sources [73]. This will provide a larger zone of quiet and increased noise control area. Also, the dual-channel configuration can be used to have accurate feedback for a user using an ANC in a 3-Dimensional space, where the feedback signal is captured from two ears instead of one. This section will review basic multi-channel ANC extensions.

A.2.1. Extension of single-channel to multi-channel ANC adaptive algorithm

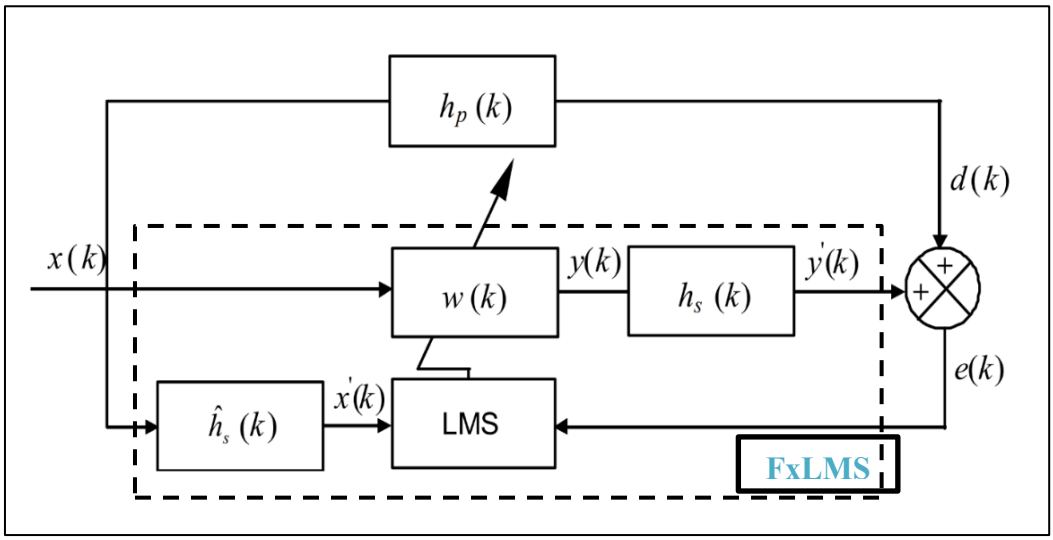

Figure A.2-1 Block diagram of FxLMS multi-channel ANC system.

In the multi-channel ANC system, the reference, anti-noise, and error signals can be more than one and may not be necessary the same number of channels. To represent the array of signals,

$r = 1, 2, \ldots, R$ is an array of reference input signals,

$e = 1, 2, \ldots, E$ is an array of error microphones,

$s = 1, 2, \ldots, S$ is an array of secondary paths or secondary sources,

$i = 1, 2, \ldots, L-1$ is the array of coefficients of the adaptive filter with an order of L,

and k is the input sample at a time.

The signal at the error microphones can be described as

$$\boldsymbol{e}_e(k) = \boldsymbol{d}_e(k) + \boldsymbol{y}'_e(k) \tag{2.34}$$

$y'_e(k)$ is the secondary noise estimate signal on the e^{th} microphone, and $d_e(k)$ is the disturbance signal on the e^{th} microphone. $y'_e(k)$ can be obtained from the actual secondary path estimate impulse response,

$$y'_e(k) = \sum_{s=1}^{S} y_s(k) * \boldsymbol{h}_{\boldsymbol{s}(s,e)}(k) \tag{2.35}$$

$\boldsymbol{h}_{\boldsymbol{s}(s,q)}(k)$ is the impulse response from the s^{th} secondary source to the e^{th} error microphone, $\boldsymbol{y}_{\boldsymbol{s}}(k)$ is a vector of driving signals for control loudspeakers, it can be expressed as,

$$\boldsymbol{y}_{\boldsymbol{s}}(k) = \sum_{r=1}^{R} \sum_{i=0}^{L-1} \boldsymbol{w}^T_{(\boldsymbol{i},\boldsymbol{r},\boldsymbol{s})}(k) \boldsymbol{x}_{\boldsymbol{r}}(k-i) \tag{2.36}$$

The filter coefficients $w^T_{(i,r,s)}(k)$ for each s^{th} control loudspeaker can be expressed as

$$\boldsymbol{w}^T_{(\boldsymbol{i},\boldsymbol{r},\boldsymbol{s})}(k) = \left[\boldsymbol{w}_{(0,r,s)}(k), \boldsymbol{w}_{(1,r,s)}(k), \dots, \boldsymbol{w}_{(L-1,r,s)}(k)\right]^T \in R^{L\times 1}$$

The reference input signals $x_r(k)$ for each r^{th} reference sensor can be expressed as

$$\boldsymbol{x}_{\boldsymbol{r}}(k) = [\boldsymbol{x}_{\boldsymbol{r}}(k)\ \ \boldsymbol{x}_{\boldsymbol{r}}(k-1), \dots, \boldsymbol{x}_{\boldsymbol{r}}(k-L+1)]^T \in R^{L\times 1}$$

To minimize the sum of the mean squared error of the signals, the instantaneous error given for each e^{th} microphone is written as

$$\hat{\boldsymbol{\xi}}(k) = \sum_{e=1}^{E} \boldsymbol{e}^{\boldsymbol{2}}(k) \tag{2.37}$$

As a result, the update equation for each r^{th} input signal for s^{th}, the secondary path is given by

$$\boldsymbol{w}_{(r,s)}(k+1) = \boldsymbol{w}_{(r,s)}(k) - 2\boldsymbol{\mu}\sum_{\boldsymbol{e=1}}^{\boldsymbol{E}} \mathbf{e}_{\mathbf{e}}(k)\boldsymbol{x}'_{(r,s,e)}(k) \tag{2.38}$$

Similarly, μ is the step-size or convergence factor, $\boldsymbol{x}'_{(r,s,e)}(k)$ are filtered reference signals, it takes a form of vector and is expressed as

$$\boldsymbol{x}'_{(r,s,e)}(k) = \left[\boldsymbol{x}'_{(r,s,e)}(k), \dots, \boldsymbol{x}'_{(r,s,e)}(k-L+1)\right]^T$$

$$\boldsymbol{x}'_{(r,s,e)}(k) = \boldsymbol{x}_r(k) * \widehat{\boldsymbol{h}}_{\boldsymbol{s}(s,e)}(k) \tag{2.39}$$

Multi-channel spatial ANC systems can increase the quiet zone in a 3-Dimensional space compared to single-channel spatial ANC systems. However, the multi-channel configuration has increased computational complexity at the cost of increasing the control region, which is one of the challenges faced when implementing a multi-channel-based ANC system. In the implementation phase of the multi-channel ANC, setting up the position of the control loudspeakers and the error microphones is important for the ANC performance and can significantly impact the ANC performance. Additionally, the number of error microphones and the control loudspeakers are important. It is ideal to have a control loudspeaker for each error microphone.

Appendix B. Selection of ANC components.

An in-ear microphone and a standard low-cost transceiver were selected for the mobility experiments of the wireless ANC system. The transceiver operates at ~ 2.4 GHz which is a standard ISM band that is reserved for industrial, medical, and scientific purposes.

B.1. Error microphone

The in-ear microphone was picked based on mobility requirements, where the user can walk freely with the in-ear microphones worn in the ears. The sony microphone has a frequency response of 20Hz – 20kHz. A MAX4466 microphone amplifier was used with the microphone. Additional low-pass filtering was used to improve the signal-to-noise ratio.

Figure B.1-1 Sony ECM-TL3 In-ear microphone

B.2. Transceivers

The wireless ANC system was built using a pair of transceivers for each channel. Each transceiver set contains a transmitter and a receiver that are battery-operated. The transceivers used for the wireless ANC system are NRF transceivers model NRF24L01+, provided with Arduino nano boards, as shown in **Figure B.1-1**. The product is also supported with a AMS1117 voltage regulator module but is replaced with a LM1117 voltage regulator due to low current supply to the transceivers.

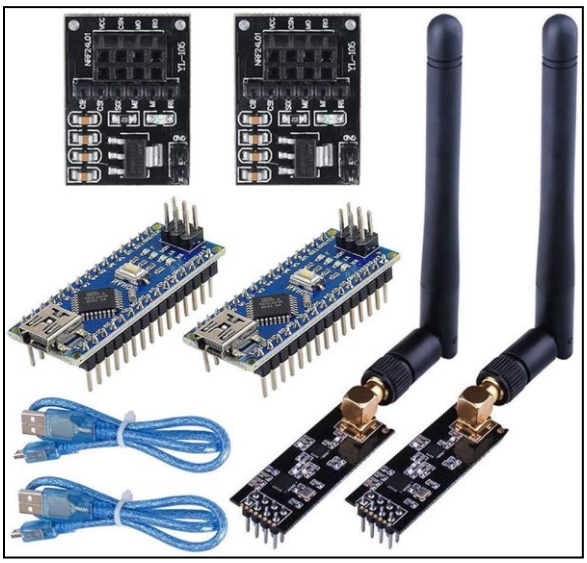

Figure B.2-1 NRF24L01+ Transceivers set

Appendix C. ANC – Air-Duct additional experiment results

C.1. Additional convergence plots.

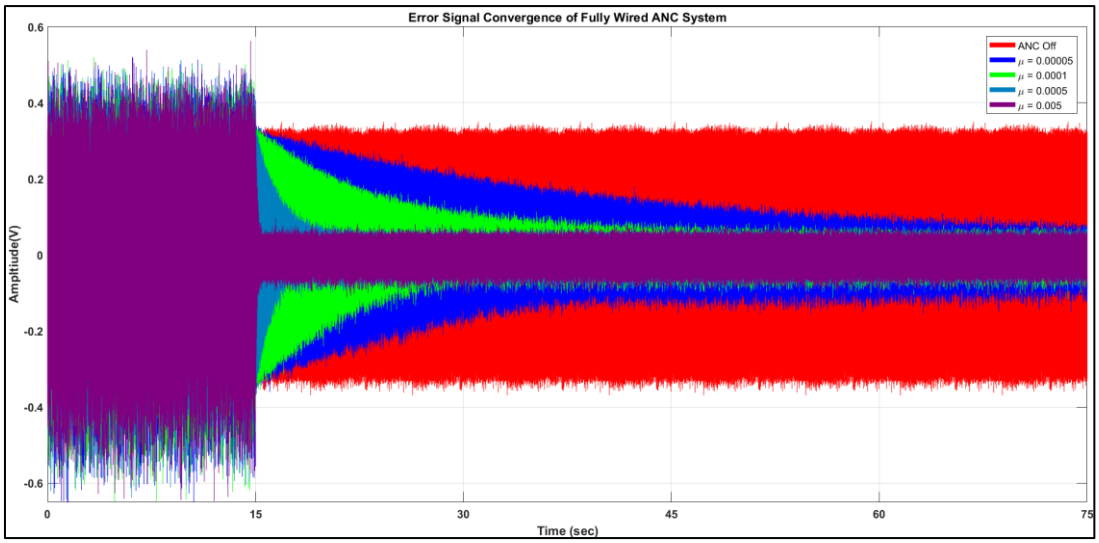

Figure C.1-1 Convergence plot for setup 1.1.1 (Air Duct Experiment) using smaller values of $\boldsymbol{\mu}$

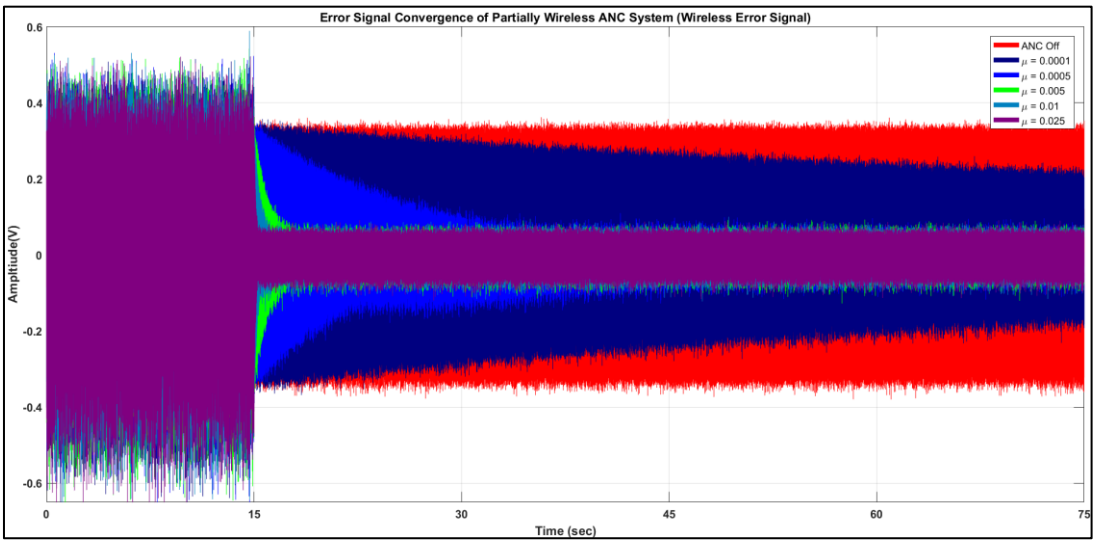

Figure C.1-2 Convergence plot for setup W.1.1 (Air Duct Experiment) using smaller values of $\boldsymbol{\mu}$

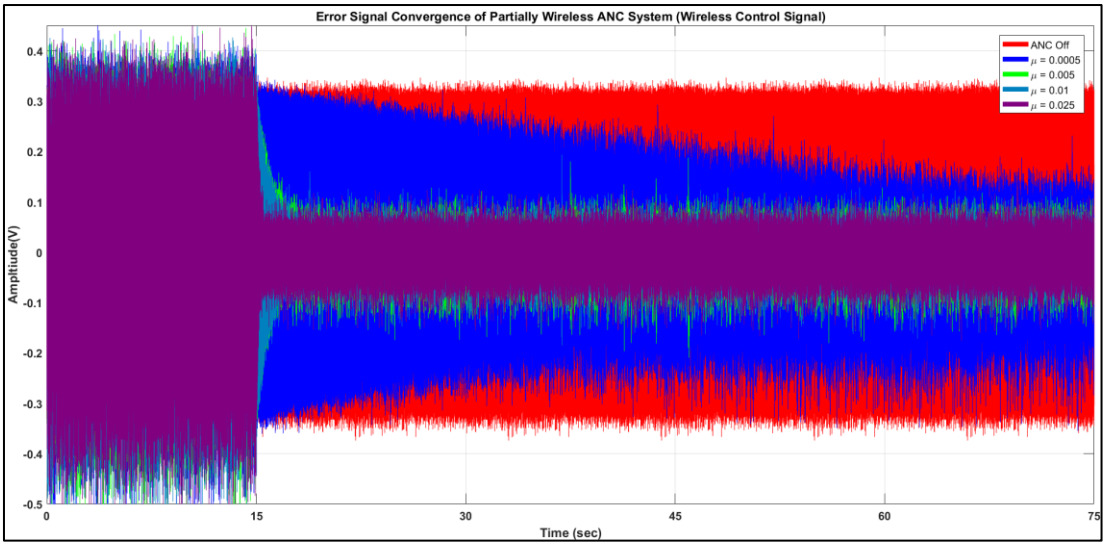

Figure C.1-3 Convergence plot for setup 1.W.1 (Air Duct Experiment) using smaller values of $\boldsymbol{\mu}$

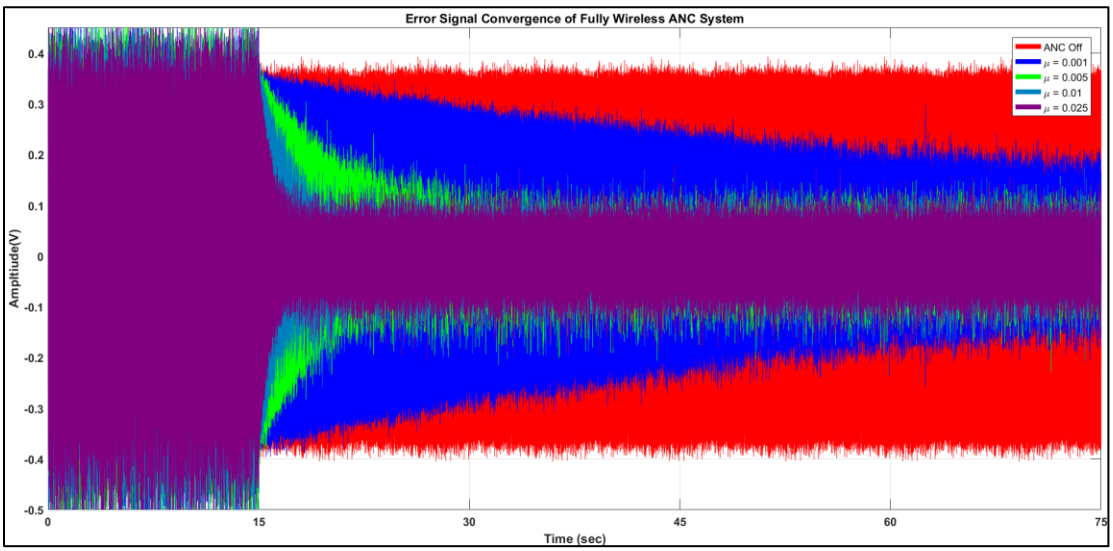

Figure C.1-4 Convergence plot for setup W.W.1 (Air Duct Experiment) for smaller values of $\boldsymbol{\mu}$

Appendix D. In-ear experiments results

D.1. Results of in-ear ANC experiments.

Table. D.1-1 Stationary experiment results compared between each setup.

Setup ID	Tonal noise reduction (dB)	Narrowband noise reduction (dB)
Local noise reduction		
Using offline system identification		
W.1.1	41.938	23.320
W.W.1	38.036	18.006
Using online system identification		
W.1.1	37.300	21.920
2W.1.1 (Left ear)	13.188	14.854
2W.1.1 (Right ear)	3.462	6.262
2W.1.1 (Average)	8.098	10.493
2W.W.1 (Left ear)	11.946	13.260
2W.W.1 (Right ear)	4.645	6.697
2W.W.1 (Average)	8.472	10.207
Noise reduction using closely spaced loudspeakers		
Using online system identification		
2W.1.1 (Left ear)	26.581	20.028
2W.1.1 (Right ear)	18.385	17.332
2W.1.1 (Average)	22.593	18.927

Setup ID	Tonal noise reduction (dB)	Narrowband noise reduction (dB)
Noise reduction using closely spaced loudspeakers		
Using online system identification		
2W.W.1 (Left ear)	28.206	20.611
2W.W.1 (Right ear)	21.458	18.995
2W.W.1 (Average)	24.838	19.923

Table. D.1-2 Steady pace head rotation experiment results compared between each setup.

Setup ID	Tonal noise reduction (dB)	Narrowband noise reduction (dB)
Local noise reduction		
Using offline system identification		
W.1.1 (μ = 0.1)	36.271	21.855
W.W.1 (μ = 0.2)	33.119	17.743
Using online system identification		
W.1.1	23.282	16.469
W.W.1	26.928	15.677
2W.1.1 (Left ear)	12.056	13.665
2W.1.1 (Right ear)	5.459	7.130
2W.1.1 (Average)	9.125	10.767
Noise reduction using closely spaced loudspeakers		
Using online system identification		
W.1.1	36.943	18.076
2W.W.1 (Left ear)	30.262	20.843
2W.W.1 (Right ear)	22.058	18.296
2W.W.1 (Average)	26.285	19.813

Table. D.1-3 Walking experiment results compared between each setup

Setup ID	Tonal noise reduction (dB)	Narrowband noise reduction (dB)
Local noise reduction		
Using online system identification		
W.1.1	18.339	12.815
W.W.1	14.710	11.623
2W.1.1 (Left ear)	12.119	9.880
2W.1.1 (Right ear)	9.880	9.265
2W.1.1 (Average)	10.928	9.567
2W.W.1 (Left ear)	10.608	6.858
2W.W.1 (Right ear)	9.378	8.850
2W.W.1 (Average)	9.972	7.797
Noise reduction using closely spaced loudspeakers		
Using online system identification		
W.W.1	8.743	8.226
2W.1.1 (Left ear)	3.799	5.602
2W.1.1 (Right ear)	8.850	9.972
2W.1.1 (Average)	5.962	7.515
2W.W.1 (Left ear)	1.801	3.401
2W.W.1 (Right ear)	8.532	8.585
2W.W.1 (Average)	4.530	5.612

Table. D.1-4 Results of Setup ID **W.1.1** for each type of experiment

Tonal noise reduction (dB)	Narrowband noise reduction (dB)
Stationary experiment	
Local noise reduction using offline system identification	
41.938	23.320
Local noise reduction using online system identification	
37.300	21.920
Steady pace head rotations experiment	
Local noise reduction using offline system identification	
36.271	21.855
Local noise reduction using online system identification	
23.282	16.469
Noise reduction with closely spaced loudspeakers using online system identification	
36.943	18.076
Walking experiment	
Local noise reduction using online system identification	
18.339	12.815

Table. D.1-5 Results of Setup ID **W.W.1** for each type of experiment

Tonal noise reduction (dB)	Narrowband noise reduction (dB)
Stationary experiment	
Local noise reduction using offline system identification	
38.036	18.006
Steady pace head rotations experiment	
Local noise reduction using offline system identification	
33.119	17.743
Local noise reduction using online system identification	
26.928	15.677
Walking experiment	
Local noise reduction using online system identification	
14.710	11.623
Noise reduction with closely space loudspeakers using online system identification	
8.743	8.226

Table. D.1-6 Results of Setup ID **2W.1.1** for each type of experiment

In-Ear Channel	Tonal noise reduction (dB)	Narrowband noise reduction (dB)
Stationary experiment		
Local noise reduction using online system identification		
Left Ear Ch	13.188	14.854
Right Ear Ch	3.462	6.262
Average	8.098	10.493
Noise reduction with closely space loudspeakers using online system identification		
Left Ear Ch	26.581	20.028
Right Ear Ch	18.385	17.332
Average	22.593	18.927
Steady pace head rotations experiment		
Local noise reduction using online system identification		
Left Ear Ch	12.056	13.665
Right Ear Ch	5.459	7.130
Average	9.125	10.767
Walking experiment		
Local noise reduction using online system identification		
Left Ear Ch	12.119	9.880
Right Ear Ch	9.880	9.265
Average	10.928	9.567

In-Ear Channel	Tonal noise reduction (dB)	Narrowband noise reduction (dB)
Noise reduction with closely space loudspeakers using online system identification		
Left Ear Ch	3.799	5.602
Right Ear Ch	8.850	9.972
Average	5.962	7.515

Table. D.1-7 Results of Setup ID **2W.W.1** for each type of experiment

In-Ear Channel	Tonal noise reduction (dB)	Narrowband noise reduction (dB)
Stationary experiment		
Local noise reduction using online system identification		
Left Ear Ch	11.946	13.260
Right Ear Ch	4.645	6.697
Average	8.472	10.207
Noise reduction with closely space loudspeakers using online system identification		
Left Ear Ch	28.206	20.611
Right Ear Ch	21.458	18.995
Average	24.838	19.923
Steady pace head rotations experiment		
Noise reduction with closely space loudspeakers using online system identification		
Left Ear Ch	30.262	20.843
Right Ear Ch	22.058	18.296
Average	26.285	19.813
Walking experiment		
Local noise reduction using online system identification		
Left Ear Ch	10.608	6.858
Right Ear Ch	9.378	8.850
Average	9.972	7.797

In-Ear Channel	Tonal noise reduction (dB)	Narrowband noise reduction (dB)
Noise reduction with closely space loudspeakers using online system identification		
Left Ear Ch	1.801	3.401
Right Ear Ch	8.532	8.585
Average	4.530	5.612

D.2. Results of in-ear ANC experiments with speech interference.

Table. D.2-1 Approximated results for stationary experiments with Speech Interference.

Setup ID	Primary noise level (dB)	Tonal noise level without speech (dB)	Tonal noise level with speech (dB)	Tonal noise reduction without speech (dB)	Tonal noise reduction with speech (dB)
Local noise reduction using offline system identification					
W.W.1	-20	-75	-65	55	45
Local noise reduction using online system identification					
W.W.1	-20	-50	-50	30	30
2W.W.1 (Average)	-20	-25	-25	5	5
Adjacent loudspeakers noise reduction using offline system identification					
W.W.1	-20	-75	-65	55	45
Adjacent loudspeakers noise reduction using online system identification					
W.W.1	-20	-55	-50	35	30
2W.W.1 (Average)	-20	-40	-40	20	20

Table. D.2-2 Approximated results for head rotation experiments with Speech Interference.

Setup ID	Primary Noise Level (dB)	Tonal Noise Level without Speech (dB)	Tonal Noise Level with Speech (dB)	Tonal Noise Reduction without Speech (dB)	Tonal Noise Reduction with Speech (dB)
Local noise reduction using online system identification					
2W.W.1 (Average)	-20	-25	-25	5	5
Adjacent loudspeakers noise reduction using online system identification					
2W.W.1 (Average)	-20	-30	-30	10	10

Table. D.2-3 Approximated results for walking experiment with Speech Interference.

Setup ID	Primary Noise Level (dB)	Tonal Noise Level without Speech (dB)	Tonal Noise Level with Speech (dB)	Tonal Noise Reduction without Speech (dB)	Tonal Noise Reduction with Speech (dB)
Local noise reduction using online system identification					
2W.W.1 (Average)	-30	-35	-35	5	5